ATTACHMENT

2-5

NUCLEAR POWER GENERATION
CF3.ID4
ATTACHMENT 7.2

TITLE: DESIGN CALCULATION COVER SHEET

Unit(s): 1&2

File No.: 21.10

Responsible Group: NPEQ

Calculation No.: OQE-014

System No. 42C

Design Calculation YES ☒ NO ☐

Quality Classification: Q

Structure, System or Component: DRY CASK STORAGE SYSTEM

Subject: Enova Engineering Calculation 0104-021-C01, "SEISMIC STABILITY ANALYSIS OF TRANSPORTER ON SOIL"

Computer/Electronic calculation YES ☐ NO ☒

Computer ID	Application Name and Version	Date of Latest Installation/Validation Test

Registered Engineer Stamp: Complete A or B

A. Insert PE Stamp or Seal Below

REGISTERED PROFESSIONAL ENGINEER
PATRICK W. HUANG
No. 36611
Patrick Huang
CIVIL
STATE OF CALIFORNIA

Expiration Date: 06/30/04

B. Insert stamp directing to the PE stamp or seal

NOTE 1: Update DCI promptly after approval.

NOTE 2: Forward electronic calculation file to CCTG for uploading to EDMS.

CF3.ID4
ATTACHMENT 7.2

TITLE: DESIGN CALCULATION COVER SHEET

RECORD OF REVISIONS

CALC No. OQE-014

Rev No.	Status	No. of Pages	Reason for Revision / Remarks	Prepared By: Initials/ LAN ID/ Date	LBIE Screen Yes/ No/ NA	LBIE Yes/ No/ NA	Check Method*	LBIE Approval PSRC Mtg. No.	LBIE Approval PSRC Mtg. Date	Checked Initials/ LAN ID/ Date	Supervisor Initials/ LAN ID/ Date	Registered Engineer Signature/ LAN ID/ Date
0	F	7 + ATTACHMENTS	Initial Issue to Support New Licensing Amendment for ISFSI	PH PWH2 10/8/02	☐ Yes ☐ No ☒ NA	☐ Yes ☐ No ☒ NA	☐ A ☐ B ☒ C	NA	NA	NA	N. J NXJ1 10/8/02	[illegible] PWH2 10/8/02
					☐ Yes ☐ No ☐ NA	☐ Yes ☐ No ☐ NA	☐ A ☐ B ☐ C					
					☐ Yes ☐ No ☐ NA	☐ Yes ☐ No ☐ NA	☐ A ☐ B ☐ C					
					☐ Yes ☐ No ☐ NA	☐ Yes ☐ No ☐ NA	☐ A ☐ B ☐ C					
					☐ Yes ☐ No ☐ NA	☐ Yes ☐ No ☐ NA	☐ A ☐ B ☐ C					

*Check Method: A: Detailed Check, B: Alternate Method (note added pages), C: Critical Point Check

Pacific Gas and Electric Company
Engineering - Calculation Sheet
Project: Diablo Canyon Unit ( )1 ( )2 (X)1&2

CALC .NO. OQE-014
REV. NO. 0
SHEET NO. i

SUBJECT SEISMIC STABILITY ANALYSIS OF TRANSPORTER ON SOIL

MADE BY PH DATE 10/8/2002 CHK'D BY NA DATE NA

REV. No.	DETAILS OF REVISION
0	Initial Issue

Pacific Gas and Electric Company
Engineering - Calculation Sheet
Project: Diablo Canyon Unit ( )1 ( )2 (X)1&2

CALC .NO. OQE-014
REV. NO. 0
SHEET NO. ii

SUBJECT SEISMIC STABILITY ANALYSIS OF TRANSPORTER ON SOIL

MADE BY PH DATE 10/8/2002 CHK'D BY NA DATE NA

TABLE OF CONTENTS

References:

1. CF3.ID4 "Design Calculations"
2. CF3.ID17 "Design Documents Prepared by External Contractors"

Attachments:

A. Enova Engineering Calculation No. 0104-021-C01 "Seismic Stability Analysis of Transporter on Soil" Date 9/23/02. (55 Pages)

B. Robert P. Kennedy "Peer Review Comments on Seismic Stability Analysis of Transporter on Soil" Date 9/24/02. (1 Pages)

Pacific Gas and Electric Company
Engineering - Calculation Sheet
Project: Diablo Canyon Unit ( )1 ( )2 (x)1&2

CALC. NO. OQE-014
REV. NO. 0
SHEET NO. 1

SUBJECT SEISMIC STABILITY ANALYSIS OF TRANSPORTER ON SOIL

MADE BY PH DATE 10/8/2002 CHECKED BY NA DATE NA

1) Introduction:

This calculation is to document the Enova Engineering Calculation No. 0104-021-C01, Revision 0, "SEISMIC STABILITY ANALYSIS OF TRANSPORTER ON SOIL" (Attachment A) according to DCPP procedure CF3.ID4 [Ref. 1].

Enova's calculation is to estimate the extent of potential sliding and rocking of a loaded transporter subjected to a hypothetical seismic event along the transporter route.

2) Review and Acceptance:

The Enova's calculation is performed based on the design requirements including in CWA's 2002PR0150, 2002PR0194 and 2002PR0269 and associated input transmittals listed in the References. The design inputs and the evaluation method have been reviewed and verified per DCPP procedure CF3.ID17 [Ref. 2], it is determined that the calculation is accurate and complete.

The methodology of Enova's calculation is also independently reviewed by Dr. Robert P. Kennedy (Attachment B).

3.) Conclusion:

Enova's calculation is acceptable per CF3.ID17 [Ref. 2].

Quality Verification Plan (QVP) AR A0552939 has been updated for the acceptance of Enova's calculation.

OQE-014 is prepared and processed per CF3.ID4 [Ref. 1].

ATTACHMENT A

ENOVA

Engineering Services

CALCULATION COVER PAGE

PROJECT NUMBER: 0104-021	CLIENT. PG&E
PROJECT TITLE: SEISMIC STABILITY ANALYSIS OF TRANSPORTER ON SOIL	
CALCULATION NUMBER: 0104-021-C01	
CALCULATION TITLE: SEISMIC STABILITY ANALYSIS OF TRANSPORTER ON SOIL	

CALCULATION DESCRIPTION·

THIS CALCULATION SUMMARIZES THE SEISMIC STABILITY ANALYSES AND RESULTS FOR THE DIABLO CANYON TRANSPORTER SUBJECT TO AMPLIFIED MOTIONS CORRESPONDING TO A HYPOTHETICAL SEISMIC EVENT ALONG THE TRANSPORT ROUTE. THIS CALCULATION IS PERFORMED IN SUPPORT OF DIABLO CANYON'S USED FUEL PROJECT.

REGISTERED PROFESSIONAL ENGINEER
SOHRAB ESFANDIARI
No. 36405
CIVIL
STATE OF CALIFORNIA

SOFTWARE USAGE: SAP2000 NON-LINEAR, VERSION 7.10

REVISION:	REVISION DESCRIPTION (INCLUDE PAGES REVISED):	TOTAL NUMBER OF PAGES:

ORIGINATOR (PRINT)	INITIALS	CHECKER (PRINT)	INITIALS	APPROVER (PRINT)	APPROVER SIGNATURE	DATE

REVISION:	REVISION DESCRIPTION (INCLUDE PAGES REVISED):	TOTAL NUMBER OF PAGES:

ORIGINATOR (PRINT)	INITIALS	CHECKER (PRINT)	INITIALS	APPROVER (PRINT)	APPROVER SIGNATURE	DATE

REVISION.	REVISION DESCRIPTION (INCLUDE PAGES REVISED):	TOTAL NUMBER OF PAGES:
0	ORIGINAL ISSUE	54

ORIGINATOR (PRINT)	INITIALS	CHECKER (PRINT)	INITIALS	APPROVER (PRINT)	APPROVER SIGNATURE	DATE
S. Esfandiari SOHRAB ESFANDIARI	SE	TY Wang T. Y. WANG	TYW	SOHRAB ESFANDIARI	S. Esfandiari	9/23/02

ENOVA

Engineering Services

CALCULATION COVER PAGE

PROJECT NUMBER: 0104-021	CLIENT: PG&E
PROJECT TITLE: SEISMIC STABILITY ANALYSIS OF TRANSPORTER ON SOIL	
CALCULATION NUMBER: 0104-021-C01	
CALCULATION TITLE: SEISMIC STABILITY ANALYSIS OF TRANSPORTER ON SOIL	

CALCULATION DESCRIPTION:

THIS CALCULATION SUMMARIZES THE SEISMIC STABILITY ANALYSES AND RESULTS FOR THE DIABLO CANYON TRANSPORTER SUBJECT TO AMPLIFIED MOTIONS CORRESPONDING TO A HYPOTHETICAL SEISMIC EVENT ALONG THE TRANSPORT ROUTE. THIS CALCULATION IS PERFORMED IN SUPPORT OF DIABLO CANYON'S USED FUEL PROJECT.

Expiration date: 6/30/04

SE

REGISTERED PROFESSIONAL ENGINEER
SOHRAB ESFANDIARI
No: 36405
CIVIL
STATE OF CALIFORNIA

SOFTWARE USAGE: SAP2000 NON-LINEAR, VERSION 7.10

REVISION.	REVISION DESCRIPTION (INCLUDE PAGES REVISED):	TOTAL NUMBER OF PAGES:

ORIGINATOR (PRINT)	INITIALS	CHECKER (PRINT)	INITIALS	APPROVER (PRINT)	APPROVER SIGNATURE	DATE

REVISION.	REVISION DESCRIPTION (INCLUDE PAGES REVISED):	TOTAL NUMBER OF PAGES:

ORIGINATOR (PRINT)	INITIALS	CHECKER (PRINT)	INITIALS	APPROVER (PRINT)	APPROVER SIGNATURE	DATE

REVISION:	REVISION DESCRIPTION (INCLUDE PAGES REVISED):	TOTAL NUMBER OF PAGES:
0	ORIGINAL ISSUE	54

ORIGINATOR (PRINT)	INITIALS	CHECKER (PRINT)	INITIALS	APPROVER (PRINT)	APPROVER SIGNATURE	DATE
S. Esfandiari SOHRAB ESFANDIARI	SE	T. Y. Wang T. Y. WANG	TYW	SOHRAB ESFANDIARI	S. Esfandiari	9/23/02

TABLE OF CONTENTS

1.0 INTRODUCTION

This calculation documents the modeling approach, analysis cases, and results for the seismic stability analysis of the Diablo Canyon (DCPP) Transporter (also called crawler), if subject to amplified ground motions.

Sliding and rocking analyses of the DCPP transporter have been performed using ISFSI Long Period (ILP) ground motions. These analysis are documented in Reference 1. ILP ground motions were developed based on rock properties similar to the power block. There were 5 sets of Time Histories developed for the ILP spectra. The purpose of the analyses to be performed here is to conservatively estimate the extent of potential sliding and rocking of a loaded transporter if it were subjected to a hypothetical seismic event, which exceeded the ILP ground motions. Per directions from PG&E (Ref. 9), a uniform amplification factor of 2 across all frequencies is to be applied to the ILP motions in order to define the hypothetical seismic event used in this study.

The objective of the seismic stability analysis is to determine the best estimate and maximum sliding displacement as well as potential uplift (as a result of potential rocking or free-flight response) that the transporter will potentially experience during a defined seismic event.

Section 2.0 describes the methodology. Design inputs are summarized in Section 3.0. Model development is discussed in Section 4.0. Various analyses cases and results are presented in Section 5.0. Conclusions are stated in Section 6.0. References are outlined in Section 7.0.

2.0 METHODOLOGY

The transporter is free to slide and rock on the road in the event that the friction resistance between the transporter and the road surface is overcome by the interia forces imposed by the earthquake. Only the case of transporter carrying a horizontal HI-TRAC is analyzed, since it is only for this scenario, that the transporter, if it slid significantly during an earthquake, could leave the road and slide down a hillside.

The sliding and rocking seismic response of the transporter is predicted using a non-linear simplified rigid body representation of the transporter subject to both horizontal and vertical time histories of input motion. The input acceleration time histories are those for the rock designated as ILP ground motions further amplified by a uniform factor of 2 (Ref. 9). There are 5 sets of time histories, which are produced to represent the ILP. These are provided to ENOVA by PG&E as design input (Ref. 2). To ascertain the response of a loaded transporter to a hypothetical seismic event, per directions from PG&E, a uniform scale factor of 2 is applied to these ILP time histories.

To capture the worst case rocking response, a 2-D cross-section of the transporter across the shorter lateral dimension is adopted (worst case for rocking). To capture the sliding behavior non-linear friction elements are used at the base, which can model the proper friction behavior in both orthogonal components along the horizontal direction. Therefore, for prediction of sliding, the model is 3-D.

The model is a non-linear model in order to correctly simulate the geometric non-linearity inherent in this problem. At the surface contact of the transporter and the road surface two distinct geometric non-linearities exist:

1. Laterally, friction is the only means of resisting lateral motion. Once friction is overcome the transporter will begin to slide relative to top of the road surface. This non-linear behavior is modeled using friction elements at the base.

2. Vertically, the transporter is free to separate from the road surface in the "up" direction due to potential rocking and free-flight modes of response. However in the "down" direction, the road surface and the supporting soil or rock media will act as a restraint to the transporter. This geometric non-linear behavior is modeled using gap/contact

elements at the base. In addition, vertical dashpots are placed under the gap element to absorb the energy dissipated due to contact of the transporter on the road surface. Also vertical springs are placed under the gap element to represent the vertical stiffness of the underlying media and transporter tracks combined.

All analyses are performed using the SAP2000 Non-linear computer program. Also, since element non-linearity is involved, all analyses are non-linear time history analysis. All non-linear time history analyses are performed using the Fast Nonlinear Analysis (FNA) Approach (See Ref. 5 for details of the methodology). To comply with SRP 3.7.1 (Ref. 8) for performing non-linear analysis, 5 sets of analyses are performed subject to the 5 sets of time histories representing the ILP motions all amplified by a uniform factor of 2.

Five sets of analyses are performed on the flat surface using a Coefficient of Friction (COF) of 0.4 consistent with the analyses performed in Ref. 1. One analysis case is performed using an upper bound COF of 0.8 to verify that consistent with the Holtec analyses (Ref. 1), rocking of the transporter is insignificant.

In addition to flat surface analysis, sliding of the transporter on a road surface having different grades longitudinally and transversely is also studied here. For analyses on Grade, two models are developed. One has a 6% grade along the longitudinal direction and 2% grade along the transverse direction of the road (Ref. 10). The second model has an 8.5% grade longitudinally and 2% grade in the transverse direction (Ref. 10). These 2 separate slopes constitute various portions of the road that the transporter whilst carrying the HI-TRAC in a horizontal position will travel on (Ref. 10). This input is provided by PG&E (Ref. 10). For the 6% grade model, 10 analyses cases will be run, 5 sets with fault parallel component of motion aligned longitudinally, and the other 5 sets the fault normal component of motion will be aligned with the longitudinal direction of the transporter. For the 8.5% model, only two analyses cases will be run. These would correspond to the two cases from the 6% model, which resulted in highest sliding displacement along the longitudinal and the transverse directions respectively.

In order to simulate the effect of gravity, a ramp function is defined where the load is ramped up to unity at 5 seconds and held constant for another 5 seconds. This ramp function uses the static gravity load case as a multiplier, hence simulating the gravity condition in a time-history analysis option. The gravity time history analysis case is defined as a pre-condition to the various seismic time history analyses cases, thus simulating presence of gravity conditions before and during application of dynamic loads.

3.0 DESIGN INPUT

The following information is used as design input for developing these analyses cases and results. All design input is provided by PG&E. All transporter dimensions are taken from DCPP Transporter provided in Page 13 of Ref. 1:

1. Transporter configuration analyzed is the scenario when the transporter is carrying the loaded HI-STORM in a horizontal orientation (Ref. 3)
2. Weight of empty transporter = 170 Kips (Ref. 1)
3. Weight of loaded HI-TRAC including allowance for upending frame = 260 Kips (Ref. 1)
4. Width of tracks= 29.5" (Ref. 1)
5. Inner distance between tracks = 152.5" (Ref. 1)
6. Length of tracks = 294" (Ref. 1)
7. Max. height of CG of empty transporter = 87" above ground (Ref. 1)
8. Max. height of CG of loaded HI-TRAC = 65"+6" (carry height) = 71" above ground (Ref. 1)
9. Mass moment of inertia of transporter about it's CG = 5,022 K-in-Sec.^{2} (Ref. 7)
10. Mass moment of inertia of loaded HI-TRAC about it's CG = 796 K-in-Sec.^{2} (Ref. 7)
11. Coefficient of friction for all sliding analyses COF = 0.4 (Ref. 3)
12. Coefficient of friction for all rocking analyses COF = 0.8 (Ref. 3)
13. Coefficient of restitution between transporter and road surface COR = 0.25 (Ref. 1)
14. Road Grade(s) for all downslope analyses cases = 6% & 8.5% along the longitudinal direction and 2% along the transverse direction (Ref. 10 & Ref. 11)
15. Input control motions for both horizontal and vertical motions = 5 sets of ILP time histories (Ref. 2) multiplied by an assumed factor of 2 (Ref. 9) to define the hypothetical seismic event
16. For Fault parallel direction use the component with fling (Ref. 4)
17. Vertical coefficient of subgrade reaction for soil = use data for soft rock (Ref. 6)

CALCULATION NUMBER	0104-021-C01	PROJECT NUMBER:	0104-021
CALCULATION TITLE:	SEISMIC STABILITY ANALYSIS OF TRANSPORTER ON SOIL		

The control motions for the ILP are 5 sets of time histories developed by PG&E. These are:

1. Lucerne valley (48 Sec. duration)
2a. Yarimca (40 Sec. duration)
3. LGPC (22 Sec. duration)
5. El Centro (40 Sec. duration)
6. Saratoga (40 Sec. duration)

Figure 3.1 through 3.3 shows the response spectra plots for the 2 horizontal directions and the vertical direction for set 6 (Saratoga) as a representative of the 5 sets. These spectra correspond to motions amplified by a uniform scale factor of 2 to represent a hypothetical seismic event. All 5 sets of time histories have spectra that match the target ILP spectra.

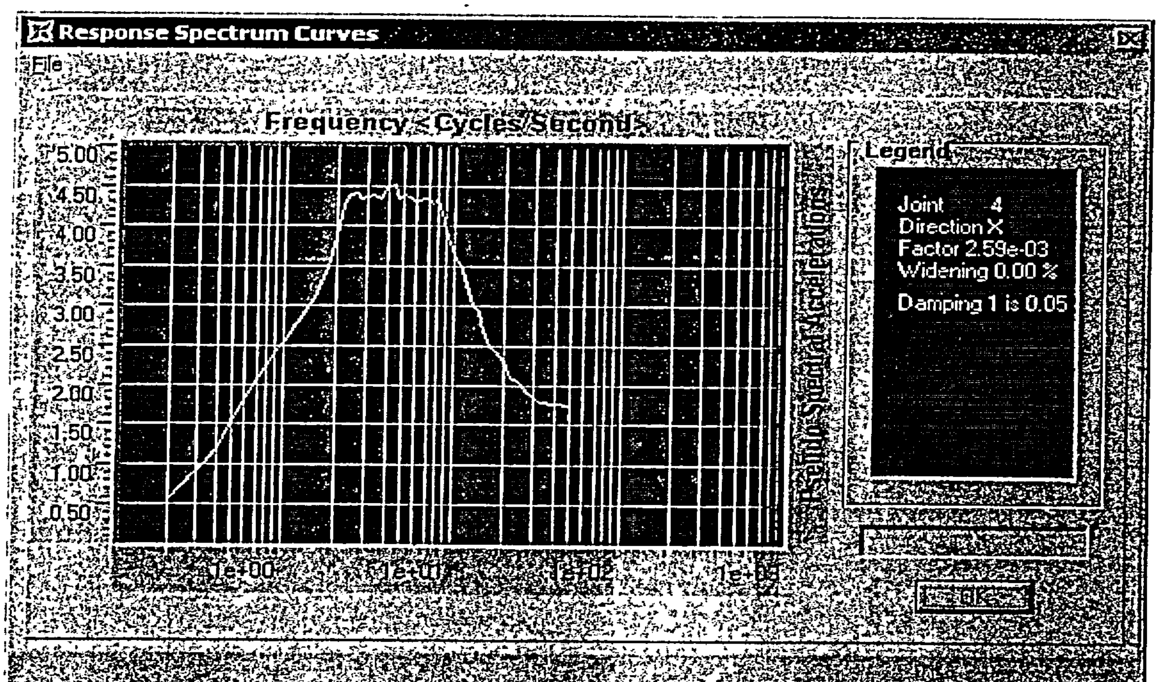

Figure 3.1: Set 6 Spectra (Fault Normal), 5% damping, Scaled by factor of 2

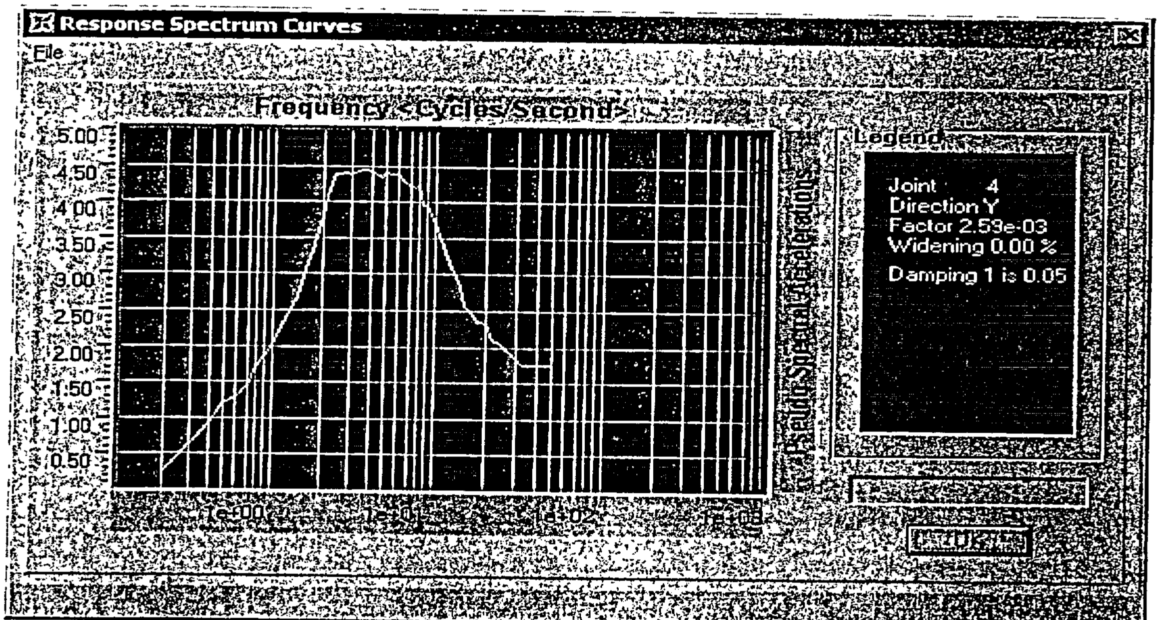

Figure 3.2: Set 6 Spectra (Fault Parallel w/fling), 5% damping, Scaled by factor of 2

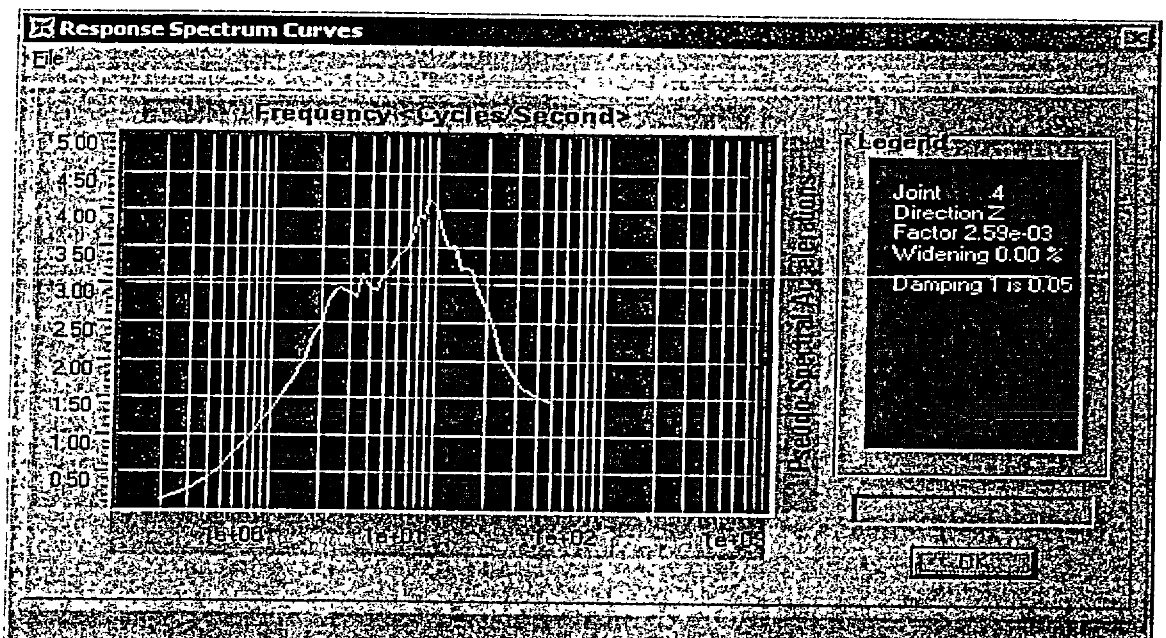

Figure 3.3: Set 6 Spectra (Vertical), 5% damping, Scaled by factor of 2

Table 3.1 below provides a summary of PGAs for the 5 sets of motion when multiplied by a factor of 2:

Time History Set	Peak Ground Acceleration (PGA) - g Fault Normal	Fault Parallel	Vertical
1	1.85	1.80	1.39
2a	1.85	1.73	1.47
3	1.75	1.77	1.39
5	1.75	1.85	1.48
6	1.76	1.77	1.47

Table 3.1: Summary of PGAs for the 5 T/H Sets

Note that vertical PGAs are greater than unity thus causing free-flight mode of response in the vertical direction.

4.0 MODEL DEVELOPMENT

4.1 Flat Surface Model

A rigid body non-linear finite element model is developed for the purpose of performing the sliding and rocking analysis of the transporter when carrying the HI-TRAC in horizontal orientation. Consistent with assumption of Ref. 1, the combined transporter and HI-TRAC is treated as a rigid body with the mass of the combined set-up lumped at the CG of the combined transporter/HI-TRAC in horizontal orientation. This model is developed using the SAP2000 Non-linear computer program. The model consists of rigid frame elements modeling the combined transporter/HI-TRAC as a rigid body, and NLLink elements modeling the interface between the transporter and the road surface. All mass and coordinate data for the transporter and the HI-TRAC is provided by PG&E as design input and are summarized in Section 3.0.

The height of the CG of the combined transporter carrying the HI-TRAC in horizontal orientation is calculated below:

Weight of empty transporter = 170 Kips
CG height of empty transporter = 87" (Max. value taken conservatively)
Weight of loaded HI-TRAC in horizontal orientation = 260 Kips (allows for 10 Kips for weight of the upending frame)
CG height of the Horizontal HI-TRAC on transporter = 65"
Nominal carry height of Horizontal HI-TRAC = 6"
CG height of the horizontal HI-TRAC above ground = 65+6 = 71"

Weight of combined transporter carrying the HI-TRAC horizontally = 430 Kips
CG height of the combined transporter/HI-TRAC = (170x87 + 260x71)/430 = 77.3"

4.1.1 GRIDLINES & COORDINATES

The following grid-line system was used to set-up the FEM. The model is created in the global X-Z plane. The grid-line is used to construct the model. The X & Z coordinates of the grid-line signify specific items of interest in the FEM.

All grid-line coordinates are with respect to the origin are defined in the Cartesian coordinate system. Tables 4.1 and 4.2 below summarize the key grid-lines and their significance.

Gridline No.	Incremental X-Dimension (inch)	Cumulative X-Coordinate (inch)	Significance
-1	-105.75	-105.75	Left edge of left track
0	0.000	0.000	Origin/CG of combined set-up
1	105.75	105.75	Right edge of right track

Table 4.1: X-Direction Key Gridlines

Gridline No.	Incremental Z-Dimension (inch)	Cumulative Z-Coordinate (inch)	Significance
0	0.00	0.00	Origin/center line of cross-section through combined transporter & HI-TRAC in shorter plane
1	77.3	77.3	CG of combined transporter carrying loaded HI-TRAC in horizontal orientation

Table 4.2: Z-Direction Key Gridlines

4.1.2 BOUNDARY CONDITIONS

Modeling the interface of the transporter and the road surface is based on a combination of Non-linear Link elements at the model's two bases (see Fig. 4.1). At each base, 2 sets of nodes are defined having identical coordinates. These are nodes 4 and 14 at the left base (X=-105.75") and 5 and 15 at the right base (X=105.75"). Nodes 14 and 15 have degrees of freedom in the vertical Z direction only and are restrained in all other directions. In the horizontal X direction, the friction element (Isolator 2) attaches nodes 4 and 5 representing the transporter to nodes 14 and 15 representing the ground.

In the vertical Z direction, the gap/contact part of the isolator 2 element connects nodes 4 and 5 to 14 and 15 respectively. Nodes 14 and 15 are in turn attached to the ground using a parallel combination of damper and spring elements, which are in parallel to each other and in series with the gap/contact element. The damper and the spring elements are defined as one-joint Nllink elements. By definition, all one joint Nllink elements are assumed to be grounded at the other end of the element (Ref. 5).

The damper is specified as a non-linear Nllink element, whilst the spring is specified as a linear Nllink element. This modeling arrangement simulates a damper in parallel with the contact spring of the isolator 2 element. However, since the isolator 2 element does not have a built-in damper inside the element, the resulting behavior is achieved by adding a separate spring element with the desired vertical stiffness of the base node, Kv, and assigning the contact stiffness of the Isolator 2 element an order of magnitude higher than Kv. These 2 elements when acting in series will have a net vertical stiffness of Kv, which in turn is parallel to the damper. Figure 4.1 shows this arrangement schematically.

At the interface of the Nllink element and the base nodes of the transporter, the model is free to slide (when sliding frictional resistance is overcome), as well as free to uplift in the vertical +Z direction. The model has no other physical restraints.

4.1.3 MATERIAL PROPERTIES

Since the transporter/HI-TRAC model is desired to be a rigid body model, all frame elements have rigid properties. This is achieved by defining a new material called "RIGID" which is assigned the following properties:

Young's Modulus (E):	16,000.00 KSI
Poison's ratio:	0.20
Weight density:	0.00
Mass density	0.00
Coefficient of thermal expansion:	0.00

4.1.4 FRAME SECTION PROPERTIES

The following arbitrary rigid properties are assigned to all RIGID frame elements. Section properties are assigned so that the fixed base structure would exhibit a fundamental frequency in excess of 33 Hz..

Cross-Sectional Area (A):	10,000 in^2
Shear area in local directions 2 & 3	8,333 in^2
Moment of Inertia about local axes 2 & 3:	8,333,333 in^4
Torsional Constant:	1,408,334 in^4

These properties are based on an arbitrary cross-sectional dimensions of 100 in x 100 in assigned to all rigid links.

4.1.5 NON-LINEAR ELEMENT PROPERTY

The Nllink element in SAP2000 is capable of modeling a number of distinct non-linear behavior. For the application of modeling the transporter/ground interface, the following properties of Nllink elements are used:

1. Isolator 2 element representing the friction (X) and gap/contact (Z)
2. Damper element
3. Spring element

Horizontally, Isolator2 properties will be used. This is a biaxial friction-pendulum isolator element that has coupled friction properties for the two shear deformations, post-slip stiffness in the shear directions, gap behavior in the axial direction, and linear stiffness properties for the three rotational degrees of freedom (not used in these analyses). The element is capable of inputting different coefficients of friction for fast velocity versus slow velocity conditions, however for these analyses a constant friction coefficient is used at all velocities.

By setting the radius of the surface to infinity, a flat surface is depicted; thus post slip stiffness is set to zero. The pre-slip stiffness in the shear deformation direction (U2) and the contact stiffness in the down axial direction (-Z) need to be set to some value, which is relatively rigid. At the same time these values should be set not too high so that problems with solution convergence due to iteration of non-linear equations of motion are avoided.

The following stiffness properties are selected for the Nllink Isolator 2 elements (elements 1 & 2):

Contact stiffness K in axial (U1) direction:	1E6 K/in
Pre-slip stiffness in the shear (U2) direction:	1E6 K/in
Lower Bound Friction Coefficient to predict max. sliding:	0.4
Upper Bound Friction Coefficient to predict max. rocking:	0.8

The Nllink spring element stiffness is representative of the vertical stiffness of the transporter/ground interface when the transporter tracks impact the ground either as a result of uplift due to rocking or as a result of free-flight. This stiffness is the summation of vertical stiffness of the soil/shale and any flexibility that is offered by the transporter tracks.

The coefficient of subgrade modulus in the vertical direction for soil/shale media is not available at this time. Conservatively, the subgrade modulus for soft rock under the mat will be used here, as an upper bound estimate. The soil value will be lower. The coefficient of subgrade reaction for soft rock is defined in Ref. 6 as follows:

$Ks = Es/B\ [1/(1-v^2)]$

Where:

Es = Young's modulus = 0.2E3 KSI for soft rock (Ref. 6, Page 5)
v = Poisson's ratio = 0.31 for soft rock (Ref. 6, Page 5)
B = Width of transporter track = 29.5" (Ref. 1)

$Ks = 0.2E3/29.5\ [1/(1-0.31^2)] = 7.5\ K/in^3$

Multiplying this Ks by the area under each track of the transporter, the vertical stiffness of soft rock under each transporter track is:

Kv = 294 x 29.5 x 7.5 = 65,051 K/in

Check frequency of the transporter whilst supported by this spring constant:

$f = 1/2\pi\ [K/M]^{0.5}$
$f = 1/2\pi\ [2x65{,}051x386.4/430]^{0.5} = 54\ Hz.$

This frequency is higher than 33 Hz., assumed by Holtec (Ref. 1) in stability analysis of transporter on rock. To be consistent with Ref. 1 assumption, use Kv that would result in a frequency of 33 Hz.:

$33 = 1/2\pi\ [2\text{x}Kv\text{x}386.4/430]^{0.5}$
$Kv = 23{,}922$ K/in

Use of 33 Hz. frequency is justified due to anticipated additional flexibility offered by:

1. The transporter tracks
2. Soil/Shale vertical stiffness which will be softer than soft rock

The Nllink damper element represents energy dissipation upon contact and is calculated as follows:

$2Cv = 2\xi\ (2KM)^{0.5}$

Where:

K = 23,922 (Vertical stiffness at the track/ground interface)
M = 430/386.4 = 1.1128 K-Sec^2/in (Mass of the structure)
ξ = Modal damping set to 0.4 representing a coefficient of restitution of 0.25 for this interface. This assumption is consistent with that used in Ref. 1 for stability analysis of the transporter on rock.

Damping constant Cv = 92.3 K-sec/in

4.1.6 MODEL MASS

Based on design input provided by PG&E (Ref. 1), the following mass and mass moment of inertia are used:

Total Weight of transporter carrying loaded HI-TRAC horizontally:	430.00 Kips
Mass of loaded transporter:	1.1128 K-Sec^2/in

98% of the total mass is assigned to node 2 (CG of loaded transporter) and 1% is assigned to each of the Nllink Isolator 2 elements. This is recommended by SAP2000 technical manual in order to obtain a more stable solution using Nllink elements. Thus:

Mass assigned to node 2 (CG of transporter):	1.0906	K-Sec^2/in
Weight assigned to node 2 (CG of transporter):	421.4	Kips
Mass assigned to each Isolator 2 element:	0.0111	K-Sec^2/in
Weight assigned to each Isolator 2 element:	4.3	Kips

The Nllink element forces under gravity loading are checked here. From any of the analysis cases, the Nllink element forces are extracted for the gravity case and these are summarized below:

Force in Nllink 5 (spring): 215.0 Kips = 0.5 (430) = 215.0 Kips
Force in Nllink 1 (contact): 212.9 Kips = 215.0 - 0.5 (4.3) = 212.85 Kips

Therefore static equilibrium is maintained.

The mass moment of inertia of the loaded transporter about the longitudinal axis of the transporter is calculated as follows based on the mass moment of inertia data for the empty transporter and the loaded HI-TRAC in the horizontal position provided by Ref. 7. These values are:

For empty Transporter, $I_{Longitudinal}$ = 1.9405E9 lb-mass-in^2 = 5,022 K-Sec^2-in
For loaded HI-TRAC, $I_{Longitudinal}$ = 3.076E8 lb-mass-in^2 = 796 K-Sec^2-in

The vertical CG height for both the empty transporter and the loaded HI-TRAC is reported as 69.5" above the ground (note that these dimensions are slightly different than the CG heights used for DCPP transporter, since the dimensions used in Ref. 7 are for the generic transporter, The DCPP transporter with higher CG will provide for higher potential for rocking).

Calculate the mass moment of inertia about CG of combined transporter and loaded HI-TRAC for DCPP, CG height previously calculated as 77.3" above ground:

$I_{Longitudinal} = 5{,}022 + 796 + 430/386.4\ (77.3\text{-}69.5)^2 = 5{,}886$ K-Sec^2-in

Use this value in the model for mass moment of inertial about global Y axis of the model.

4.1.7 MODEL PLOTS

Figure 4.1. shows the model plot including joint numbering.

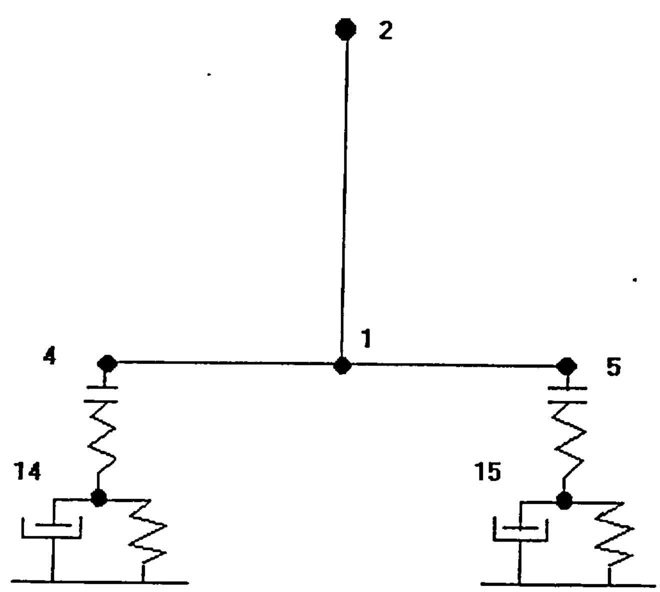

Figure 4.1: Math Model

4.2 Model for 6% Grade

The analyses results for flat surface analyses cases (see Section 5.0) indicate that subject to amplified hypothetical seismic event motion, the transporter does not exhibit any rocking behavior. As such, the model to be used for all downslope analyses cases, was further simplified to that of a single stick representing the CG height of the combined transporter carrying the HI-TRAC in a horizontal orientation. Figure 4.2 shows the model along with node numbering scheme:

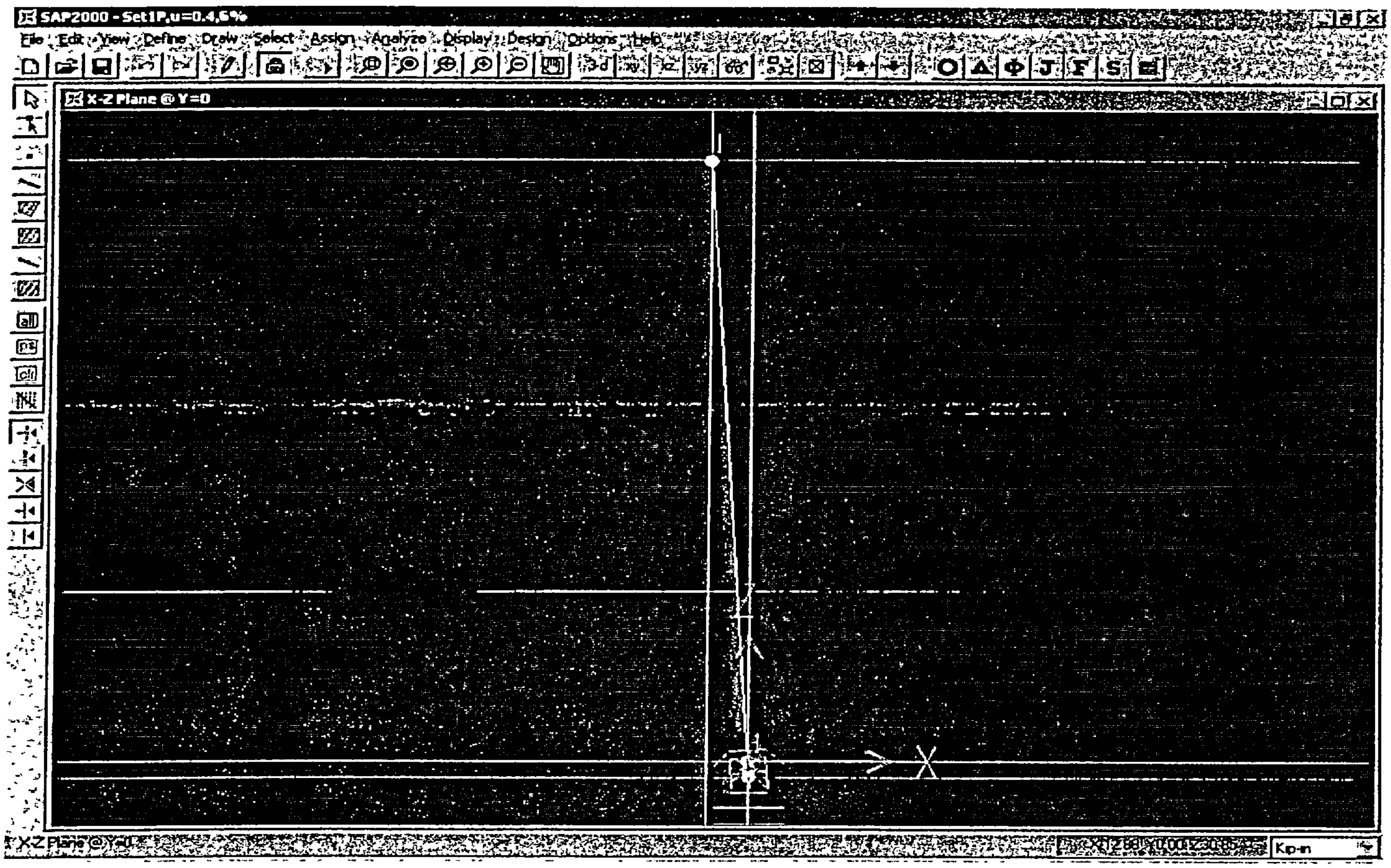

Figure 4.2: 6% Grade Model

In this model, the following node numbers are assigned:

Node 1: CG of combined Transporter/HI-TRAC
Node 4: Top of contact element (road/transporter interface)
Node 3: Bottom of contact element (top of spring/dashpot element)
Node 5: Bottom of spring/dashpot element (fixed restraint)

This model represents 6% grade along the longitudinal direction of the transporter (parallel to the road) and a 2% slope along the transverse direction of the transporter (perpendicular to the road). The 2% slope exists on the road and represents a 2% downhill slope towards the hill side (Ref. 10).

4.2.1 COORDINATES

To allow for 6% grade longitudinally and 2% grade along the transverse direction, and to allow for transformation of coordinates, the contact element, and the spring/dashpot elements are assigned an arbitrary height of 1". The stick representing the combined transporter/HI-TRAC has a height of 77.3" as before (to the CG).

To simulate the 6% grade along the longitudinal direction and 2% grade along the transverse direction, the coordinates of these nodes are transformed as follows:

First a rotation α is performed about the Y axis to represent the 6% slope longitudinally which is represented along the X-Z plane in this model, where:

$\tan\alpha = 0.06$
$\alpha = 3.4336^\circ$

Next, a rotation of β is performed about axis X' (the transformed X axis) to allow for the 2% transverse slope, where:

$\tan\beta = 0.02$
$\beta = 1.1458^\circ$

This results in the following transformed coordinates:

Node 1: X coordinate = -77.3 Sin 3.4336 = -4.6297"
Y coordinate = -77.3 Cos 3.4336 Sin 1.1458 = -1.5429"
Z coordinate = +77.3 Cos 3.4336 Cos 1.1458 = 77.1458"

Node 4: X coordinate = 0"
Y coordinate = 0"
Z coordinate = 0"

Node 3: X coordinate = +1 Sin 3.4336 = +0.0599"
Y coordinate = +1 Cos 3.4336 Sin 1.1458 = +0.02"
Z coordinate = -1 Cos 3.4336 Cos 1.1458 = -0.998"

Node 5: X coordinate = +2 Sin 3.4336 = +0.1198"
Y coordinate = +2 Cos 3.4336 Sin 1.1458 = +0.0399"
Z coordinate = -2 Cos 3.4336 Cos 1.1458 = -1.996"

4.2.2 BOUNDARY CONDITIONS

Node 5 is restrained in all directions. Node 1 is free in all directions. Node 4 is free to move in 3 translational directions but is restrained against all 3 rotations. Node 3 has local degrees of freedom assigned such that it would only allow movement along the local axial axis of the contact element (connecting nodes 3 to 4) and dashpot/spring elements (connecting node 3 to 5).

4.2.3 MATERIAL PROPERTIES

Material properties are unchanged from the flat surface model. See Section 4.1.3.

4.2.4 FRAME SECTION PROPERTIES

Frame section properties are unchanged from the flat surface model. See Section 4.1.4.

4.2.5 NON-LINEAR ELEMENT PROPERTY

The Nllink element properties are unchanged from the flat surface model. See Section 4.1.5. However, since the two sets of spring and dashpot elements are combined into one element for the 6% grade model, the stiffness of the spring element is twice that of the previous model:

Kv = 2x23,922 = 47,844 K/in

The corresponding vertical damper is calculated as follows:

$Cv = 2\xi\,(KM)^{0.5}$

Where:

K = 47,844 (Vertical stiffness at the track/ground interface)
M = 430/386.4 = 1.1128 K-Sec^2/in (Mass of the structure)
ξ = Modal damping set to 0.4 representing a coefficient of restitution of 0.25 for this interface.

Damping constant Cv = 184.6 K-sec/in

4.2.6 MODEL MASS

The mass at CG is unchanged from the flat surface model. See Section 4.1.6. Same as the flat surface model, 98% of the mass is assigned to CG, and 2% is assigned to the Nllink element to ensure stability of the Nllink element.

Mass assigned to node 1 (CG of transporter):	1.0906	K-Sec^2/in
Weight assigned to node 1 (CG of Transporter):	421.4	Kips
Mass assigned to Isolator 2 element:	0.0222	K-Sec^2/in
Weight assigned to Isolator 2 element:	8.6	Kips

4.3 Model for 8.5% Grade

The 6% grade model is further modified to produce an 8.5% grade model representing portions of the road that have 8.5% grade along the longitudinal direction. The transverse slope remains as 2%. Figure 4.3 shows the 8.5% grade model along with node numbering scheme:

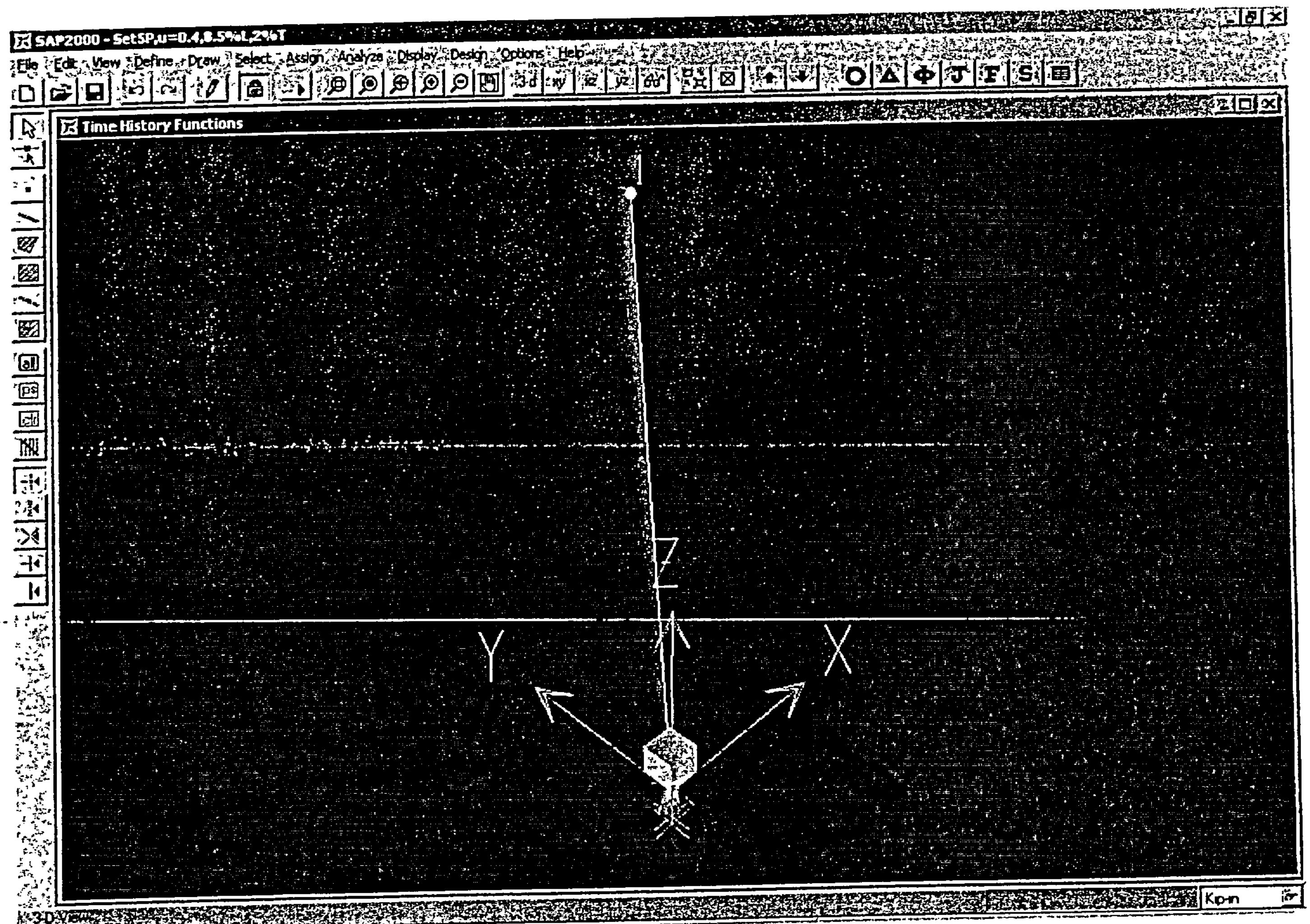

Figure 4.3: 8.5% Grade Model

The node numbers, element numbers and non-linear link element numbers and properties remain the same as the 6% model. Only the node coordinates are altered to represent the geometry associated with the 8.5% grade.

This model represents 8.5% grade along the longitudinal direction of the transporter (parallel to the road) and a 2% slope along the transverse direction of the transporter (perpendicular to the road). The 2% slope exists on the road and represents a 2% downhill slope towards the hill side (Ref. 10).

4.3.1 COORDINATES

To allow for 8.5% grade longitudinally and 2% grade along the transverse direction, and to allow for transformation of coordinates, the contact element, and the spring/dashpot elements are assigned an arbitrary height of 1". The stick representing the combined transporter/HI-TRAC has a height of 77.3" as before (to the CG).

To simulate the 8.5% grade along the longitudinal direction and 2% grade along the transverse direction, the coordinates of these nodes are transformed as follows:

First a rotation α is performed about the Y axis to represent the 8.5% slope longitudinally which is represented along the X-Z plane in this model, where:

$\tan \alpha = 0.085$
$\alpha = 4.8585°$

Next, a rotation of β is performed about axis X' (the transformed X axis) to allow for the 2% transverse slope, where:

$\tan \beta = 0.02$
$\beta = 1.1458°$

This results in the following transformed coordinates:

Node 1: X coordinate = -77.3 Sin 4.8585 = -6.5469"
Y coordinate = -77.3 Cos 4.8585 Sin 1.1458 = -1.5402"
Z coordinate = +77.3 Cos 4.8585 Cos 1.1458 = 77.0069"

Node 4: X coordinate = 0"
Y coordinate = 0"
Z coordinate = 0"

Node 3: X coordinate = +1 Sin 4.8585 = +0.0847"
Y coordinate = +1 Cos 4.8585 Sin 1.1458 = +0.0199"
Z coordinate = -1 Cos 4.8585 Cos 1.1458 = -0.9962"

Node 5: X coordinate = +2 Sin 4.8585 = +0.1694"
Y coordinate = +2 Cos 4.8585 Sin 1.1458 = +0.0398"
Z coordinate = -2 Cos 4.8585 Cos 1.1458 = -1.9924"

4.3.2 BOUNDARY CONDITIONS

Boundary conditions are the same as the 6% model. See Section 4.2.2.

4.3.3 MATERIAL PROPERTIES

Material properties are unchanged from the flat surface model. See Section 4.1.3.

4.3.4 FRAME SECTION PROPERTIES

Frame section properties are unchanged from the flat surface model. See Section 4.1.4.

4.3.5 NON-LINEAR ELEMENT PROPERTY

The Nllink element properties are unchanged from the 6% model. See Section 4.2.5.

4.3.6 MODEL MASS

Model mass is the same as the 6% model. See Section 4.2.6.

5.0 *ANALYSES CASES & RESULTS*

This Section summarizes various analysis cases performed and the results for each case. Table 5.1 below summarizes various analysis cases performed. For all flat surface analyses cases, the longitudinal axis of the transporter is aligned with the Fault Parallel component of the input motion.

For all grade analysis cases for the 6% model, two sets of analyses were performed for each time history set. The first set aligned the fault normal component of the motion along the 6% grade with a sign convention of "+X" representing upslope along the longitudinal direction, and the fault parallel component of motion applied along the transverse direction, with "+Y" representing upslope direction. These analyses cases are denoted by the time history set No., followed by letter "N" indicating fault normal component placed along the longitudinal direction.

The second set of analyses cases reversed the application of fault parallel component and the fault normal component such that the fault parallel component was aligned along the longitudinal direction. These analyses cases are denoted by "P" standing for fault parallel or component of the motion being aligned along the transporter longitudinal direction.

All together, for 6% grade model, 10 analyses cases were run, 5 corresponding to the 5 TH sets with "P" designation and 5 with "N" designation as described above. These are designated as analyses cases 7 through 16 respectively.

The third set of analyses on grade were performed for the 8.5% grade model. Two analyses cases were run for this model, corresponding to the two cases that resulted in the highest longitudinal and transverse sliding displacements from the 6% model. These are named analyses cases 17 & 18 respectively. Judging from the results of the 6% grade model, the two analyses cases chosen for the 8.5% model are 5N and 5P.

Table 5.1 below summarizes all analyses cases performed:

Analysis Case	Time History Set	Grade	COF
1	Set 1	0%	0.4
2	Set 2a	0%	0.4
3	Set 3	0%	0.4
4	Set 5	0%	0.4
5	Set 6	0%	0.4
6	Set 6	0%	0.8
7	Set 1N	6% longitudinal, 2% transverse	0.4
8	Set 2aN	6% longitudinal, 2% transverse	0.4
9	Set 3N	6% longitudinal, 2% transverse	0.4
10	Set 5N	6% longitudinal, 2% transverse	0.4
11	Set 6N	6% longitudinal, 2% transverse	0.4
12	Set 1P	6% longitudinal, 2% transverse	0.4
13	Set 2aP	6% longitudinal, 2% transverse	0.4
14	Set 3P	6% longitudinal, 2% transverse	0.4
15	Set 5P	6% longitudinal, 2% transverse	0.4
16	Set 6P	6% longitudinal, 2% transverse	0.4
17	Set 5N	8.5% longitudinal, 2% transverse	0.4
18	Set 5P	8.5% longitudinal, 2% transverse	0.4

Table 5.1: Summary of Analyses Cases

5.1 Flat Surface Analyses Results

Table 5.2 below provides a summary of maximum sliding displacements for the 2 orthogonal directions (longitudinal and transverse), as well as uplift displacement at both corner nodes for all the flat surface analyses cases (1 through 6).

Analysis Case	T/H Set	COF	Peak Longitudinal Displacement (in)	Peak Transverse Displacement (in)	Peak Uplift Displacement (in)
1	1	0.4	49.6	40.0	0.47
2	2a	0.4	30.5	27.3	0.53
3	3	0.4	27.3	53.2	0.20
4	5	0.4	37.1	65.3	0.24
5	6	0.4	48.4	54.1	0.45
Average for 5 sets at COF=0.4			**38.5**	**48.0**	**0.38**
6	6	0.8	13.9	11.8	0.46

Table 5.2: Summary of Maximum Sliding & Uplift Displacements for Flat Surface Cases

The best estimate of sliding and uplift displacements are obtained by averaging these 5 cases. This averaging is allowed as per SRP Guidelines, Section 3.7.2 (Ref. 8) since the average of the 5 sets of time histories were used to match the target spectrum. These best estimates are shown in bold letters. The largest sliding displacement, i.e. 48.0" is applicable to both directions (transverse & longitudinal), since the direction of input motion components for H1 & H2 are interchangeable.

Figures 5.1 through 5.6 show the sliding displacements for the 6 cases analyzed for the flat surface cases. Each plot contains both components of sliding, i.e., sliding along longitudinal axis of the transporter (Y component) and sliding along transverse axis of the transporter (X components). Figures 5.7 through 5.12 show the uplift displacements at the 2 nodes (nodes 4 & 5) at the base of the structure. Close examination of the vertical uplift displacement plots are a good indication of whether the vertical uplift displacement is as a result of the transporter rocking or due to free flight mode because of vertical component being greater than 1g. These plots indicate that the uplift displacements are primarily due to free-flight mode and not rocking. Comparing Figures 5.11 and 5.12 (uplift for set 6 for COF=0.4 & 0.8) indicates that the amount of uplift is almost identical (0.45" for COF=0.4 vs. 0.46" for COF=0.8) which indicates the uplift is essentially due to the free-flight response and not rocking mode of response. Furthermore, Figure 5.13 shows a closer examination of the uplift plot for Analysis case 6 (COF=0.8), which is most prune to rocking due to high friction coefficient, between times 5 & 8 Sec. into the excitation. As seen from this Figure, the uplift displacements at joints 4 & 5 happen primarily together indicating free-flight response. Therefore, it is concluded that subject to these high ground motions, the transporter is not susceptible to rocking because of its low CG height to width ratio.

In Figures 5.1 through 5.13 they following notations are used in the plots:

Joint 4:	Sliding displacement at Joint 4 along X axis (Transverse direction)
Joint 4-1:	Sliding displacement at Joint 4 along Y axis (Longitudinal direction)
Joint 4-2:	Uplift displacement at Joint 4 along Z axis (Up direction)
Joint 5:	Uplift displacement at Joint 5 along Z axis (Up direction)

5.2 6% Grade Analyses Results

For the 6% model, 10 cases were run. These correspond to the 5 TH sets, once with the fault normal component of the motion aligned along the longitudinal direction, and the second time with the fault parallel component aligned along the longitudinal direction. The same sign convention was applied consistently for all 10 analyses cases, stated below:

a. The "+" longitudinal motion was applied along -X meaning down-slope of 6% grade.
b. The "+" transverse motion was applied along +Y meaning up-slope of 2% grade.

The reason for this alignment of signs is that based on the flat surface analyses cases, each of the five Fault Parallel and five Fault Normal time histories used produce a preferred plus or minus direction of sliding as can be seen in Figures 5.1 through 5.5. Direction of preferred sliding is defined as the direction of large initial sliding displacement. Based on this definition, this preferred direction of sliding for all 5 sets is shown here in Table 5.3.

Time History Set	Fault Parallel	Fault Normal
1	+	-
2a	-	-
3	-	+
5	+	+
6	+	+

Table 5.3: Preferred Sliding Direction on Flat Surface

This sign convention ensures that for example, for all "N" cases, where fault normal component is applied along longitudinal direction, 3 of the 5 cases would tend to produce preferred sliding downslope of longitudinal and also upslope of transverse direction. The same sign convention is maintained for all the "P" cases, except that the 2 horizontal components of input motion are inter-changed. The downslope sliding results are significantly affected by whether the preferred sliding direction is placed downslope or upslope. The main objective of the sliding study on grade is twofold:

1. To estimate, the "conservative biased mean" of sliding downslope of longitudinal direction

2. To estimate, the "conservative biased mean" of sliding upslope of transverse direction, since this is the direction facing the open side of the road

Therefore, by aligning the signs as described above (since 3 out of 5, or 60% of the cases are aligned favorably), the analyses cases will produce conservative bias means (or best estimates) along downslope in the longitudinal direction and along upslope in the transverse direction. By the same argument, the results will produce unconservative bias means along the upslope in the longitudinal direction, and downslope along the transverse direction, however it is noted that these 2 directions are of no interest in this study.

Figures 5.14 through 5.23 show the sliding displacement plots for these 10 cases. Each plot contains the longitudinal and the transverse sliding displacements. These are X & Y output plots. Also plotted are Z direction plots. Because of the 6% grade, the Z direction plot represents the vertical component of the sliding displacement of the transporter as it slides down slope of the 6% grade. This value does not represent the actual uplift of the transporter. The actual uplift is calculated and discussed separately. The following convention applies for these plots:

Joint 4: Sliding displacement at base node along X axis (Longitudinal direction)
Joint 4-1: Sliding displacement at base node along Y axis (Transverse direction)
Joint 4-2: Component of sliding displacement at base node along Z axis (Up direction)

Table 5.4 below provides a summary of maximum (both positive and negative) sliding displacements for the 2 orthogonal directions (longitudinal and transverse), for all the analyses cases performed on the 6% grade (7 through 16). The following sign convention applies:

a. Positive longitudinal is max. along upslope for 6% grade
b. Positive transverse is max. along upslope for 2% grade

Analysis Case	T/H Set	COF	Peak Longitudinal Displacement (in)	Peak Transverse Displacement (in)
7	1N	0.4	-50.7/+18.5	-7.1/+35.2
8	2aN	0.4	-78.0/+21.3	-34.5/+0.1
9	3N	0.4	-113.9/+2.8	-35.2/+5.2
10	5N	0.4	-162.7/+7.4	-4.1/+23.2
11	6N	0.4	-83.5/+2.9	-3.0/+45.8
Average "N" Cases			**-97.8/+10.6**	**-16.8/+21.9**
12	1P	0.4	-104.9/+1.7	-53.7/+6.8
13	2aP	0.4	-14.8/+19.7	-25.9/+14.1
14	3P	0.4	-68.9/+14.7	-5.7/+41.7
15	5P	0.4	-106.4/+0.2	-11.8/+56.2
16	6P	0.4	-77.4/+7.7	-4.4/+52.6
Average "P" Cases			**-74.5/+7.7**	**-20.3/+34.3**

Table 5.4: Summary of Maximum Sliding Displacements for 6% Grade Cases

The average of the each of these 5 cases represent a biased conservative estimate of the mean of the sliding displacements for that particular set (N or P) along either the downslope for the longitudinal or upslope along the transverse directions, respectively. To arrive at the biased conservative best estimate of sliding displacements for the case of transporter on 6% grade, the highest of the two sets of best estimates is conservatively taken, rather than average of all 10 cases. This results in 97.8" of sliding displacement down slope of the 6% grade along the longitudinal direction, and +34.3" along the upslope of the 2% transverse grade of the road.

The values reported in Table 5.4 for upslope sliding displacements along the longitudinal direction (10.6") and downslope sliding displacements along transverse direction (20.3") are biased unconservative, because of alignment of the signs of the input time histories as discussed earlier. These values are ignored, since sliding displacements in these 2 directions are of no interest.

Notes:

1. The average of longitudinal displacements reported of 97.8" is along the X direction of the model. To arrive at downslope sliding displacement along the longitudinal axis of the road, this value must be divided by Cos 3.434 degrees (6% slope) arriving at a sliding displacement along the grade of 97.8/Cos 3.434o = 98.0". This correction for the 2% slope results in the same numbers reported along the Y axis of the model, since Cos 1.1458 = 1.0.

2. The uplift displacements are not reported, since as the transporter slides downslope, this results in a negative Z movement as well (because of the 6% slope) which is typically higher than the uplift displacement due to free flight. The actual uplift displacements due to free-flight mode of response are expected to be very similar to those on the flat surface, due to the very slight slope of the grade. This is checked for one case of 2a, which had resulted in the highest uplift for the flat model. The net uplift displacements are calculated as follows:

Net Uplift = $\delta Z - \delta X$ (Tan 3.434) - δY (Tan 1.146) – Ignoring the very small contribution

Where:

δZ = Vertical displacement calculated by the program for 6% grade
δX = Global X axis (longitudinal) displacement calculated by the program for 6% grade

Figure 5.24 shows the net uplift plot for case 2aN. As seen from this Figure, max. uplift displacement (separation from road surface for the 6% grade) is 0.51" compared to 0.53" for the corresponding flat surface case. The slight difference is attributed to the slight 6% grade. The shape of the uplift pattern is very similar between the two cases of 6% grade and Flat (See Figure 5.24 versus Figure 5.8). As such it is concluded that the uplift due to free-flight response is very close for 6% grade vs. the flat surface due to the fact that the uplift is due to vertical component only, and that the slope is quite small.

Figures 5.14 through 5.23 show the sliding displacement for the 10-downslope analyses cases. In these Figures, the following notations are used in the plots:

Joint 4: Sliding displacement at Joint 4 along X axis (Longitudinal direction)
Joint 4-1: Sliding displacement at Joint 4 along Y axis (Transverse direction)
Joint 4-2: Uplift displacement at Joint 4 along Z axis (Up direction)

5.3 *8.5% Grade Analysis Results*

Based on the 6% grade analysis results, case 5N resulted in highest longitudinal sliding displacement downslope, whereas case 5P resulted in highest transverse sliding displacement upslope (see Table 5.4). These 2 cases are run for the 8.5% grade model. Table 5.5 below summarizes the results:

Analysis Case	T/H Set	COF	Peak Longitudinal Displacement (in)	Peak Transverse Displacement (in)
17	5N	0.4	-208.0/+6.0	-4.0/+25.5
18	5P	0.4	-141.0/+0.1	-11.7/+58.2

Table 5.5: Summary of Maximum Sliding Displacements for 8.5% Grade Cases

Comparing the results from Table 5.4 to Table 5.5, the max. longitudinal sliding displacement increases from 162.7" to 208.0" (28% increase), when the grade of the road is increased from 6% to 8.5%. Max. transverse sliding displacement increases from 56.2" to 58.2" (3.6% increase). This slight change in transverse sliding is expected since the longitudinal sliding changes, because of the larger grade, thus resulting in a different net vector sliding which would slightly affect the transverse sliding, even though the transverse grade is kept constant at 2%.

It is noted that the reported sliding displacements for the 2 cases ran are expected to be the max. sliding displacements in the longitudinal and transverse directions. The "best estimate" values are expected to be less if all 5 sets of T/H cases were to be run and results are averaged.

Figures 5.25 and 5.26 show the sliding displacement plots for these 2 analyses cases for the 8.5% grade model.

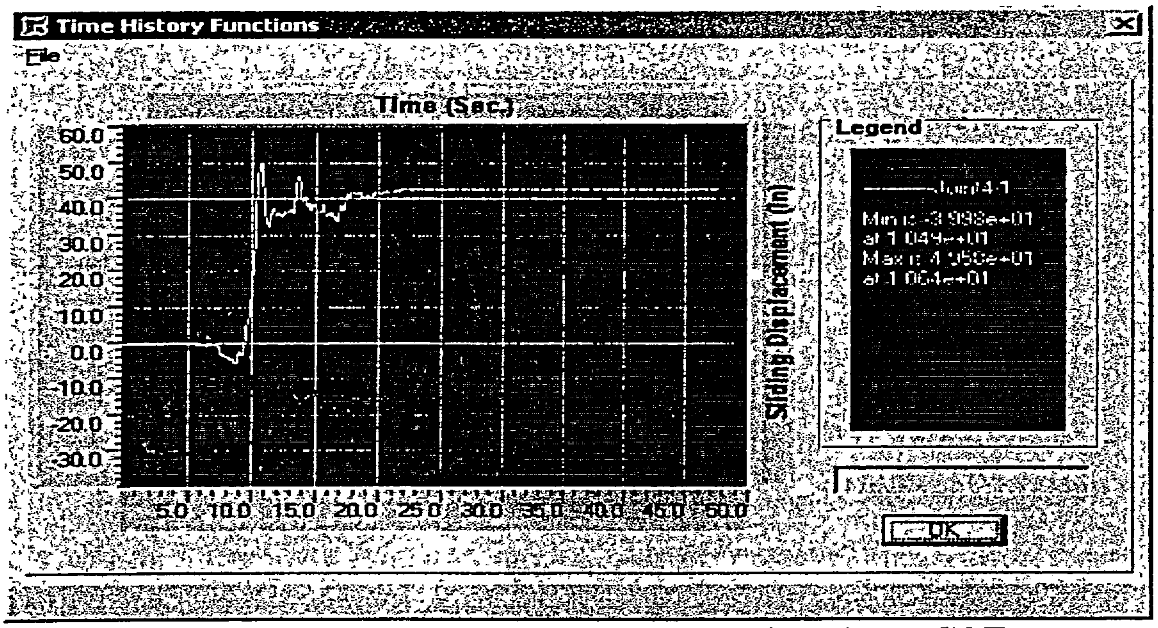

Figure 5.1: Sliding Displacements for Flat Surface, Set 1, COF=0.4

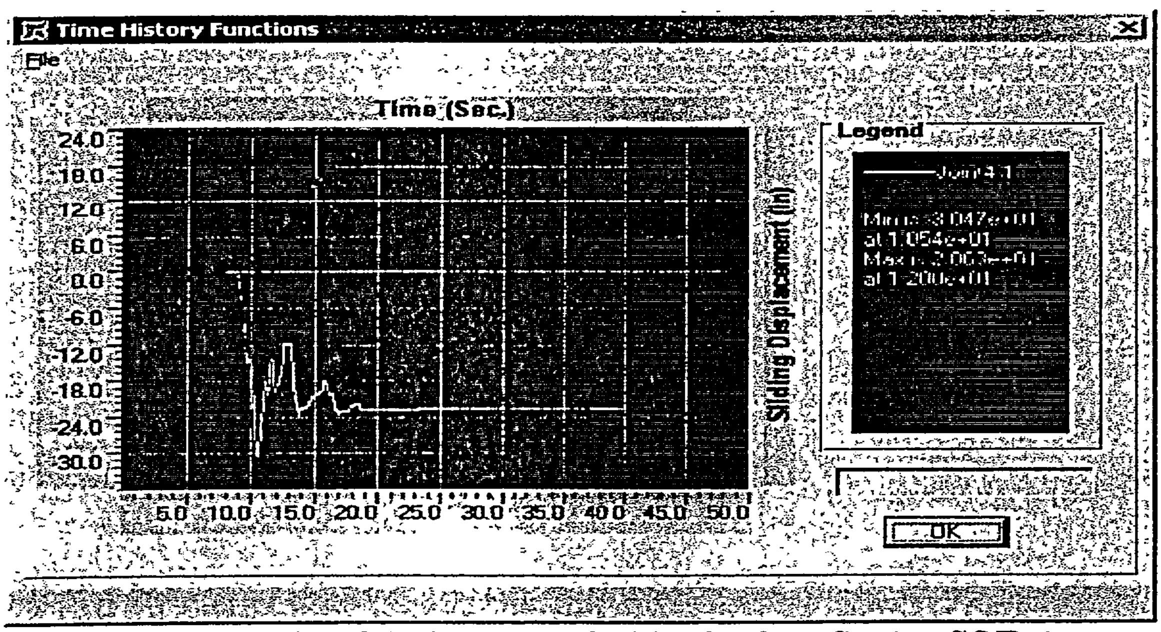

Figure 5.2: Sliding Displacements for Flat Surface, Set 2a, COF=0.4

ENOVA

Engineering Services

CALCULATION SHEET

CALCULATION NUMBER: 0104-021-C01	PROJECT NUMBER: 0104-021
CALCULATION TITLE: SEISMIC STABILITY ANALYSIS OF TRANSPORTER ON SOIL	

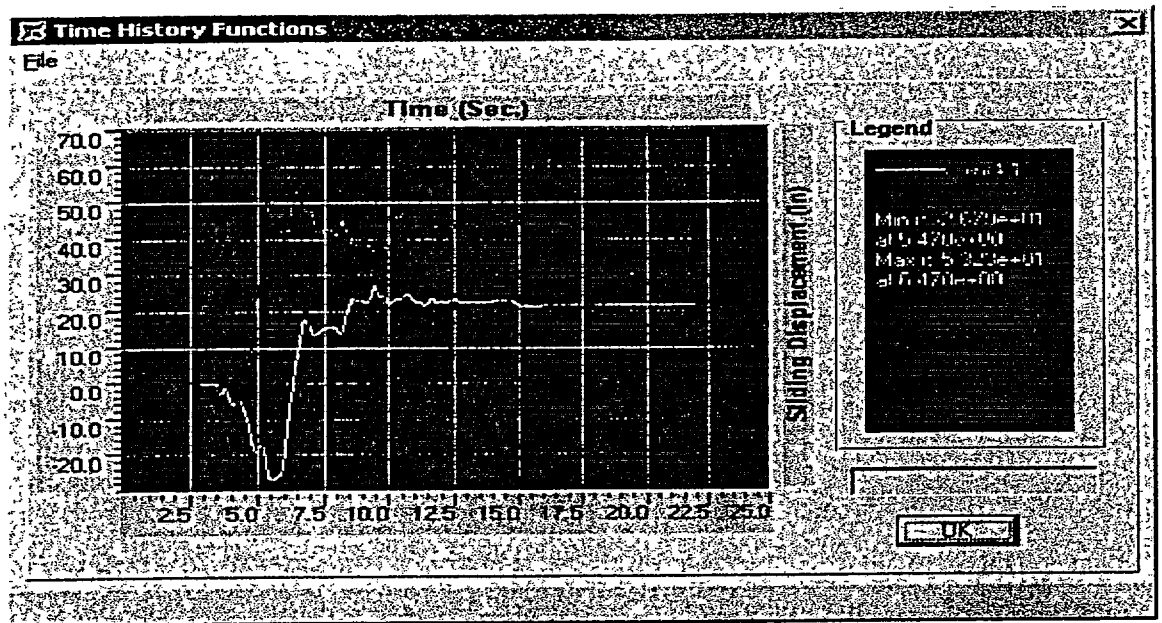

Figure 5.3: Sliding Displacements for Flat Surface, Set 3, COF=0.4

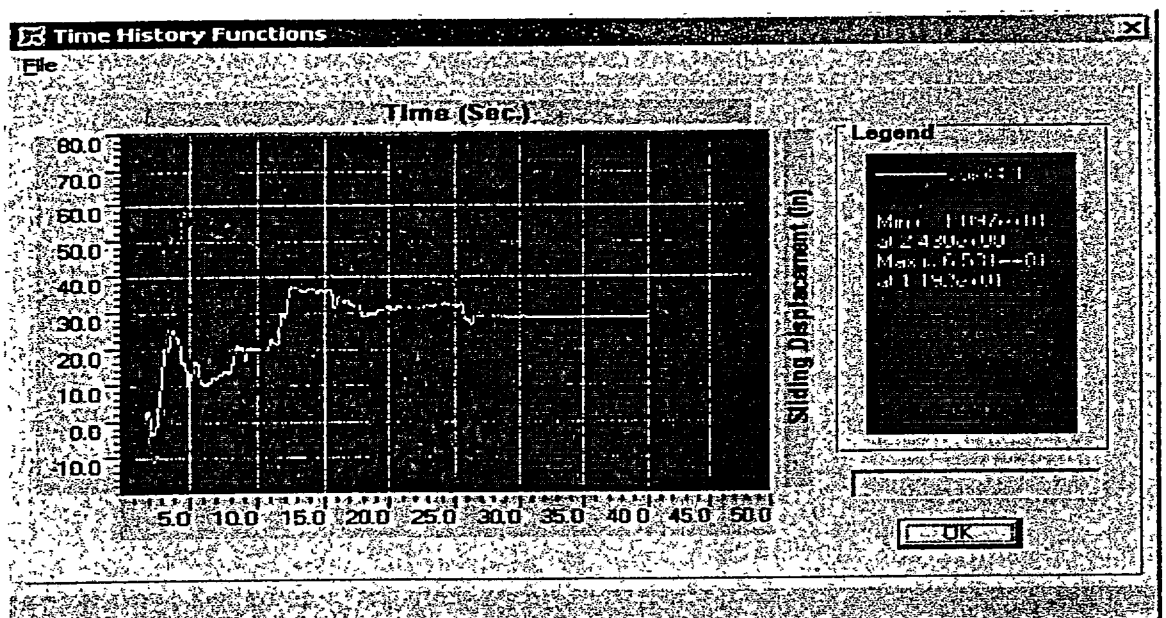

Figure 5.4: Sliding Displacements for Flat Surface, Set 5, COF=0.4

0	SE	9/17/02	TYW	9/22/02					
Rev.	Originator	Date	Checker	Date	Rev.	Originator	Date	Checker	Date

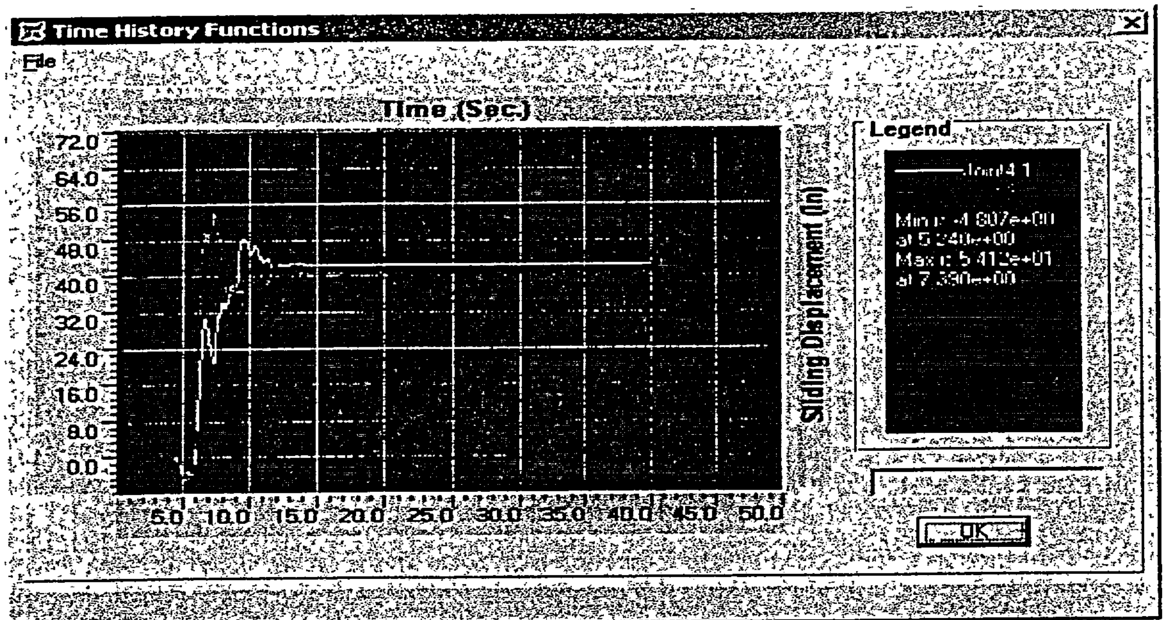

Figure 5.5: Sliding Displacements for Flat Surface, Set 6, COF=0.4

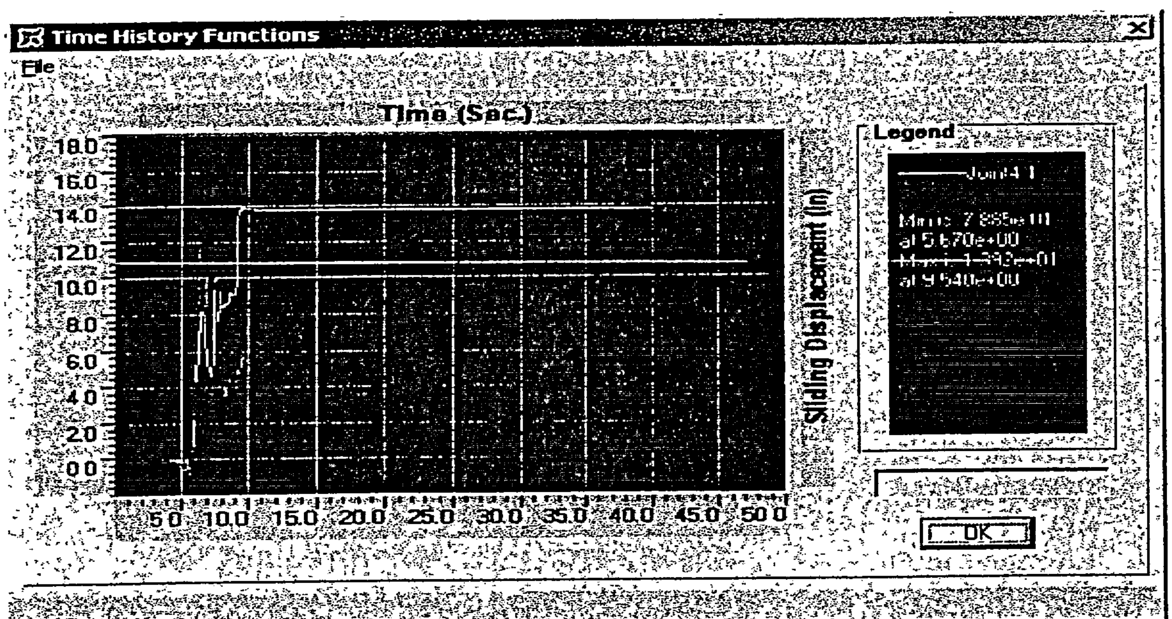

Figure 5.6: Sliding Displacements for Flat Surface, Set 6, COF=0.8

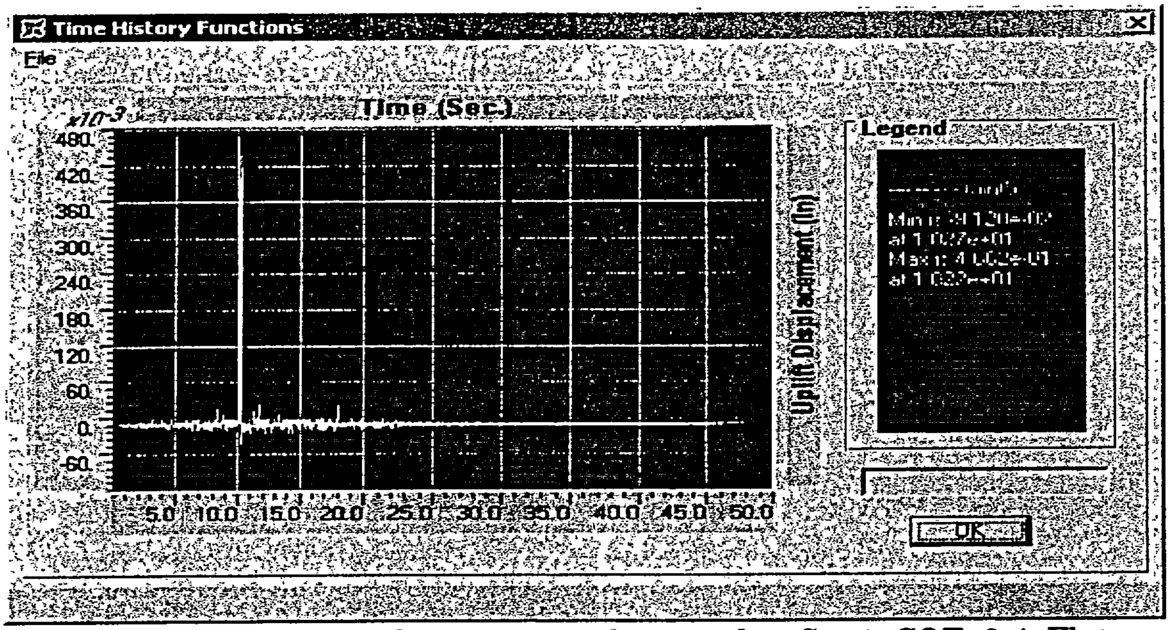

Figure 5.7: Uplift Displacements at base nodes, Set 1, COF=0.4, Flat

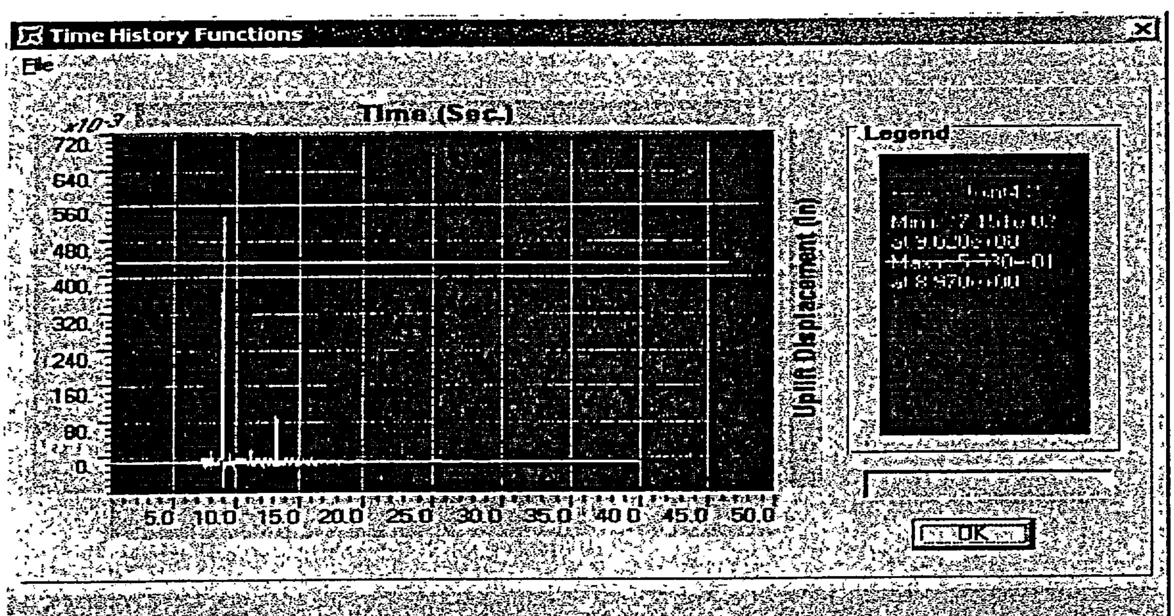

Figure 5.8: Uplift Displacements at base nodes, Set 2a, COF=0.4, Flat

ENOVA

Engineering Services

CALCULATION SHEET

CALCULATION NUMBER: 0104-021-C01	PROJECT NUMBER: 0104-021
CALCULATION TITLE: SEISMIC STABILITY ANALYSIS OF TRANSPORTER ON SOIL	

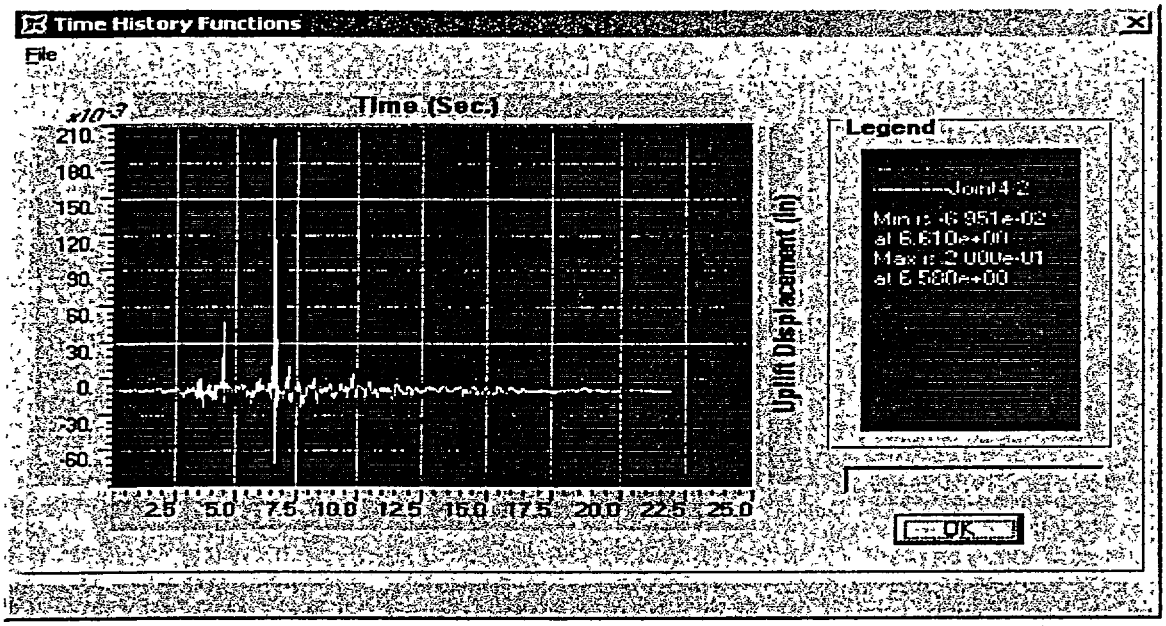

Figure 5.9: Uplift Displacements at base nodes, Set 3, COF=0.4, Flat

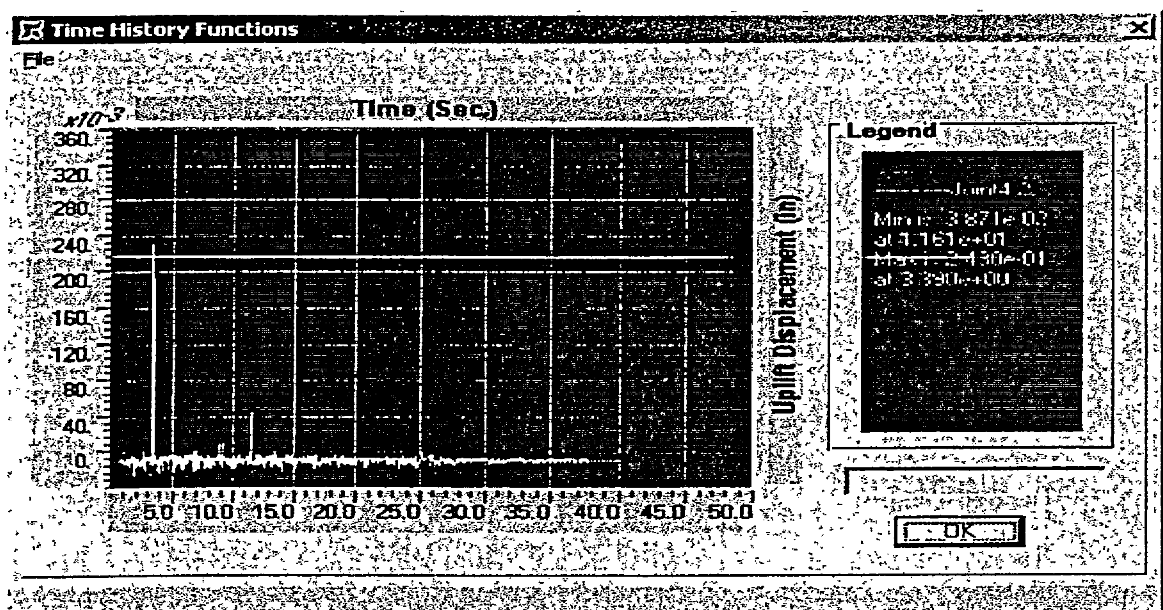

Figure 5.10: Uplift Displacements at base nodes, Set 5, COF=0.4, Flat

0	SE	9/17/02	TYW	9/22/02					
Rev.	Originator	Date	Checker	Date	Rev.	Originator	Date	Checker	Date

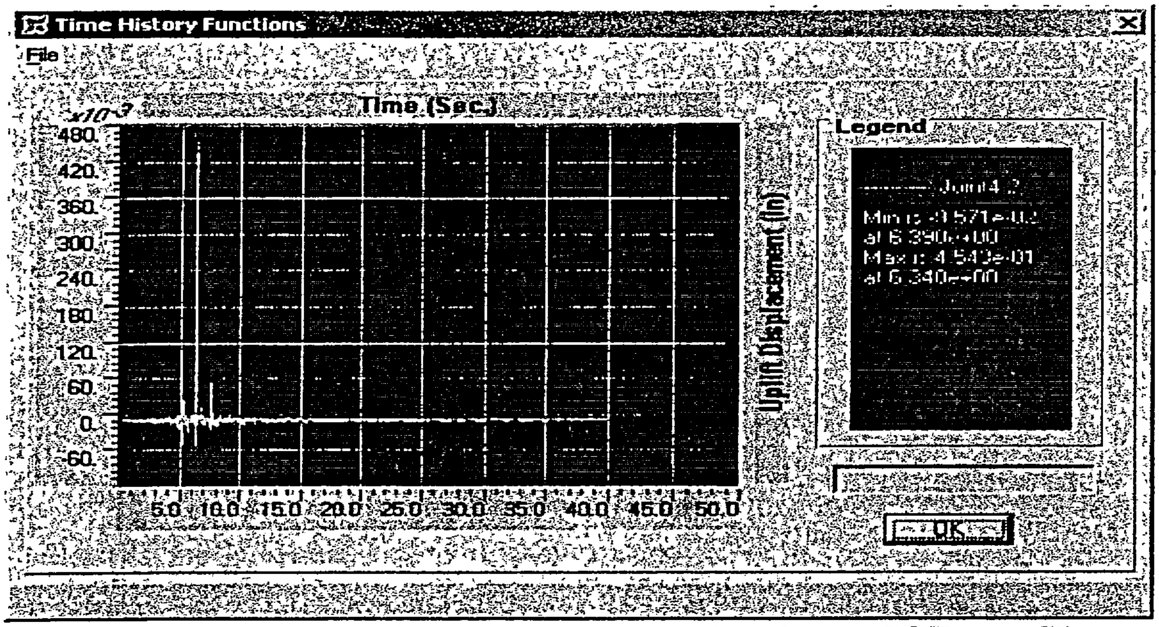

Figure 5.11: Uplift Displacements at base nodes, Set 6, COF=0.4, Flat

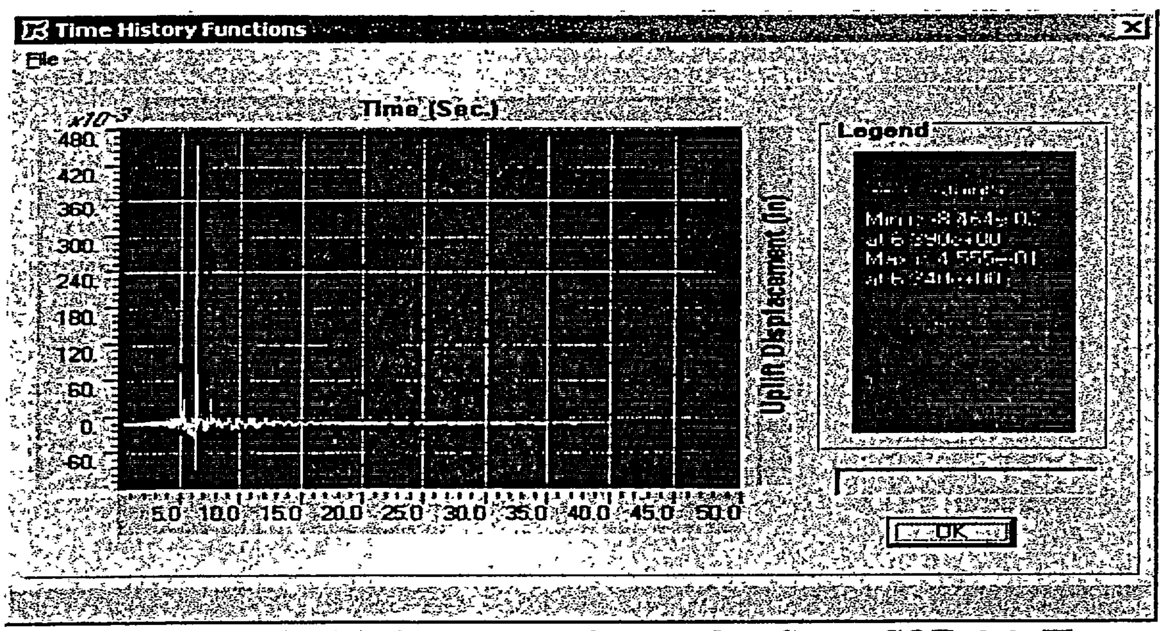

Figure 5.12: Uplift Displacements at base nodes, Set 6, COF=0.8, Flat

CALCULATION NUMBER: 0104-021-C01	PROJECT NUMBER 0104-021
CALCULATION TITLE: SEISMIC STABILITY ANALYSIS OF TRANSPORTER ON SOIL	

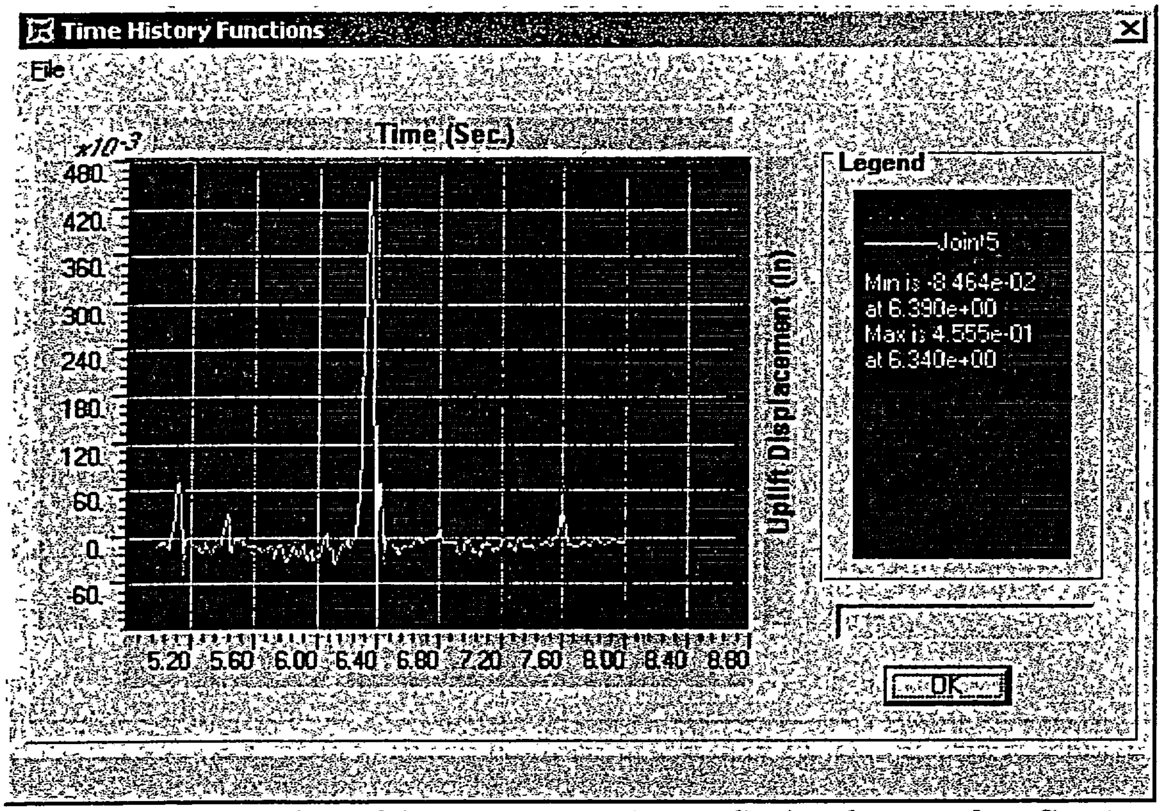

Figure 5.13: Close-up of Uplift Displacements (5<t<8 Sec.) at base nodes, Set 6, u=0.8

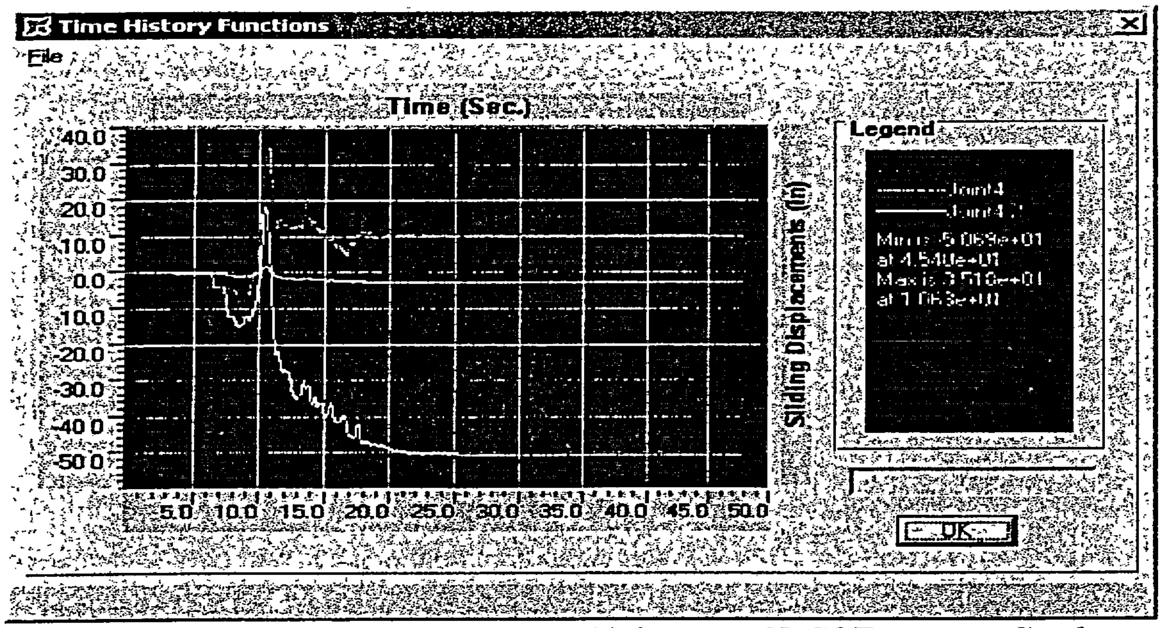

Figure 5.14: Sliding Displacement(s) for case 1N, COF=0.4, 6% Grade

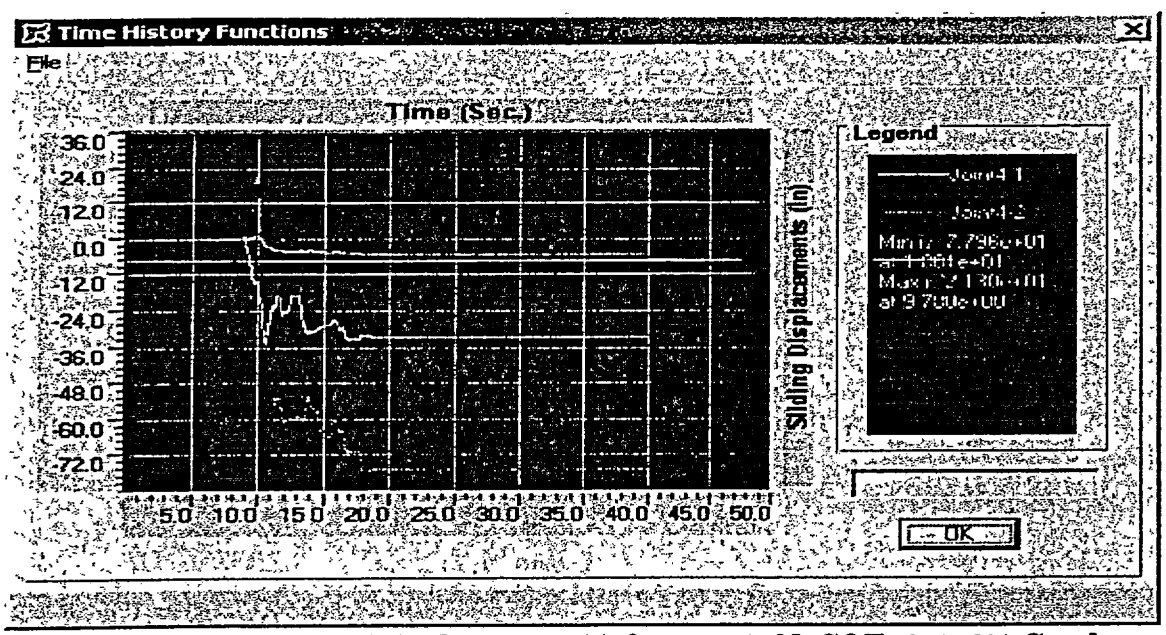

Figure 5.15: Sliding Displacement(s) for case 2aN, COF=0.4, 6% Grade

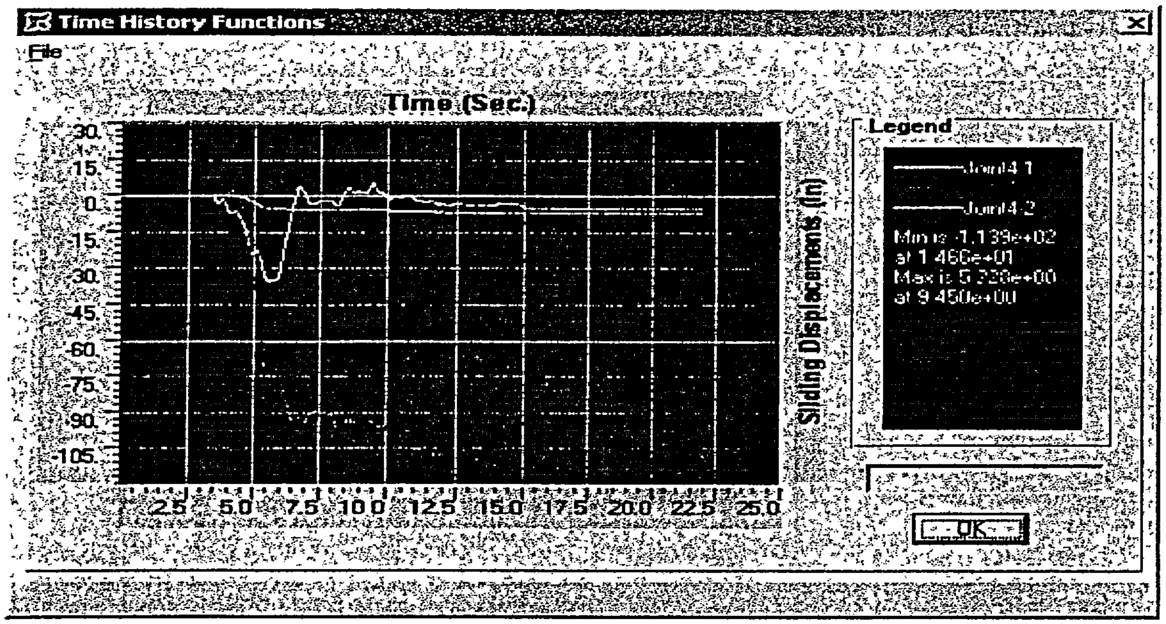

Figure 5.16: Sliding Displacement(s) for case 3N, COF=0.4, 6% Grade

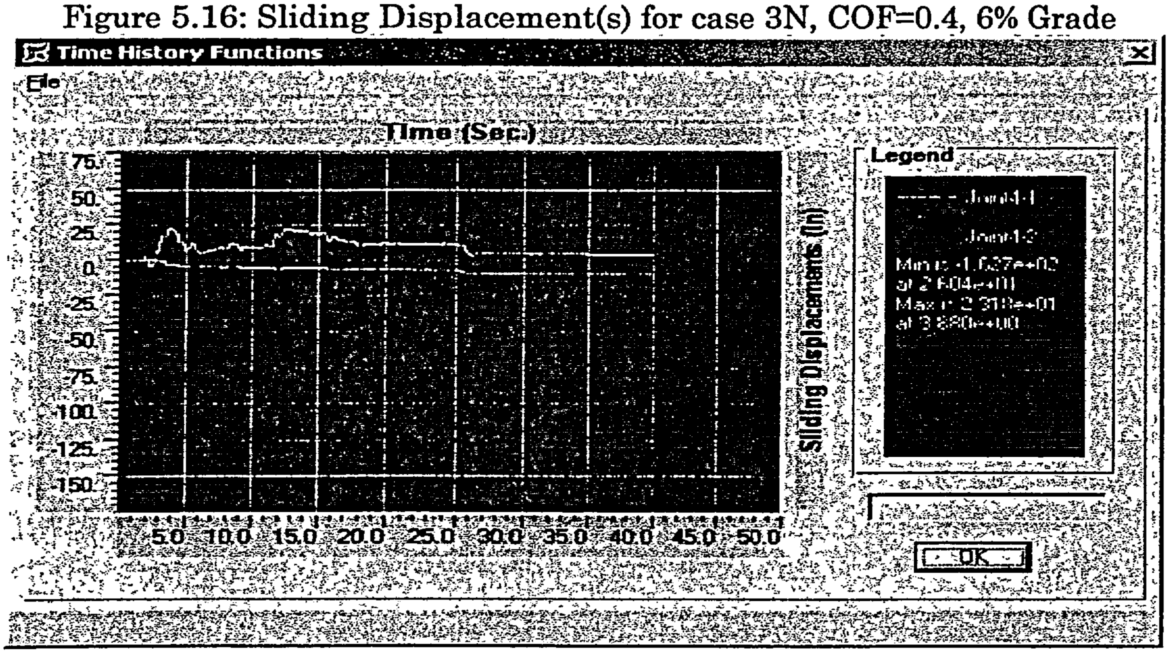

Figure 5.17: Sliding Displacement(s) for case 5N, COF=0.4, 6% Grade

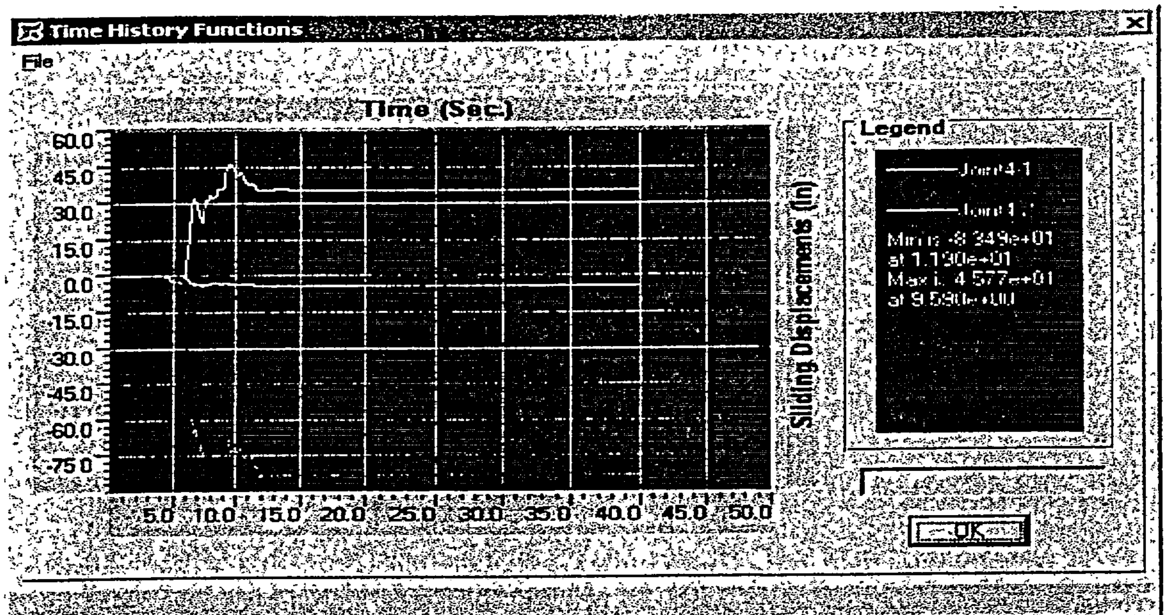

Figure 5.18: Sliding Displacement(s) for case 6N, COF=0.4, 6% Grade

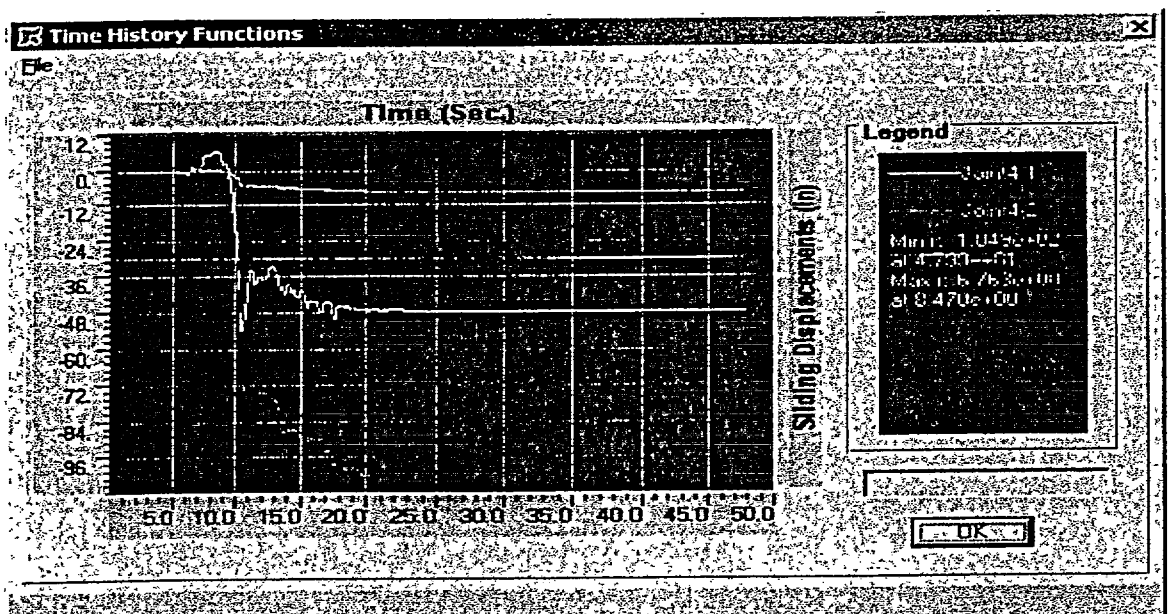

Figure 5.19: Sliding Displacement(s) for case 1P, COF=0.4, 6% Grade

ENOVA

Engineering Services

CALCULATION SHEET

CALCULATION NUMBER:	0104-021-C01	PROJECT NUMBER:	0104-021
CALCULATION TITLE:	SEISMIC STABILITY ANALYSIS OF TRANSPORTER ON SOIL		

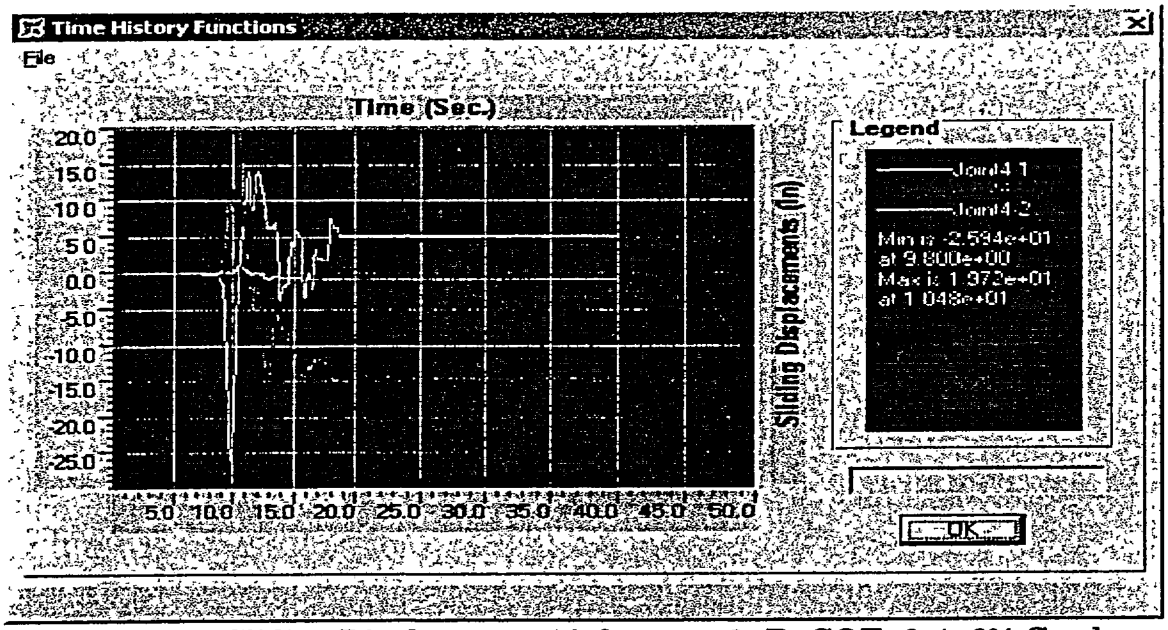

Figure 5.20: Sliding Displacement(s) for case 2aP, COF=0.4, 6% Grade

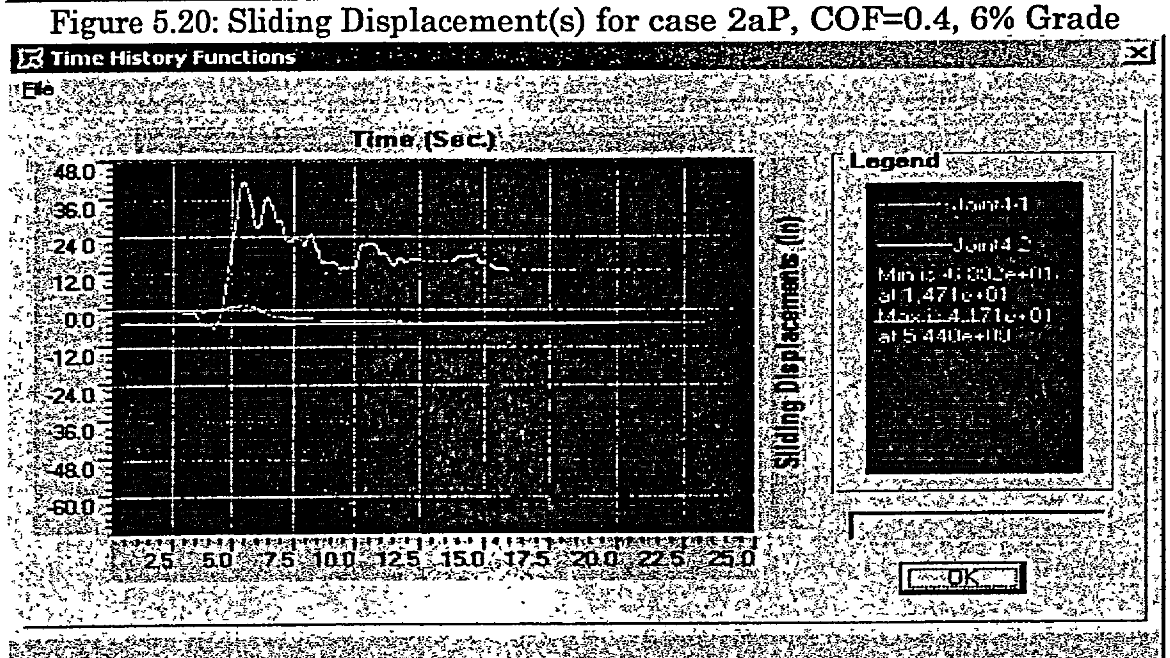

Figure 5.21: Sliding Displacement(s) for case 3P, COF=0.4, 6% Grade

0	SE	9/17/02	TYW	9/22/02					
Rev.	Originator	Date	Checker	Date	Rev.	Originator	Date	Checker	Date

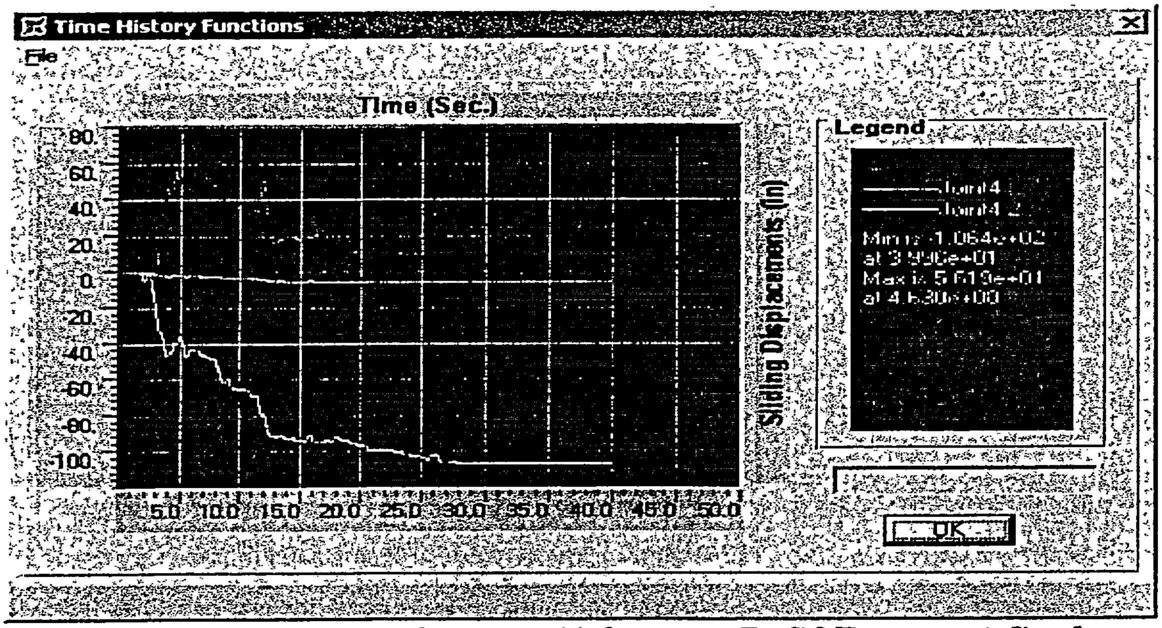

Figure 5.22: Sliding Displacement(s) for case 5P, COF=0.4, 6% Grade

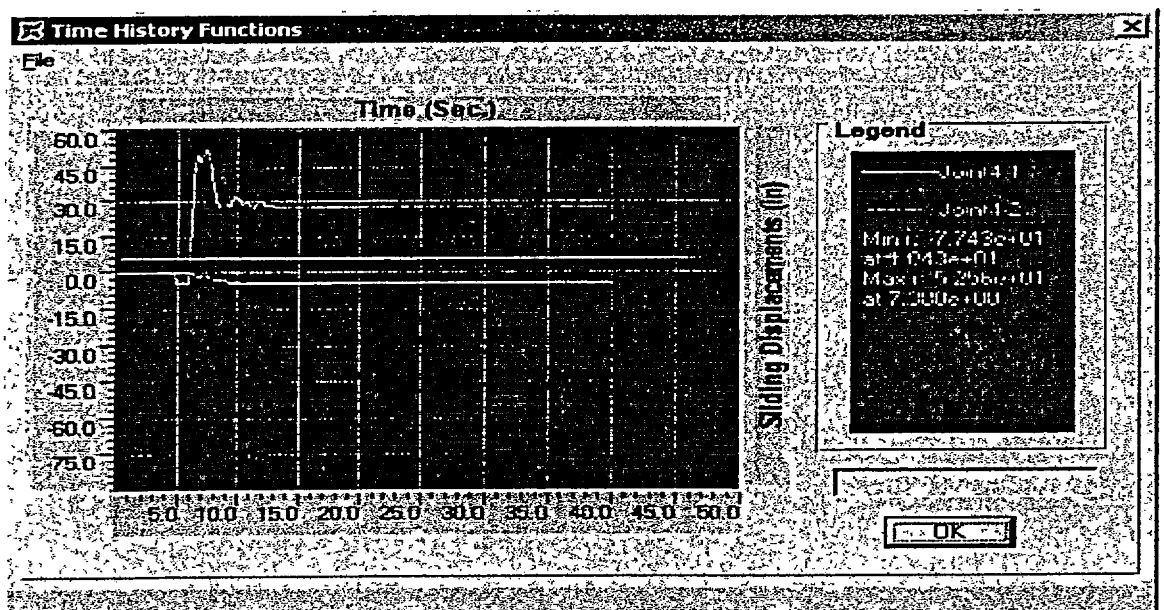

Figure 5.23: Sliding Displacement(s) for case 6P, COF=0.4, 6% Grade

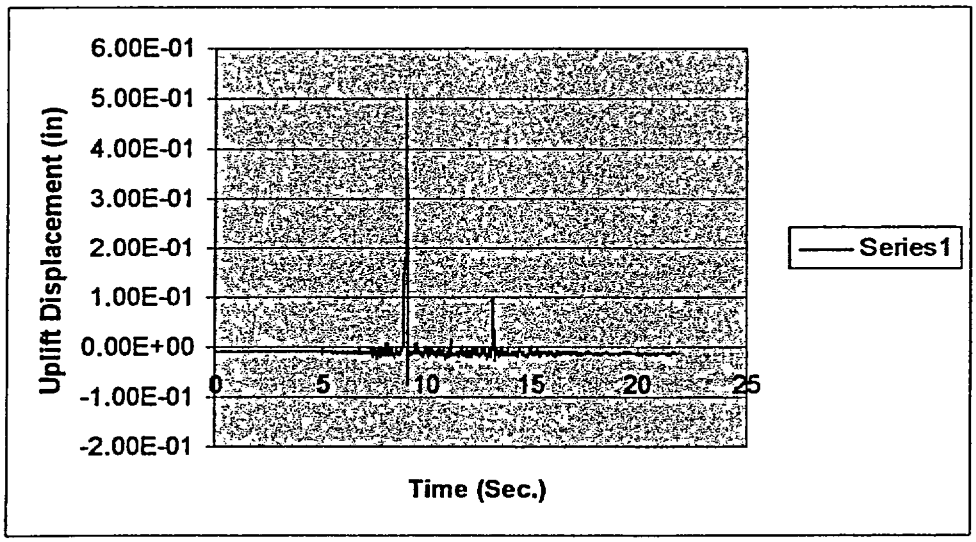

Figure 5.24: Net Uplift for Case 2aN, COF=0.4, 6% Grade

ENOVA

Engineering Services

CALCULATION SHEET

CALCULATION NUMBER: 0104-021-C01	PROJECT NUMBER: 0104-021
CALCULATION TITLE: SEISMIC STABILITY ANALYSIS OF TRANSPORTER ON SOIL	

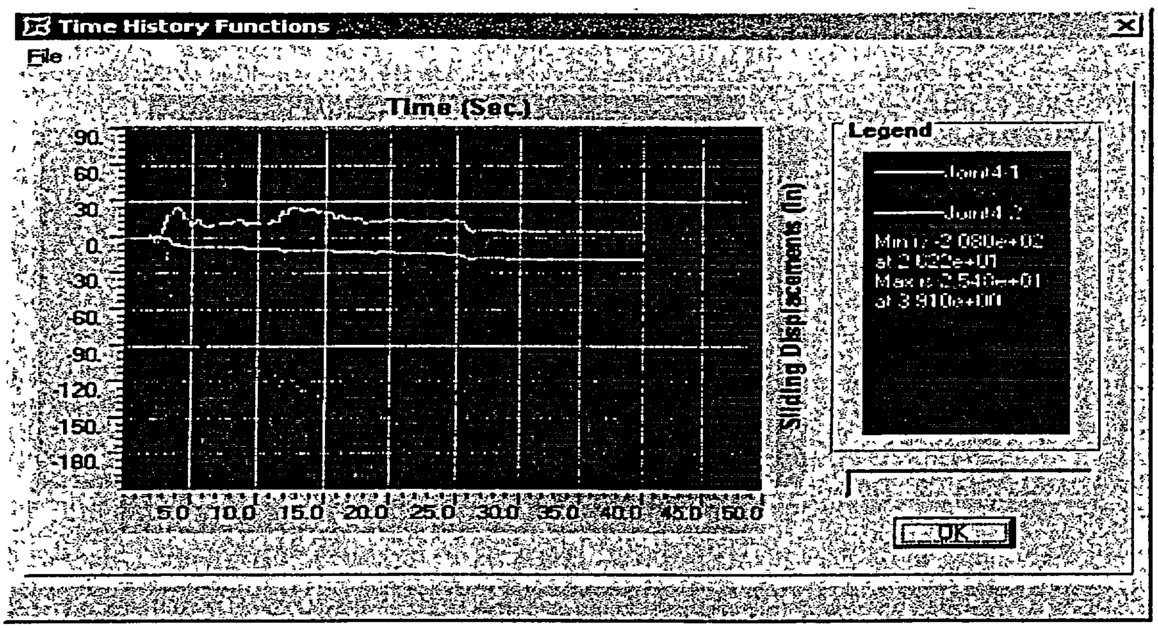

Figure 5.25: Sliding Displacement(s) for case 5N, COF=0.4, 8.5% Grade

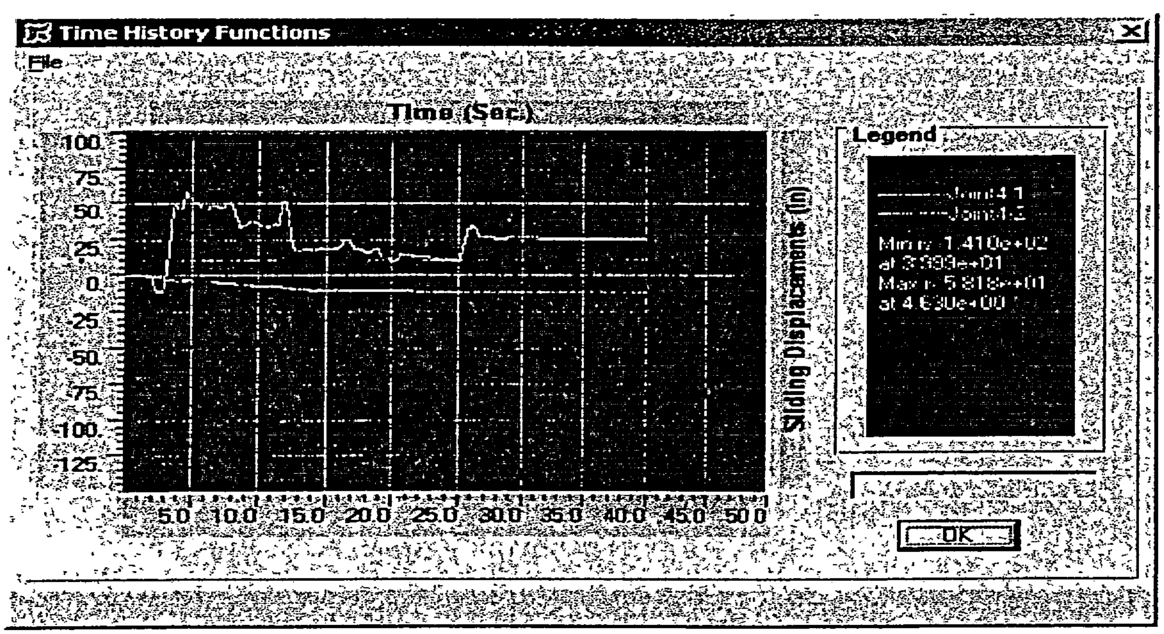

Figure 5.26: Sliding Displacement(s) for case 5P, COF=0.4, 8.5% Grade

0	SE	9/17/02	TYW	9/22/02					
Rev.	Originator	Date	Checker	Date	Rev.	Originator	Date	Checker	Date

6.0 CONCLUSIONS

The following conclusions are arrived at regarding stability of the DCPP transporter carrying the HI-TRAC in horizontal orientation subject to a hypothetical seismic event representing conservative amplification of ground motions along the transporter route. The estimates sliding displacements are based on a dynamic COF of 0.4 between the transporter track and the road surface. The rocking analysis was done using a dynamic COF of 0.8 to maximize potential for rocking.

The conclusions are:

1. The DCPP transporter is not susceptible to rigid body rocking due to its low CG height to width ratio.
2. The vertical component of motion having a PGA of (1.44g avg.) which is higher than 1g gravity results in free-flight of the transporter. The best estimate of peak free-flight uplift displacement is 0.38".
3. The best estimate of sliding displacement on flat surface is 48.0".
4. The conservatively biased best estimate of sliding displacement downslope on a 6% longitudinal grade is 97.8", whereas the estimated max. sliding displacement downslope on a 6% grade is 162.7" corresponding to T/H set 5N.
5. The conservatively biased best estimate of sliding displacement upslope of a 2% transverse grade on a 6% grade road is 34.3", whereas the estimated max. sliding displacement upslope on a 2% grade is 56.2" corresponding to T/H set 5P.
6. The estimated maximum sliding displacement down slope on an 8.5% longitudinal grade is 208.0".
7. The estimated maximum sliding displacement upslope of a 2% transverse grade on an 8.5% grade road is 58.2".

Tables 5.2, 5.4, and 5.5 provide the individual sliding displacements for all analyses cases for the flat road, 6% longitudinal grade, and 8.5% longitudinal grade portions of the road respectively.

7.0 REFERENCES

1. "Transporter Stability on Diablo Canyon Dry Storage Travel Path", Holtec Report No. HI-2012768, Rev. 2, 11/14/01.
2. PG&E letter to ENOVA dated 4/17/02, Subject: Diablo Canyon Used Fuel Storage Project – Diablo Canyon Units 1 & 2, Analysis Inputs Transmittal for CWA 2002PR0150.
3. CWA 2002PR0150 – Specification for performing transporter stability analysis subject to soil motions, 4/16/02.
4. PG&E letter to ENOVA dated 11/2/01, Subject: Diablo Canyon Used Fuel Storage Project – Diablo Canyon Units 1 & 2, Non-linear Sliding Analysis of the ISFSI Mat at DCPP.
5. Computers & Structures, Inc., SAP2000 Analysis Reference Manual.
6. "Development of Coefficient of Subgrade Reaction for DCPP ISFSI Pad Stability Checks (GeoSciences # GEO.DCPP.01.07), PG&E Calculation No. 52.27.100.717, Rev. 0, 11/13/01.
7. PG&E letter to ENOVA dated 5/7/02, Subject: Diablo Canyon Used Fuel Storage Project – Diablo Canyon Units 1 & 2, Analysis Inputs Transmittal for CWA 2002PR0150.
8. USNRC Standard Review Plan, Rev. 2, Part of NUREG 0800.
9. PG&E letter to ENOVA dated 9/17/02, Subject: Diablo Canyon Used Fuel Storage Project – Diablo Canyon Units 1 & 2, Analysis Inputs Transmittal for CWA 2002PR0269.
10. PG&E letter to ENOVA dated 5/31/02, Subject: Diablo Canyon Used Fuel Storage Project – Diablo Canyon Units 1 & 2, Analysis Inputs Transmittal for CWA 2002PR0194.
11. CWA 2002PR0194 –Specification for performing transporter stability analysis subject to soil motions on sloped road, 5/31/02.
12. CWA 2002PR0269 –Specification for performing transporter stability analysis subject to soil motions on sloped road, 7/11/02.

APPENDIX A

COMPUTER RUN USAGE LOG

This Section contains an index of all SAP2000 computer files generated in support of these analyses. The index in page A-2 shows all file names for analyses cases in support of various analyses cases as summarized in Section 5.0 of this Calculation file. The file names correspond to the input file. All other analyses files created by SAP have the same prefix file name and different extensions and are contained on the same folder location.

ENOVA

Engineering Services

COMPUTER RUN USAGE LOG

PROJECT TITLE:	SEISMIC STABILITY ANALYSIS OF TRANSPORTER ON SOIL		CLIENT:	PG&E.
PROJECT NUMBER:	0104-021			
SOFTWARE/VERSION:	RUN IDENTIFIER: FOLDER/FILE	DATE OF RUN:	DESCRIPTION VARIOUS ANALYSIS CASES	ASSOCIATED CALCULATION (INCLUDE REV.)
SAP2000 VERSION 7.10	U=0 4,FLAT,SET1	7/19/02	COF=0 4, SET 1, FLAT SURFACE	0104-021-C01, REV 0
SAP2000 VERSION 7.10	U=0 4,FLAT,SET2A	7/19/02	COF=0 4, SET 2A, FLAT SURFACE	0104-021-C01, REV 0
SAP2000 VERSION 7 10	U=0 4,FLAT,SET3	7/19/02	COF=0 4, SET 3, FLAT SURFACE	0104-021-C01, REV 0
SAP2000 VERSION 7 10	U=0 4,FLAT,SET5	7/19/02	COF=0 4, SET 5, FLAT SURFACE	0104-021-C01, REV 0
SAP2000 VERSION 7 10	U=0 4,FLAT,SET6	7/18/02	COF=0 4, SET 6, FLAT SURFACE	0104-021-C01, REV 0
SAP2000 VERSION 7.10	U=0 8,FLAT,SET6	7/19/02	COF=0.8, SET 6, FLAT SURFACE	0104-021-C01, REV 0
SAP2000 VERSION 7 10	SET1N,U=0.4,6%L,2%T	7/22/02	COF=0 4, SET 1, 6% GRADE LONGITUDINAL, 2% GRADE TRANSVERSE, FAULT NORMAL COMPONENT DOWNSLOPE	0104-021-C01, REV 0
SAP2000 VERSION 7 10	SET2AN,U=0 4,6%L,2%T	7/22/02	COF=0 4, SET 2A, 6% GRADE LONGITUDINAL, 2% GRADE TRANSVERSE, FAULT NORMAL COMPONENT DOWNSLOPE	0104-021-C01, REV 0
SAP2000 VERSION 7 10	SET3N,U=0 4,6%L,2%T	7/22/02	COF=0.4, SET 3, 6% GRADE LONGITUDINAL, 2% GRADE TRANSVERSE, FAULT NORMAL COMPONENT DOWNSLOPE	0104-021-C01, REV 0
SAP2000 VERSION 7 10	SET5N,U=0 4,6%L,2%T	7/22/02	COF=0.4, SET 5, 6% GRADE LONGITUDINAL, 2% GRADE TRANSVERSE, FAULT NORMAL COMPONENT DOWNSLOPE	0104-021-C01, REV 0
SAP2000 VERSION 7 10	SET6N,U=0 4,6%L,2%T	7/22/02	COF=0 4, SET 6, 6% GRADE LONGITUDINAL, 2% GRADE TRANSVERSE, FAULT NORMAL COMPONENT DOWNSLOPE	0104-021-C01, REV 0
SAP2000 VERSION 7 10	SET1P,U=0 4,6%L,2%T	7/22/02	COF=0 4, SET 1, 6% GRADE LONGITUDINAL, 2% GRADE TRANSVERSE, FAULT PARALLEL COMPONENT DOWNSLOPE	0104-021-C01, REV 0
SAP2000 VERSION 7.10	SET2AP,U=0 4,6%L,2%T	7/22/02	COF=0.4, SET 2A, 6% GRADE LONGITUDINAL, 2% GRADE TRANSVERSE, FAULT PARALLEL COMPONENT DOWNSLOPE	0104-021-C01, REV 0
SAP2000 VERSION 7 10	SET3P,U=0 4,6%L,2%T	7/22/02	COF=0 4, SET 3, 6% GRADE LONGITUDINAL, 2% GRADE TRANSVERSE, FAULT PARALLEL COMPONENT DOWNSLOPE	0104-021-C01, REV 0
SAP2000 VERSION 7.10	SET5P,U=0 4,6%L,2%T	7/23/02	COF=0.4, SET 5, 6% GRADE LONGITUDINAL, 2% GRADE TRANSVERSE, FAULT PARALLEL COMPONENT DOWNSLOPE	0104-021-C01, REV 0
SAP2000 VERSION 7 10	SET6P,U=0 4,6%L,2%T	7/23/02	COF=0 4, SET 6, 6% GRADE LONGITUDINAL, 2% GRADE TRANSVERSE, FAULT PARALLEL COMPONENT DOWNSLOPE	0104-021-C01, REV 0

S. Espadin

PROJECT ENGINEER

9/17/02

DATE

ENOVA

Engineering Services

COMPUTER RUN USAGE LOG

PROJECT TITLE:	SEISMIC STABILITY ANALYSIS OF TRANSPORTER ON SOIL		CLIENT:	PG&E
PROJECT NUMBER:	0104-021			
SAP2000 VERSION 7.10	SET5N,U=0.4,8 5%L,2%T	7/23/02	COF=0.4, SET 5, 8 5% GRADE LONGITUDINAL, 2% GRADE TRANSVERSE, FAULT NORMAL COMPONENT DOWNSLOPE	0104-021-C01, REV. 0
SAP2000 VERSION 7.10	SET5P,U=0.4,8 5%L,2%T	7/24/02	COF=0 4, SET 5, 8 5% GRADE LONGITUDINAL, 2% GRADE TRANSVERSE, FAULT PARALLEL COMPONENT DOWNSLOPE	0104-021-C01, REV. 0

S. Eifendi — PROJECT ENGINEER

9/17/02 — DATE

FORM 6B

ATTACHMENT B

Peer Review Comments on Seismic Stability
Analysis of Transporter on Soil

R.P. Kennedy Robert P. Kennedy
September 24, 2002

I have carefully reviewed Rev. 0 dated 9/23/02 of ENOVA Calc. 0104-021-C01 entitled *Seismic Stability Analysis of Transporter on Soil.* This calculation has incorporated all of my comments on earlier drafts. Therefore, I concur with all aspects of this calculation. I have no comments or recommendations for changes.

28625 Mountain Meadow Road, Escondido, CA 92026
(760)751-3510 • (760) 751-3537 (Fax)

ATTACHMENT

2-6

PACIFIC GAS & ELECTRIC COMPANY

PROBABILISTIC RISK ASSESSMENT

CALCULATION FILE NO. **PRA02-10 Revision 0**

SUBJECT: Probabilistic Evaluation of Seismically Induced Cask Drop, Overturn of the Transporter, or Sliding of the Transporter off the Transport Route

PREPARED BY: ______________ DATE: 10/3/02
Amir Afzali

VERIFIED BY: ______________ DATE: 10/3/02
James Young

VERIFIED IN ACCORDANCE WITH: CF3.ID15

APPROVED BY: ______________ DATE: 10/3/02
Amir Afzali

This file contains: 3 pages

RECORD OF REVISIONS

REV. 0 Original calculation.

PURPOSE

The purpose of this calculation file is to provide the basis for asserting that a seismically induced cask drop, during transportation between the nuclear power plant and the Diablo Canyon ISFSI pad, is not credible.

DISCUSSION

As part of the NRC review of the Diablo Canyon ISFSI Safety Analysis Report, the Staff asked PG&E to provide sufficient justification of why a seismic event that may cause cask drop, overturn of the transporter, or sliding of the transporter off the transport route is not credible (RAI2-19). A probabilistic evaluation is performed to provide the required justification.

ASSUMPTIONS AND ASSERTIONS

It is assumed that the transport time for the cask along the transport route is 12 hours.

CALCULATIONS

PG&E has performed a seismic evaluation of cask transporter under ground accelerations of twice the ILP earthquake acceleration. The evaluation demonstrates that the cask transporter would remain stable and would not overturn or leave the roadway (Reference 1).
The objective of the calculation herein is to determine the conditional probability of occurrence of earthquakes with greater than two times the ILP ground motion during the dry cask transport.

Per Reference 2, the extrapolated hazard for a spectral acceleration of two times the ILP ground motion is 1.2E-07/yr. For conservatism, the number was rounded up to 1.5E-07/yr to account for uncertainty in the data extrapolation. Therefore, the annual frequency for earthquakes greater than two times the ILP ground motion is 1.5E-7/yr. The conditional probability is determined by multiplying the frequency by the assumed time of transport (12 hrs.) As a result, the conditional probability of occurrence of earthquakes with greater than two times the ILP ground motion during the dry cask transport is 2.1E-10.

CONCLUSIONS

Comparing the results of this calculation with the Regulatory Guide 1.91 criteria (Reference 3), the risk of damage due to seismically induced cask drop, overturn of the transporter, or sliding of the transporter off the transport route is well below 1.0E-6 threshold and is considered insignificant.

REFERENCES

1. Response to RAI 2-19 of Diablo Canyon ISFSI Safety Analysis Report, Dated October 2002.

2. PG&E Letter from Norm Abrahamson to R. Klimczak, "Return Period for Two Times the ILP Ground Motion" in Response to AR A0564589.

3. "Regulatory Guide 1.91, "Evaluation of Explosions Postulated to Occur On Transportation Routes Near Nuclear Power Plants," February 1978.

ATTACHMENT

2-7

WLA

BORING LOG

Field	Entry
Project	DCPP Patton Cove Landslide
Job No	1223-48
Boring No.	PC-1
Boring Location	
Type & Diameter of Boring	Mud Rotary, Tricone Bit, 4"/HQ core
Elevation @ Top of Hole / Total Depth	TBD/130'
Sampling Method	SPT and ModCal SplitSpoon Samplers to 57'/HQcore to depth
Sample Driving Hammer and Drop	140lb/30" drop cathead/rope
Drilling Contractor and Rig	All Terrain Exploration Drilling/Failing 1500
Date Started	20 Nov 2000
Date Completed	22 Nov 2000
Depth to groundwater	N.D.
Logged By	CMB
Notes	redrafted from original for clarity 11/02

SPT N (60): 0 10 20 30 40 50 60

Uncorrected Blows per 6-inch drive	Depth (feet)	Soil Type (USCS)	Sampler Type	Recovery (inches)	Pocket Pen. (TSF)	Shear Torvane (TSF)	Description	Remarks
18, 28, 36	5–6.5		2.5-inch O.D. split spoon	18"	4.0		Gravelly CLAY ( ), color various dark brown (eg 7.5YR3/1) to black (7.5 YR2.5/1); very stiff to hard; damp; common to abundant subrounded, subangular, angular clasts to 4"; clasts are sandstone, dolomite, limestone; coarse ~20-30% color inconsistent w/ crude layering: (FILL)	gravel
20, 36, 32	10–11.5		2.5-inch O.D. split spoon	15"			Similar to above; angular clasts to 1.0"	
12, 16, 14	11.5–13			11"	3.75-4.0			

Depth (feet): 0 1 2 3 4 5 6 7 8 9 10 11 12 13 14 15

Fill

? ? ? ? (at 14 ft)

Native colluvium/fan deposits

3.0-inch O.D. split spoon sampler | 2.5-inch O.D. split spoon sampler | Standard Penetration Test (SPT) sampler

WLA

BORING LOG

Project	Job No	Boring No
DCPP Patton Cove Q_{ls}		PC-1

SPT N_1(60) 0 10 20 30 40 50 60

Uncorrected Blows per 6-inch drive	Depth (feet)	Soil Type (USCS)	Sampler Type	Recovery (inches)	Pocket Pen (TSF)	Shear Torvane (TSF)	Description	Remarks
6, 10, 10	15–16.5			11"	1.5		CLAY w/ Gravel; (<15% gravel) color very dark grey (10 YR3/1); similar to above but more consistent color; damp, stiff to very stiff; clasts are angular, up to 1.5", of dolomite, sandstone; clay is med. plasticity, medium toughness. (Colluvium/Fan Deposit - Holocene)	sample w/ no losses
4, 6, 7	16.5–18			10"			gravel clasts are oxidized, highly weathered | red + tan color, white carbonate stringers (soil development)	Samples - 11:10
	19						— — ? — — — ? — — — ? — —	
15, 30, 32	20–21.5			15"	4.5-refusal		Sandy CLAY ( ): brown (7.5 YR5/4); very stiff to hard; damp, sand is very fine grained, well sorted; some silt; occasional gravels to ~0.75", subangular; fines are low-med plasticity; med. toughness. (Old Colluvium/Fan Deposits - Pleistocene)	
15, 18, 25	21.5–23			16"				Sample 11:30
8, 12, 18	25–26.5			15"	3.5-4.5		similar to above	Samples 11:45
4, 5, 9	26.5–28			17"				
	28.5							driller reports harder material @ 28.5'
6, 7, 10	30–31.5			14"	2.5-3.5		similar to above, more moist (w/ capillary zone above water table?)	
	32							

3.0-inch O.D. split spoon sampler | 2.5-inch I.D. split spoon sampler | Standard Penetration Test (SPT) sampler

WLA

BORING LOG

Project	Job No	Boring No
DCPP Patton Cove Q_{cs}		PC-1

SPT $N_1(60)$: 0 10 20 30 40 50 60

Uncorrected Blows per 6-inch drive	Depth (feet)	Soil Type (USCS)	Sampler Type	Recovery (inches)	Pocket Pen. (TSF)	Shear Torvane (TSF)	Description	Remarks
6 8 8	32–33			18"			Similar to above; grades to brown (10YR 4/3); grades less sand, more silty	
	33–35						Grades siltier	
7 13 11	35–36.5			7"	2.5-3.0			Samples @ 12:30
5 6 9	36.5–38			4"			Similar to above; large dolomite clast (2") in shoe; continued siltier, less sandy	
	39							
20 13 13	40–41.5			13"	2.0-2.5		Similar to above. Silty CLAY ( ); brown (10YR 4/3); damp, stiff to very stiff; high plasticity, med. toughness; angular clasts of dolomite to 0.5", occasionally to 1"; few clasts of reddish sandstone; high dry strength; coarse component ~5% (Old Fan Deposit/Colluvium - Pleistocene)	40' Driller reports hard drilling Samples @ 12:50
6 7 8	41.5–43			17"				
	44							
6 12 18	45–46.5			15"	3.75-4.0		same as above	
6 10 10	46.5–48			18"				samples 13:20-13:30
	49							

3.0-inch O.D. split spoon sampler; 2.5-inch I.D. split spoon sampler; Standard Penetration Test (SPT) sampler

WLA

BORING LOG

Project	Job No	Boring No
DCPP Pattern Cove Q_{ls}		PC-1

Depth (feet)	SPT N1(60)	Uncorrected Blows per 6-inch drive	Soil Type (USCS)	Sampler Type	Recovery (inches)	Pocket Pen. (TSF)	Shear Torvane (TSF)	Description	Remarks
49								— ? — — ? — — ? — — ? —	
50–51		13, 12, 16		2.5-inch I.D. split spoon	14"	1.5-3.5		Clayey SAND to Sandy Silty CLAY ( ); color varies, mottled 10YR5/3 greyish brown to yellowish brown (10YR5/8), sand is fine to medium grained, well sorted, dense, damp to moist; very stiff/dense, some zones of highly to completely weathered shale/mudstone, yellowish-brown (Highly to Completely Weathered Bedrock)	Samples 13:50-14:00
51.5–53		9, 12, 12			16"				
54									hard zone at 54' on.
55–57		50/6", 45, 45, 50/5"			4"	refuse		SILTSTONE shale; very dark greyish brown (10YR 3/2); dry to damp, hard; moderately weathered; R_0-R_1; slightly fissile/friable, highly fractured; fracture walls are highly weathered (Bedrock)	samples 14:25-14:35
57								Switch to core @ 57'	
58–66									

3.0-inch O.D. split spoon sampler 2.5-inch I.D. split spoon sampler Standard Penetration Test (SPT) sampler

LOG of ROCK BORING PC-1

Page 35 of 10

Project: DCPP Patton Cove Landslide	Job Number: 1223-48	Boring Location: middle of southbound lane; across from Stop Sign of Reservoir Rd	Total Depth
Type & Diameter of Boring: Double Barrel Core Barrel, HQ core, 4" Barrel	Elevation and Datum	Ground Water Depth: N.D.	Depth to Bedrock: 54'
Drilling Contractor and Rig: All Terrain Exploration Drilling / Failing 1500	Length of Core Barrel and Bit: 10'	No. of Core Boxes	Date Started: 20 Nov 2000
Casing Size and Depth: 6" set to ~3'	Borehole Inclination: vert	Logged By: CMB	Date Completed: 22 Nov 2000

WLA

Depth (feet)	Log	Drill Rate (min/ft)	Run No.	Recovery/Cut	% Recovery	RQD	Weathering	Fracture Spacing	Strength	Lithologic Description	Description of Discontinuities	Remarks
0–56										Mud Rotary Drilling w/ drive samples to 57.0'	Boring reamed to 57' HQ coring begins @ 57'	
57–59		10 min / Ft	1	1.6 / 2.0	80%	0	C_w	V_c	R_o	SILTSTONE/CLAYSTONE C_w, R_o, V_c, crushed, pervasive intense fracturing, no preferred orientation; weathered to clay-like consistency. Very Dark Grey (7.5YR 3/1)	numerous pervasive fractures throughout core run.	Begin 16:35 11/21/00 end 16:55 stop for day
59–61		11 min / ft	2	2.0 / 2.0	100%	0	H_w-M_w	V_c	R_o-R_1	SILTSTONE, black (7.5YR 2.5) with dark grey; closely - very closely fractured, med-highly weathered; fine grained, fractures are oxidized along surfaces, can be indented by fingernail, bedding not apparent; some yellowish alteration along fractures. Weathering is concentrated along fractures and also pervasive through rock mass, though less intense.	Crushed zone (Mc) J_o (Mc?), 45°, Pl, Sl, ? J_o, 30°, Pl St, Sl, Ti - SiO Crushed zone (Mc)	begin 07:27 11/22/00 note only major fractures shown, intact, unbroken core has numerous small fractures end 07:49
61–63		12 min / ft	3	1.9 / 2.0	95%	1.0 / 2.0 0.5	M_w-Sl_w	Cl	R_o-R_1		Mc (Be?), 10°, St, Sl, Op J_o (Be?), 10°, St, Sl-Pl, Op, brown clay coating Crushed zone (Mc)	begin 08:01 numerous tight small fractures not evident unless core is mechanically broken by hand end 08:28
63–65		10 min / ft	4	1.9 / 2.0	95%		M_w-Sl_w	Cl	R_o-R_1		Crushed zone (Mc) J_o, 15°, Wa, Sl, Ti - Fi, Qtz fill Crushed zone (Mc) zone of shale/clay, 75°, Wa, Sl, Op? Mc, 0-15°, St, Ro, Op	begin 08:34 Slow steady coring end 08:54

Weathering. Fr-Fresh, SW-Slight MW-Moderate, HW-Highly, CW-Completely, and RS-Residual soil Fracture Spacing VW -Very Wide (>3'), Wi Wide (1-3'), Mo Moderate (0.3'-1'), Cl Close (0.1'-0.3'), and VC-Very Close (<0.1'). Strength R6-Extremely Strong, R5-Very Strong, R4-Strong, R3-Medium Strong, R2 Weak, R1-Very Weak, and R0-Extremely Weak Lithologic Description Rock type, color texture, grain size etc Discontinuities Be-Bedding, Fa-Fault, Fo-Foliation, Jo-Joint, Mc-Mechanical break, Sh-Shear, and Ve-Vein. Joint descriptions Dip Surface shape (Pl-Planar, St-Stepped, or Wa-Wavy) Roughness (Sm-Smooth, Sl-Slightly Rough, Ro-Rough, and VR-Very Rough), Aperture (Fi-Filled, He-Healed Op-Open and Ti-Tight), type of infilling slickensides, etc

ROCK BORING LOG

Project	Job Number	Date	Boring No.
DCPP Patton Cove Qcs		21 Nov 2000	PC-1

WLA

Depth (feet)	Log	Drill Rate (min/ft)	Run No.	Recovery/Cut	% Recovery	RQD	Weathering	Fracture Spacing	Strength	Lithologic Description	Description of Discontinuities	Remarks
65–67		9 min/ft	5	2.0/2.0	100%	0.8/2.0 (0.4)	Mw-Sw	Cl	R_0-R_1	similar to above	J_o (Me), 5°, Pl-St, Sl, Op; Ve, 30°, Pl, Sl, Fi-T1, Qtz (Weathered) 6?; J_o(Me) 0°, Pl, Sl-Sm, Op; Crushed Zone (Me)	begin 09:02; end 09:20
67–69	No Recov.	7 min/ft	6	1.1/2.0	55%	0	Mw	Vc	R_0-R_1		No Recov.; Crushed Zone of highly Weathered Siltstone/Claystone, Mechanical breakage along Pre-existing tight fractures	begin 09:31; end 09:45
69–71		12.5 min/ft	7	2.0/2.0	100%	0	Mw	Cl	R_0-R_1	Highly-Completely Weathered Zone, to stiff clay, brown; SILTSTONE/CLAYSTONE similar to above. color black (7.5YR 2.5) fine grained, moderately weathered, oxidation along fractures, bedding difficult to determine. silicious	Crushed Zone (Me)	begin 09:56; end 10:21
71–73	No Recovery	12 min/ft	8	0.6/2.0	30%	0	Mw	Vc	R_1-R_2		No Recovery; Mechanically broken fragments to 2"; weathered and oxidized surfaces	begin 10:34; end 10:58
73–74	No Recov.	13 min/ft	9	0/2.0	0%	0	-	-	-		No Recovery	begin 11:08; end 11:20
74–76		12 min/ft	10	1.9/2.0	95%		Sw	Cl	R_1	CLAYSTONE, black (7.5YR2.5) massive, bedding cannot be determined, can be indented by fingernail	J_o (Me), 35-45°, Ro, Oxidized 0.5" into rock; numerous tight slickensided fractures and partings throughout core run; Me, 0°, St, Ro, Op	begin 11:28; end 11:50
76–79	No Recov.	9 min/ft	11	1.9/3.0	63%	0.5/3.0	Sw	Cl	R_0-R_1	harder zone, similar to above but R_2	No Recov.; J_o, 75-90°, Pl-Wa, Sl, Op, Slickensides; Me, 0°, St, Ro, Op; J_o, 45, Pl-St, Sl, Op; J_o(Me) 0-10°, St, Ro, Op; J_o 75°, Pl, Sl, Op	begin 12:10; end 12:37
79–80	N.R.	13 min/ft	12	1.5/1.8	83%	0	Mw-Sw	Vc-Cl	R_0-R_1	back to before (R_0-R_1) claystone	N.R.; Crushed Zone (Me)	begin 12:45

Weathering: Fr-Fresh, SW-Slight, MW-Moderate, HW-Highly, CW-Completely, and RS Residual soil. Fracture Spacing: VW-Very Wide (>3'), Wi Wide (1-3'), Mo-Moderate (0.3-1'), Cl Close (0.1'-0.3'), and VC-Very Close (<0.1'). Strength: R6 Extremely Strong, R5-Very Strong, R4-Strong, R3-Medium Strong, R2-Weak, R1-Very Weak, and R0-Extremely Weak. Lithologic Description: Rock type, color, texture, grain size, etc. Discontinuities: Be-Bedding, Fa Fault, Fo-Foliation, Jo-Joint, Me-Mechanical break, Sh-Shear, and Ve-Vein. Joint descriptions: Dip, Surface shape (Pl-Planar, St-Stepped, or Wa-Wavy), Roughness (Sm-Smooth, Sl-Slightly Rough, Ro-Rough, and VR-Very Rough), Aperture (Fi-Filled, He-Healed, Op-Open and Ti-Tight), type and amount of infilling, slickensides, etc.

ROCK BORING LOG

Project	Job Number	Date	Boring No
DCPP Patton Cove		21 Nov 2000	PC-1

WLA

Depth (feet)	Log	Drill Rate (min/ft)	Run No.	Recovery/Cut	% Recovery	RQD	Weathering	Fracture Spacing	Strength	Lithologic Description	Discontinuities	Description of Discontinuities	Remarks
80–81			12 (cont)	← see above →						Similar to above:		Me, 0°, Pl, Sm, Op Me, ~5°, Pl, Ro, Op Crushed Zone (Me)	end 13:11
81–83.3	N.R.	34 min / 2.7'	13	1.7 / 2.7	63%	0	Sw-Mw	Vc-Cl.	R_1	CLAYSTONE/SILTSTONE color grey (Gley 5/N), highly fx, slight weathering pervasive; moderate along fractures, massive;	N.R.	Crushed Zone (Me) J_o (Me), 10°, St, Sl-Ro, Op J_o, 0-5°, St, Sl-Ro, Op Crushed Zone (Me)	begin 13:23 (5 minute stop for water truck) end 14:08
83.3–86	N.R.	29 min / 2.5'	14	1.5 / 2.5	60%	0	Sw	Vc	R_1-R_2		N.R.	Crushed Zone (Me) J_o, 30°, Pl, Sm-Sl, Op-Ti J_o (Me?), 45°, St-Wa, Sl, Op J_o, 75°-80°, St Wa, Sl, Op J_o 15°, St, Sl, Op	begin 14:11 end 14:20 start 14:28 end 14:48
86–95										End of HQ Core; Return to Mud Rotary			

Weathering: Fr-Fresh, SW-Slight, MW-Moderate, HW-Highly, CW-Completely, and RS-Residual soil. Fracture Spacing: VW-Very Wide (>3'), Wi-Wide (1'-3'), Mo-Moderate (0.3'-1'), Cl-Close (0.1'-0.3'), and VC-Very Close (<0.1'). Strength: R6-Extremely Strong, R5-Very Strong, R4-Strong, R3-Medium Strong, R2-Weak, R1-Very Weak, and R0-Extremely Weak. Lithologic Description: Rock type, color, texture, grain size, etc. Discontinuities: Be-Bedding, Fa-Fault, Fo-Foliation, Jo-Joint, Me-Mechanical break, Sh-Shear, and Ve-Vein. Joint descriptions: Dip, Surface shape (Pl-Planar, St-Stepped, or Wa-Wavy), Roughness (Sm-Smooth, Sl-Slightly Rough, Ro-Rough, and VR-Very Rough), Aperture (Fi-Filled, He-Healed, Op-Open and Ti-Tight), type and amount of infilling, slickensides, etc.

WLA

BORING LOG

Project	Job No	Boring No.
DCPP Patton Cove		PC-1

SPT $N_1(60)$ 0 10 20 30 40 50 60	Uncorrected Blows per 6-inch drive	Depth (feet)	Soil Type (USCS)	Sampler Type	Recovery (inches)	Pocket Pen. (TSF)	Shear Torvane (TSF)	Description	Remarks
		85						HQ Core to 86.0'	reamed upper 86' of hole begin drilling @ 86' @ 16:22
		86							
		87							
		88							
		89							
		90							90' 16:53
		91						continued grey claystone cuttings	
		92							
		93							
		94							
		95							95' 17:17
		96							
		97							
		98							
		99							
		100							100' 17:42 end for day resume 07:10 11/22/00
		101							
		102							

3.0-inch O.D. split spoon sampler — 2.5-inch I.D. split spoon sampler — Standard Penetration Test (SPT) sampler

WLA

BORING LOG

Project	Job No	Boring No
DCPP Patton Cove		PC-1

Uncorrected Blows per 6-inch drive	Depth (feet)	Soil Type (USCS)	Sampler Type	Recovery (inches)	Pocket Pen. (TSF)	Shear Torvane (TSF)	Description	Remarks
	102							
50/1"	110			1"			CLAYSTONE; color grey (Gley 5/N); dry to damp; fresh; R_1-R_2; slightly friable; very hard; fine grained. (Bedrock-Tof_c)	110' 08 04 Sample 08:25 Start 08:39
	115							115' 09 02
	119							

SPT $N_1(60)$: 0 10 20 30 40 50 60

3.0-inch O D split spoon sampler | Bag Sample of Cuttings ~~2.5-inch I D. split spoon sampler~~ | Standard Penetration Test (SPT) sampler

WLA

BORING LOG

Project	Job No	Boring No
DCPP Patton Cove		PC-1

SPT $N_1(60)$ 0 10 20 30 40 50 60	Uncorrected Blows per 6-inch drive	Depth (feet)	Soil Type (USCS)	Sampler Type	Recovery (inches)	Pocket Pen. (TSF)	Shear Torvane (TSF)	Description	Remarks
		119							
		120							120' @ 0927
		121							
		122							
		123							
		124							124' @ 0943
		125							
		126							126' @ 0951
		127							
		128							128' @ 0959
		129		☒				same as above - grey claystone	
		130						end drilling 130.0' BOH install inclo and grout to surface	130' @ 10:12
		131							
		132							
		133							
		134							
		135							
		136							

☐ 3.0-inch O.D. split spoon sampler ☒ Bag Sample of Cuttings ~~2.5-inch I.D. split spoon sampler~~ ▮ Standard Penetration Test (SPT) sampler

ATTACHMENT

3-1

NUCLEAR POWER GENERATION
CF3.ID4
ATTACHMENT 7.2

TITLE: DESIGN CALCULATION COVER SHEET

Unit(s): 1 & 2 Diablo Canyon Power Plant

File No.: 72.10.05

Responsible Group: NCFM

Calculation No.: M-1058

No. of Pages 13

Design Calculation YES ☒ NO ☐

System No. 42C

Quality Classification Q

Structure, System or Component: Independent Spent Fuel Storage Facility

Subject: Cask Transfer Facility Seismic Restraint Configuration

Computer/Electronic calculation YES ☐ NO ☒

Computer Model	Computer ID	Program Location	Date of Last Change

Registered Engineer Stamp: Complete A or B

A. Insert PE Stamp or Seal Below	B. Insert stamp directing to the PE stamp or seal
06/30/2003 Expiration Date:	

NOTE 1: Update DCI promptly after approval.
NOTE 2: Forward electronic calculation file to CCTG for uploading to EDMS.

CF3.ID4
ATTACHMENT 7.2

TITLE: DESIGN CALCULATION COVER SHEET

RECORD OF REVISIONS

CALC No. M-1058

Rev No.	Status	Reason for Revision Remarks	Prepared By: Initials/ LAN ID/ Date	LBIE Screen Yes/ No/ NA	LBIE Yes/ No/ NA	Check Method*	LBIE Approval PSRC Mtg. No.	 PSRC Mtg. Date	Checked Initials/ LAN ID/ Date	Supervisor Initials/ LAN ID/ Date	Registered Engineer Signature/ LAN ID/ Date
0	F	Original Issue	RDH RDH7 10/19/01	☒ Yes ☐ No ☐ NA	☐ Yes ☒ No ☐ NA	☐ A ☐ B ☐ C			PH PWH2 10/19/01	RLK RLK1 10/19/01	Richard D. Hagler RDH7 10/19/01
1	F	See Page 3	RDH RDH7 10/23/01	☒ Yes ☐ No ☐ NA	☐ Yes ☒ No ☐ NA	☐ A ☐ B ☐ C			PH PWH2 10/23/01	RLK RLK1 10/23/01	Richard D. Hagler RDH7 10/23/01
2	F	See Page 3	RDH RDH7 12/10/01	☒ Yes ☐ No ☐ NA	☐ Yes ☒ No ☐ NA	☐ A ☐ B ☐ C			PH PWH2 12/11/01	RLK RLK1 12/11/01	RDH RDH7 12/11/2001
				☐ Yes ☐ No ☐ NA	☐ Yes ☐ No ☐ NA	☐ A ☐ B ☐ C					
				☐ Yes ☐ No ☐ NA	☐ Yes ☐ No ☐ NA	☐ A ☐ B ☐ C					

*Check Method: A: Detailed Check, B: Alternate Method (note added pages), C: Critical Point Check

SUBJECT Cask Transfer Facility Seismic Restraint Configuration

MADE BY Rich Hagler DATE 12/10/2001 CHECKED BY Patrick Huang DATE 12/11/2001

Change Summary

Revision	Change Description	Affected Pages	Reason for Change
0	Original Issue	N/A	N/A
1	Revised to eliminate MPC weight	1-5, 7-12	MPC lateral loading is resisted by the tiedowns to the HI-TRAC. Added radial section of tiedown geometry.
2	Removed transfer cask tiedown and relocated restraint locations for cask transporter tiedown only	1-13	Holtec reanalysis of the CTF structure

Pacific Gas and Electric Company
Engineering – Calculation Sheet
Project Diablo Canyon Unit ( ) 1 ( ) 2 (X) 1 & 2

SUBJECT Cask Transfer Facility Seismic Restraint Configuration

MADE BY Rich Hagler DATE 12/10/2001 CHECKED BY Patrick Huang DATE 12/11/2001

Table of Contents

Pacific Gas and Electric Company
Engineering – Calculation Sheet
Project Diablo Canyon Unit ( ) 1 ( ) 2 (X) 1 & 2

CALC. NO. M-1058
REV. NO. 2

SUBJECT Cask Transfer Facility Seismic Restraint Configuration

MADE BY Rich Hagler DATE 12/10/2001 CHECKED BY Patrick Huang DATE 12/11/2001

List of Sketches

1. Purpose:

The purpose of this calculation is to determine the location and capacity of seismic restraints adjacent to the cask transfer facility (CTF) structure to secure the cask transporter during multi-purpose canister (MPC) load handling operations.

The four in-ground restraints are to be located ninety degrees apart to provide a ground-level attachment point for restraint of the cask transporter.

2. Background:

The proposed deployment of the HI-STORM 100SA system at DCPP introduces additional load handling operations in and around the plant facilities in the Owner Controlled and Protected Areas. The cask transporter is required to be restrained during MPC handling operations per Input 4.8

3. Assumptions:

None

4. Input:

4.1 Deleted.
4.2 Deleted.
4.3 Deleted.
4.4 Deleted.
4.5 Deleted.
4.6 Deleted.
4.7 Deleted.
4.8 Holtec Design Criteria Document HI-2002501, "Functional Specification for the Diablo Canyon Cask Transporter," [11.1.8]
4.9 PG&E Company Specification 10012-N-NPG, "Dry Cask Storage System," [11.1.9].
4.10 Holtec Design Criteria Document HI-2002511, "Design Criteria Document for the ISFSI Pad for Anchored HI-STORM 100 Deployment at the Diablo Canyon Power Plant," [11.1.10]
4.11 PG&E Company Memo to File 72.10.05, "Cask Transporter Track Contact Surface Area Requirement," [11.1.11]

5. Methodology:

Standard engineering mechanics principals and geometric relationships are used to determine the results.

6. Acceptance Criteria:

None

7. Body of the Calculation:

7.1 Restraint Location

In order for the tiedown foundation structure to be independent of the surface slab surrounding the CTF in-ground lift, the tiedown location is chosen to be 48 in. from the lateral edge of the surface slab The surface slab is chosen as 300 in. (25 ft.) wide laterally centered on the CTF in-ground lift structure. Therefore, the lateral distance to the tiedown location is 150 in. + 48 in = 198 in. This is 87 in. laterally from the side of the cask transporter (see Sketch 7.2-1).

7.2 Cask Transporter Seismic Restraint Forces

Determine bounding restraint force for the cask transporter

Cask transporter is required to be seismically restrained during MPC load handling operations. The weight of this configuration is 170 kips (input 4.8).

Since the cask transporter is rigid (Input 4.8 Section 4.11), horizontal acceleration at the CTF structure surface is ZPA for the LTSP or 0.83g (input 4.9 App. A, Figure A.1.7).

$$a_h = \sqrt{(0.83g)^2 + (0.83g)^2} = 117g$$

The cask transporter horizontal force to be restrained is 1.17g (170 kips) = 198.9 kips.

The center of gravity of the cask tranporter is located 132 in. (input 4 10, Section 4.7) from the edge of the contact surface of the tracks at its rear (see Sketch 7.2-1). The lifting beam centerline is located at 173.64 in. (input 4.10, Section 4.7) from the edge of the contact surface of the tracks at its rear. The contact surface of the track plates is 26 in. wide per input 4.11.

The maximum force in a given restraint will occur when the maximum horizontal seismic force acts opposite in direction to the restraint as shown in Sketch 7.2-1. The other three restraints are conservatively neglected to resist the lateral force Friction forces resisting cask transporter sliding are conservatively neglected.

The attachment point is located to be on the side of the transporter at a maximum height of 84 in., the resultant force in the restraint is:

$$F_r = \frac{198.9}{\cos\left(\tan^{-1}\left(\frac{84}{\sqrt{2(87)^2}}\right)\right)} = 241.0 \text{ kips}$$

The angle of inclination from the ground surface is·

$$\alpha = \tan^{-1}\left(\frac{84}{\sqrt{2(87)^2}}\right) = 34.32 \text{ degrees}$$

<u>Determine magnitude and direction of restraint force for the cask transporter</u>

When the earthquake motion is along the transverse and longitudinal directions of the transporter, sliding and overturning of the transporter may occur. The sliding and overturning forces are resisted by two restraints The maximum height of the CG is 87 in. per Input 4.10 Section 4.7.

Longitudinal Overturning

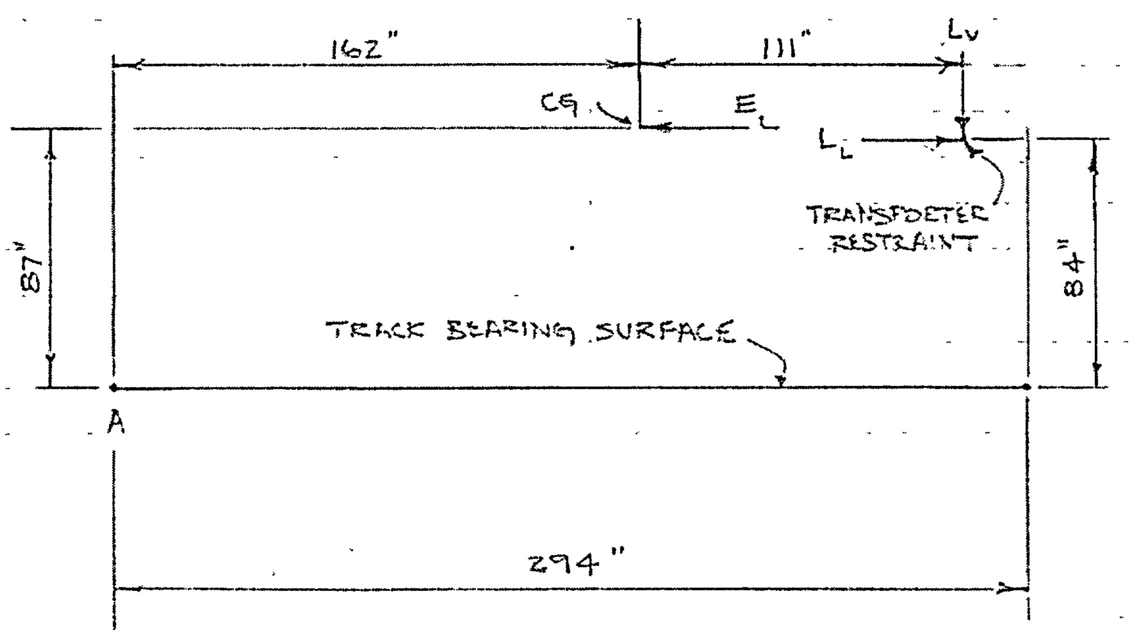

Cask Transporter Longitudinal Overturning Diagram

Summing moments about Point A to determine the induced force L developed by the opposing pair of restraints (+ = CCW):

E_L(87 in.) – L_L(84 in) - L_V(273 in.) = 0
170k(0.83g)(87 in) – L(cos34.32)(cos45)(84 in.) - L(sin34.32)(273 in.) = 0; L = 60.48 kips

L_L = L(cos34.32)(cos45) = 35.3 kips
L_V = L(sin34.32) = 34.1 kips.

Transverse Overturning

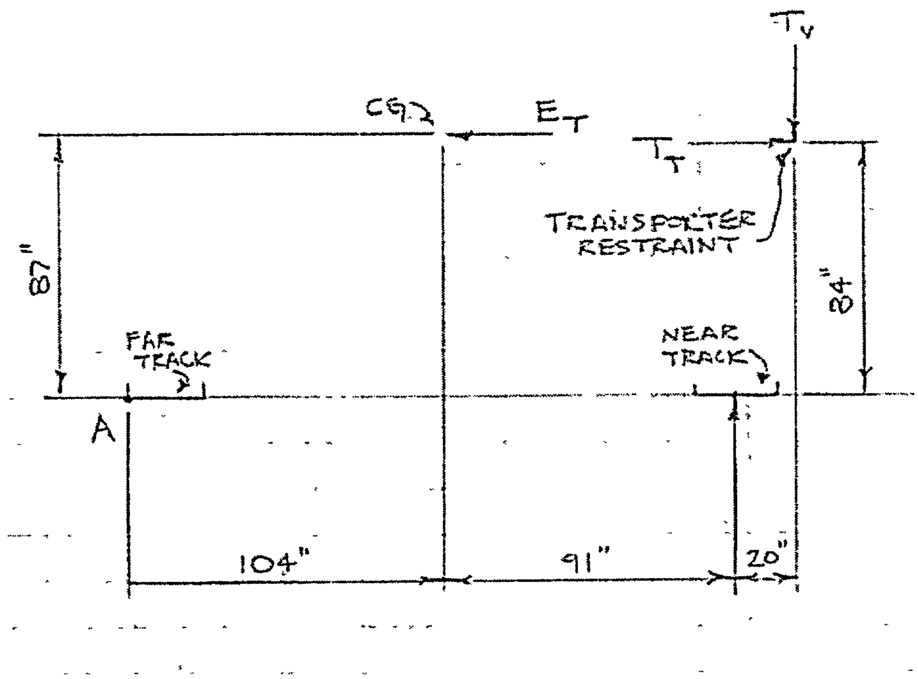

Cask Transporter Transverse Overturning Diagram

Summing moments about Point A to determine the induced force T developed by the opposing pair of restraints (+ = CCW):

E_T(87 in.) – T_L(84 in) - T_V(215 in.) = 0
170k(0.83g)(87 in.) – T(cos34.32)(cos45)(84 in.) - T(sin34.32)(215 in.) = 0; T = 72.1 kips

T_T = T(cos34.32)(cos45) = 42.1 kips;
T_V = T(sin34.32) = 40.7 kips.

Since the cask transporter is rigid (Input 4.8 Section 4.11), vertical acceleration at the CTF structure surface is 0 7g for the LTSP (input 4.9 App. A, Figure A 1.8).

Vertical Inertia

The vertical force due to seismic is 170k(0.7g) = 119 kips.

Sliding

The vertical force due to sliding is F_f(sin34.32) = 241k(sin34.32) = 135.9 kips

Combining all seismically-induced vertical forces per Input 4.9 Section 6 2.5.5.V on a per track basis:

Note The transverse forces are counteracted by only one track.

$R_E = \sqrt{(119/2)^2 + ((135.9+34.1)/2)^2 + (135.9+40.7)^2}$ = 204.8 kips per track

R = Transporter Dead Load + R_E

R = (170/2)k + 204.8k = 289.8 kips per track

Pacific Gas and Electric Company
Engineering – Calculation Sheet
Project Diablo Canyon Unit ( ) 1 ( ) 2 (X) 1 & 2

CALC. NO. M-1058
REV. NO. 2
SHEET NO. 11 OF 13

SUBJECT Cask Transfer Facility Seismic Restraint Configuration

MADE BY Rich Hagler DATE 12/10/2001 CHECKED BY Patrick Huang DATE 12/11/2001

Sketch 7.2-1 Cask Transporter Restraint During MPC Load Handling

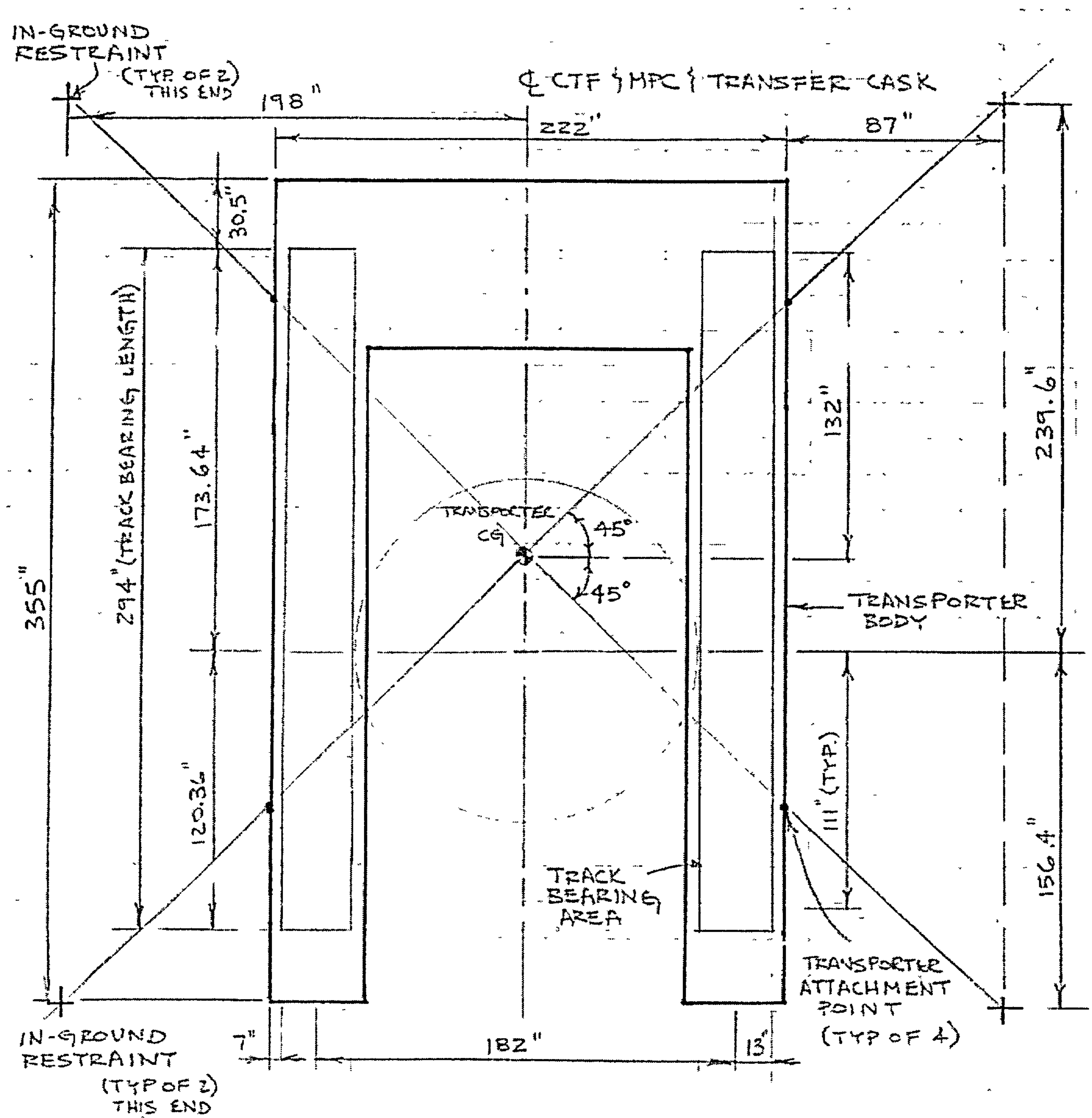

8. Results:

8.1 The resulting magnitudes and locations are.

Cask Transporter Restraint	241.0 kips maximum at 34.32 degrees from ground surface
CTF Structure Surface Reaction	289 8 kips maximum per track

Sketch 7.2-1 depicts the plan layout of the in-ground restraints at the CTF.

9. Conclusion:

N/A.

10. Impact Evaluation:

This calculation provides design input to the design of the CTF reinforced concrete structure (Ref. 11.2.1).

The CTF structure is to be licensed under 10 CFR Part 72 (Ref. 11.2.3). This calculation does not apply to the existing 10 CFR Part 50 power plant.

Once Reference 11.2.3 has been approved by NRC, PG&E will implement the HI-STORM 100SA system at DCPP using applicable administrative control programs (i.e., design change, modification control).

11. References:

11.1 Input
11.1.1 Deleted.
11.1.2 Deleted.
11.1.3 Deleted.
11.1.4 Deleted.
11.1.5 Deleted.
11.1.6 Deleted.
11.1.7 Deleted.
11.1.8 Holtec Design Criteria Document HI-2002501, "Functional Specification for the Diablo Canyon Cask Transporter," Revision 5, 11/09/2001 [4 8].
11.1.9 PG&E Company Specification 10012-N-NPG, "Dry Cask Storage System," Revision 2, 06/26/2001 [4.9].
11.1.10 Holtec Design Criteria Document HI-2002511, "Design Criteria Document for the ISFSI Pad for Anchored HI-STORM 100 Deployment at the Diablo Canyon Power Plant," Revision 2, 07/12/2001 [4.10].
11.1.11 PG&E Company Memo to File 72.10.05, "Cask Transporter Track Contact Surface Area Requirement," dated 10/19/2001 [4.11].

11.2 Output
11.2.1 PG&E Calculation 52.27.100 708, "CTF Reinforced Concrete."
11.2.2 Deleted.

11.2.3 PG&E DC ISFSI 10CFR72 License Application, 2001.

11.3 Other
11.3.1 PG&E Company Procedure CF3.ID4, "Design Calculations," Revision 7, 06/01/2001.

12. Appendices or Attachments:

None.

ATTACHMENT

4-1

Attachment A

Excerpts

From

<u>Wind Effects on Structures: Fundamentals and Applications to Design</u>

By Emil Simiu and Robert Scanlan

WIND EFFECTS ON STRUCTURES

Fundamentals and Applications to Design

Third Edition

EMIL SIMIU

NIST Fellow, Building and Fire Research Laboratory, National Institute of Standards and Technology, Gaithersburg, Maryland

ROBERT H. SCANLAN

Professor, Department of Civil Engineering, The Johns Hopkins University, Baltimore, Maryland

A Wiley-Interscience Publication

JOHN WILEY & SONS, INC.

New York / Chichester / Brisbane / Toronto / Singapore

This text is printed on acid-free paper

Library of Congress Cataloging-in-Publication Data:

Simiu, Emil

Wind effects on structures: fundamentals and applications to design / Emil Simiu, Robert H. Scanlan. — 3rd ed.

p. cm.

Includes index.

ISBN 0-471-12157-6 (cloth : alk. paper)

1. Wind-pressure. 2. Buildings—Aerodynamics. 3. Wind resistant design. I. Scanlan, Robert H. II. Title.

TA654.5.S55 1996

624.1'76—dc20 96-5238

Printed in the United States of America

10 9 8 7 6 5 4 3 2

Calculation No. 52.27.55.51, Rev. 0
Sheet A-2

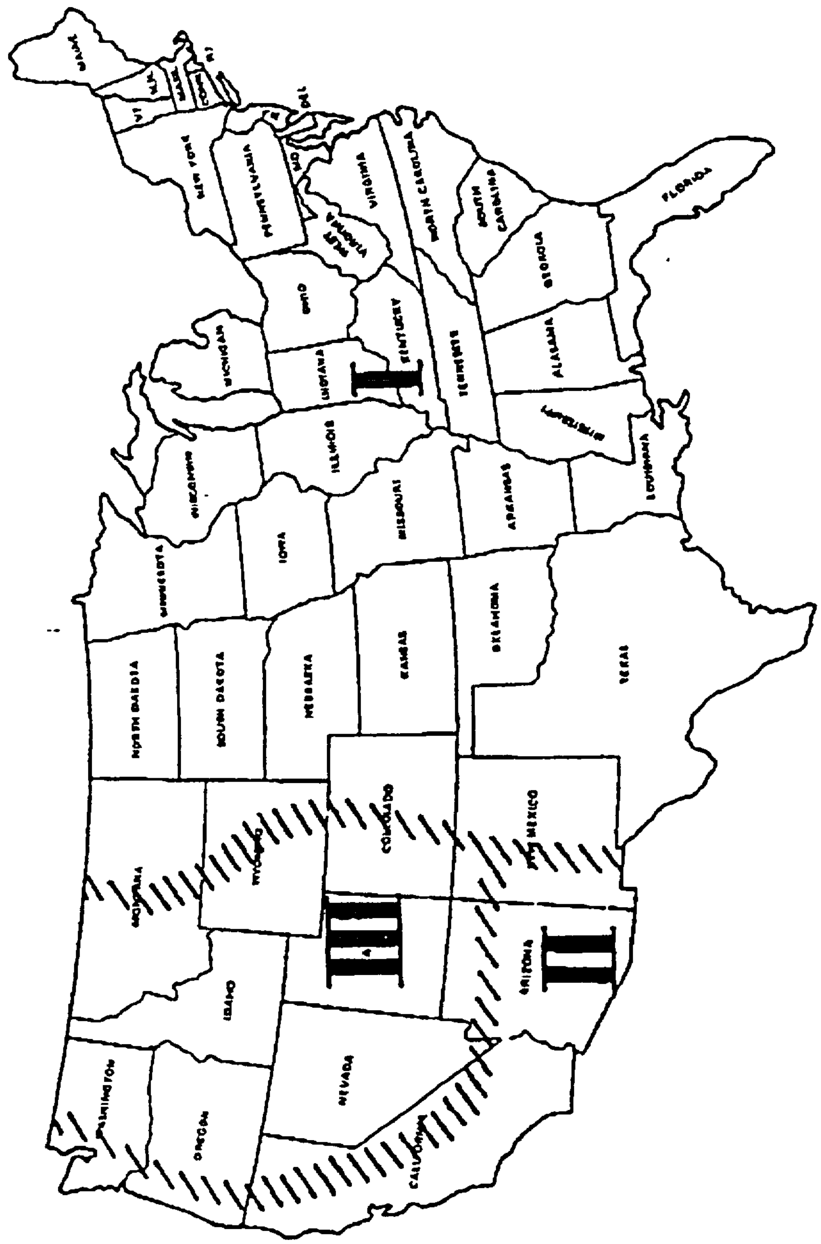

FIGURE 3.5.4. Tornado intensity regions [3-35].

TABLE 3.5.1. Regional Tornado Winds

Region	Maximum Speed V_{max} (mph)	Rotational Speed V_{rot} (mph)	Translational Speed V_{tr} (mph)	Radius of Maximum Rotational Wind Speed R_m (ft)
I	360	290	70	150
II	300	240	60	150
III	240	190	50	150

2. Temporal variations in tornado reporting efficiency. The number of reported annual tornado occurrences in the United States has increased from about 250 in 1950 to 850 in 1979. The growing trend in the number of reported tornadoes during this period has been ascribed to a corresponding increase in population density. An explicit relation to this effect has been proposed in [3-47]. Corrections accounting for tornado reporting efficiencies were effected in [3-45] by averaging the 1971–1978, 1970–1978, 1969–1978, and 1950–1978 data and assuming that the true occurrence rates are equal to the largest of these estimates.
3. Possible errors in the rating of tornado intensities on the basis of observed damage. The reason for the occurrence of such errors is that maximum tornado winds are in practice not measured, but inferred, largely on the basis of professional judgment, from observations of damage to buildings, signs, and so forth [3-42].
4. Inhomogeneous distribution along the tornado path of buildings and various other objects susceptible of being damaged. In the possible absence of such objects over the portions of the tornado path where the winds are highest—or even over the entire tornado path—the rating of the tornado is bound to be in error. The effect of corrections for such errors is to increase the estimated probability of occurrence of tornadoes with higher intensities.
5. Variation of tornado intensity along the tornado path. Accounting to this factor results in smaller estimated risks of high tornado winds than would be the case if the maximum tornado winds (by which tornado intensities

TABLE 3.5.2. Regional Pressure Drops and Pressure Drop Rate

Region	Total Pressure Drop (psi)	Rate of Pressure Drop (psi/s)
I	3.0	2.0
II	2.25	1.2
III	1.5	0.6

16.3 TORNADO-BORNE MISSILE SPEEDS

To estimate speeds attained by an object moving under the action of aerodynamic forces induced by tornado winds, a set of assumptions is required

- On the aerodynamic characteristics of the object.
- On the detailed features of the wind flow field.
- On the initial position of the object with respect to the ground and to the tornado center, and its initial velocity.

Objects commonly considered as potential missiles in the design of nuclear power plants are bluff bodies such as wooden planks, steel rods, steel pipes, utility poles, and automobiles.

The purpose of this section is to review approaches to the tornado-borne missile problem based on (1) deterministic modeling, (2) probabilistic modeling involving numerical simulations, and (3) modeling of missile transport as a Markov diffusion process.

16.3.1 Deterministic Modeling of Missile Motions

Equations of Motion and Aerodynamic Modeling. The motion of an object may be described in general by solving a system of three equations of balance of momenta and three equations of balance of moments of momenta. In the case of a bluff body, one major difficulty in writing these six equations is that the aerodynamic forcing functions are not known.

It is possible to measure in the wind tunnel aerodynamic forces and moments acting on a bluff body under static conditions for a sufficient number of positions of the body with respect to the mean direction of the flow. On the basis of such measurements, the dependence of the forces and moments on position and corresponding aerodynamic coefficients can be obtained. Aerodynamic forces and moments can then be calculated following the well-known pattern used in airfoil theory; for example, if an airfoil has a time-dependent vertical motion $h(t)$ in a uniform flow with velocity V, and if the angle of attack is α = const, the lift coefficient is [16-8]

$$C_L = \frac{dC_L}{d\alpha}\left(\alpha + \frac{1}{V}\frac{dh}{dt}\right) \tag{16.3.1}$$

This procedure for calculating aerodynamic forces and moments may be assumed to be valid if the motions of the body concerned are small. However, in the case of unconstrained bluff bodies moving in a wind flow, the validity of such a procedure remains to be demonstrated.

In the absence of a satisfactory model for the aerodynamic description of the missile as a rigid (six-degrees-of-freedom) body, it is customary to resort to the alternative of describing the missile as a material point acted upon by a drag force

$$\mathbf{D} = \tfrac{1}{2}\rho C_D A |\mathbf{V}_w - \mathbf{V}_M|(\mathbf{V}_w - \mathbf{V}_M) \quad (16.3.2)$$

where ρ is the air density, $\mathbf{V}_w$ is the wind velocity, $\mathbf{V}_M$ is the missile velocity, A is a suitably chosen area, and C_D is the corresponding drag coefficient. This model is reasonable if, during its motion, the missile either (1) maintains a constant or almost constant attitude with respect to the relative velocity vector $\mathbf{V}_w - \mathbf{V}_M$, or (3) has a tumbling motion such that, with no significant errors, some mean value of the quantity C_DA can be used in the expression for the drag D. The assumption of a constant body attitude with respect to the flow would be credible if the aerodynamic force were applied at all times exactly at the center of mass of the body—which is highly unlikely in the case of a bluff body in a tornado flow—or if the body rotation induced by a nonzero aerodynamic moment with respect to the center of mass were inhibited by aerodynamic forces intrinsic in the body-fluid system. The question thus arises as to whether such forces are present. This question has not been studied exhaustively in the literature. However, simple experiments suggest that in the case of bluff bodies the aerodynamic damping forces have a destabilizing effect. Wind tunnel tests reported in [16-9] tend to confirm this view. The assumption that potential tornado-borne missiles will tumble during their motion appears therefore to be a reasonable one.

Assuming then that Eq. 16.3.2 is valid and that the average lift force vanishes under tumbling conditions, the motion of the missile viewed as a three-degree-of-freedom system is governed by the relation

$$\frac{d\mathbf{V}_M}{dt} = \frac{1}{2}\rho\frac{C_DA}{m}|\mathbf{V}_w - \mathbf{V}_M|(\mathbf{V}_w - \mathbf{V}_M) - g\mathbf{k} \quad (16.3.3)$$

where g is the acceleration of gravity, $\mathbf{k}$ is the unit vector along the vertical axis, and m is the mass of missile. It follows from Eq. 16.3.3 that for a given flow field and given initial conditions the motion depends only upon the value of the parameter C_DA/m. For a tumbling body this value can, in principle, be determined experimentally. Unfortunately, little information on this topic appears to be presently available. Reference [16-10] contains information on tumbling motions under flow conditions corresponding to Mach numbers 0.5 to 3.5. The data of [16-10] were extrapolated in [16-11] to lower subsonic speeds; according to this extrapolation, for a randomly tumbling cube the quantity C_DA equals, approximately, the average of the products of the projected areas corresponding to "all positions statistically possible" by the respective static drag coefficients [16-11, pp. 13-17, and 14-16]. In the absence of more experimental information, it appears reasonable to assume that the effective product C_DA is given by the expression

$$C_DA = c(C_{D_1}A_1 + C_{D_2}A_2 + C_{D_3}A_3) \qquad (16.3.4)$$

where $C_{D_i}A_i (i = 1, 2, 3)$ are products of the projected areas corresponding to the cases in which the principal axes of the body are parallel to the vector $\mathbf{V}_w - \mathbf{V}_M$ by the respective static drag coefficients, and c is a coefficient assumed to be 0.50 for planks, rods, pipes, and poles and 0.33 for automobiles. In the case of circular cylindrical bodies (rods, pipes, poles), the assumption $c = 0.50$ is clearly conservative.

Computations and Numerical Results. A computer program for calculating and plotting trajectories and velocities of tornado-borne missiles is described in [16-12]. The program includes specialized subroutines incorporating the assumed model for the tornado wind field and the assumed drag coefficients (which may vary as functions of Reynolds number). Input statements include values of relevant parameters and the initial conditions of the missile motion.

In Eq. 16.3.3 both $\mathbf{V}_M$ and $\mathbf{V}_w$ are referred to an absolute frame. The velocity $\mathbf{V}_w$ is usually specified as a sum of two parts. The first part represents the wind velocity of a stationary tornado vortex and is referred to a cylindrical system of coordinates. The second part represents the translation velocity of the tornado vortex with respect to an absolute frame of reference. Transformations required to represent V_w in an absolute frame are derived in [16-12] and incorporated in the computer program.

For tornadoes with parameters given in Tables 3.5.1 and 3.5.2 for regions I, II, and III, and referred to as Type I, Type II and Type III tornadoes, respectively, calculated values of the maximum horizontal missile speeds V_H^{max} are given in Fig. 16.3.1 as functions of the parameter C_DA/m. These values were obtained on the basis of the following assumptions:

- The tangential velocity of the tornado vortex V_t is described by Eqs. 16.1.1 and 16.1.2.
- The radial velocity component V_r and the vertical velocity component V_z are given by the expressions* [16-13]

$$V_r = 0.50V_t \qquad (16.3.5)$$

$$V_z = 0.67V_t \qquad (16.3.6)$$

  The radial component is directed toward the center of the vortex (Fig. 16.3.2); the vertical component is directed upward.
- The translation velocity of the tornado vortex V_{tr} is directed along the x axis (Fig. 16.3.2).

*For alternative models, see [3-46].

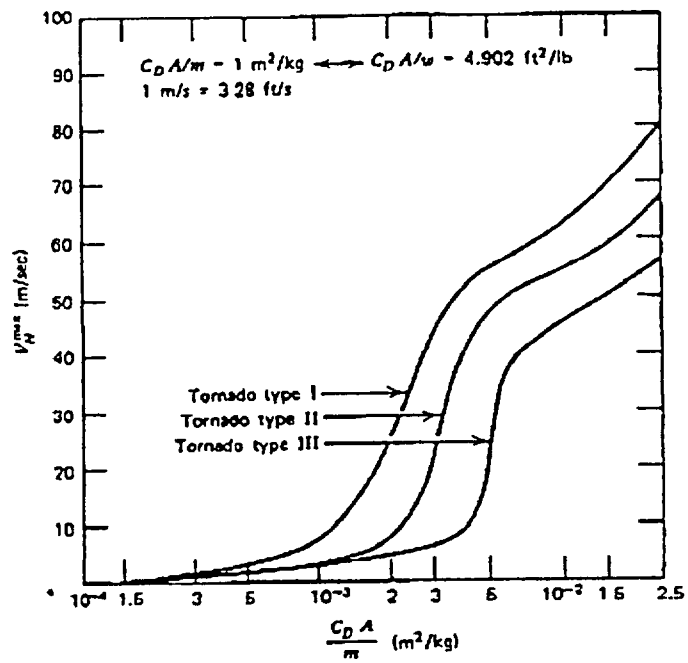

FIGURE 16.3.1. Variation of maximum horizontal missile speed as a function of C_DA/m for various types of tornadoes.

- The initial conditions (at time $t = 0$) are $x(0) = R_m$, $y(0) = 0$, $z(0) = 40$ m, $V_{M_x}(0) = V_{M_y}(0) = V_{M_z}(0) = 0$, where x, y, z are the coordinates of the center of mass of the missile and V_{M_x}, V_{M_y}, V_{M_z} are the missile velocity components along the x, y, z axes. Also at $t = 0$ the center of the tornado vortex coincides with the origin 0 of the coordinate axes.

Table 16.3.1 lists assumed characteristics of selected missiles and the corresponding horizontal speeds V_H^{max} as obtained from Fig. 16.3.1. A computer

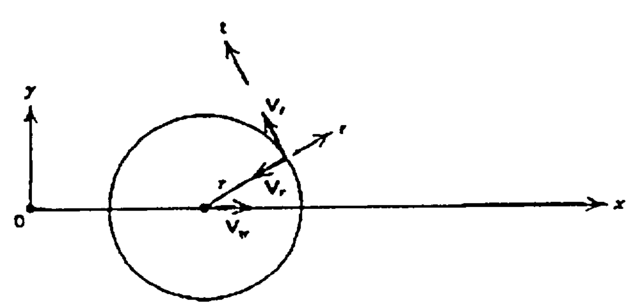

FIGURE 16.3.2. Horizontal components of tornado wind velocity.

TABLE 16.3.1. Characteristics and Maximum Horizontal Speeds of Selected Missiles

	Dimensions	Weight (lb/ft)	Mass (kg/m)	C_{D_l}	C_{D_t}	C_{D_t}	C_DA/w (ft²/lb)	C_DA/m (m²/kg)	V_H^{max} Tornado Type I	Tornado Type II	Tornado Type III
1 Wooden Plank	$3\frac{5}{8}$" × $11\frac{3}{8}$" × 12' (0 092 m × 0.289 m × 3.66m)	8.2 to 11 (e.g. 9 6)	12.2 to 16.3 (e.g. 14.3)	2.0	2.0	2.0	0.132	0.0270	272 ft/s (83 m/s)	230 ft/s (70 m/s)	190 ft/s (58 m/s)
2 6" Sch. 40 Pipe	6.625" (diam) × 15' length) (0.168 m × 4.58 m)	18.97	28.18	0.7	2.0	0.7	0 0212	0.0043	171 ft/s (52 m/s)	138 ft/s (42 m/s)	33 ft/s (10 m/s)
3 Automobile	16.4' × 6 6' × 4 3' (5 m × 2 m × 1.3m)	4000 lb (total wt)	1810 kg (total mass)	2.0	2.0	2.0	0 0343	0 0070	193 ft/s (59 m/s)	170 ft/s (52 m/s)	134 ft/s (41 m/s)
4 1" Solid Steel Rod	1" (diam) × 3' (length) (0.0254 m × 0.915 m)	2.67	4.0	1.2	2.0	1.2	0 0190	0 0040	167 ft/s (51 m/s)	131 ft/s (40 m/s)	26 ft/s (8 m/s)
5 13.5" Utility Pole	13.5" (diam) × 35' (length) (0.343 cm × 10 68 m)	27.5-36.5 (e.g. 32)	40.8–54.2 (e.g. 47.5)	0.7	2 0	0.7	0.0254	0 0052	180 ft/s (55 m/s)	157 ft/s (48 m/s)	85 ft/s (26 m/s)
6 12" Sch. 40 Pipe	12.75" (diam) × 15' (length) (0.32 m × 4.58 m)	49.56	73.6	0.7	2 0	0.7	0.016	0 0033	154 ft/s (47 m/s)	92 ft/s (28 m/s)	23 ft/s (7 m/s)

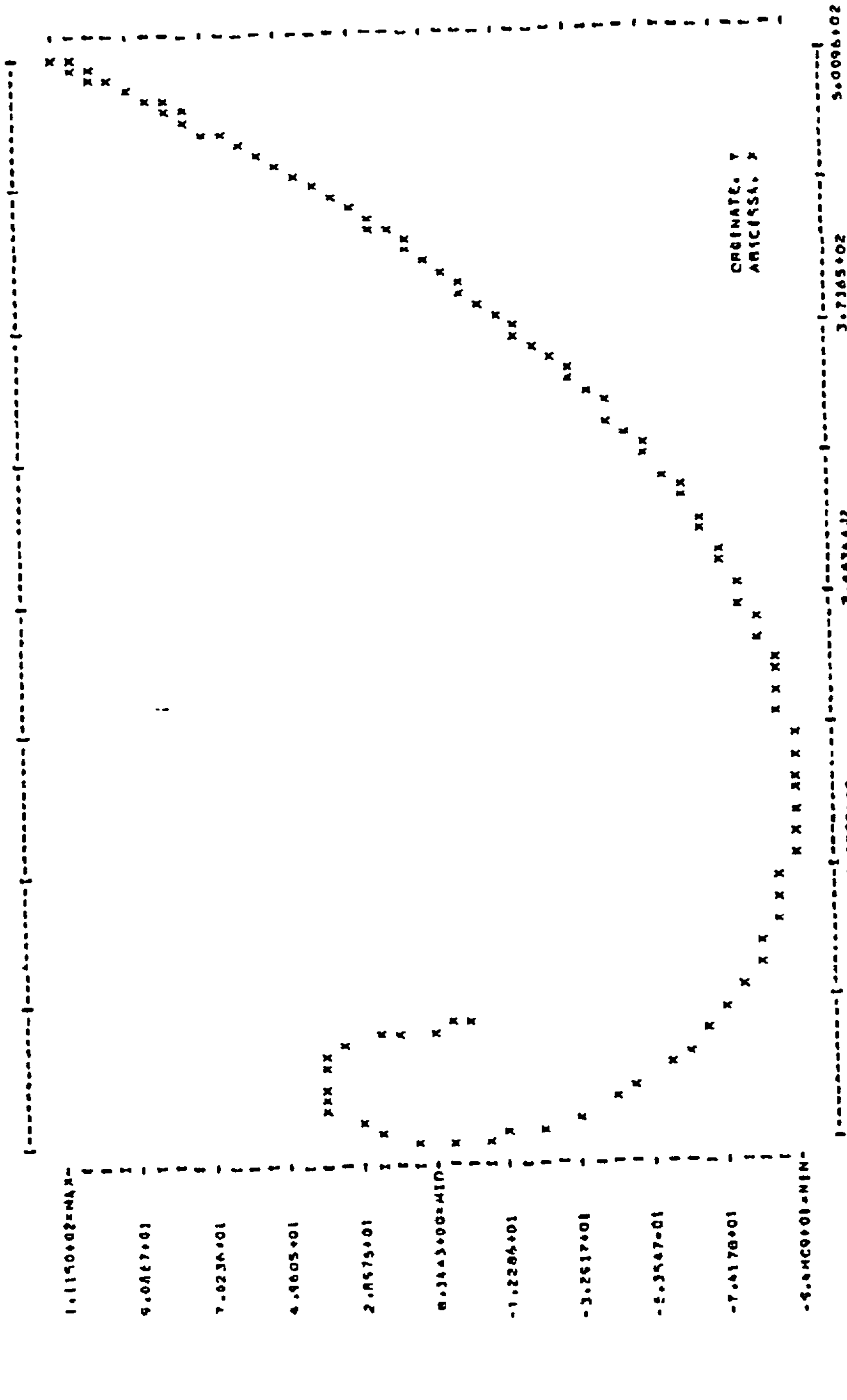

FIGURE 16.3.3. Horizontal projection of calculated missile trajectory (coordinates in meters).

Pacific Gas and Electric Company
Engineering - Calculation Sheet
Project: Diablo Canyon Unit ( )1 ( )2 (X) 1&2

Engineering
CALC. NO. 52.27.55.51
REV. NO. 0
SHEET NO. C-1 OF

SUBJECT Attachment C - Various Data Pertaining to Horizontal Wind Velocities for Tornado Missiles
MADE BY MB M. Brady DATE 11/09/99 CHECKED BY BS/ DATE

Attachment C

Basis for Various Data

Pertaining to Horizontal Wind Velocities for Tornado Missiles

As Derived from Figure 16.3.1 of

Wind Effects On Structures: Fundamentals and Applications to Design

To Facilitate Missile Hazard Assessments

Task: Establish a correlation power factor to convert the maximum horizontal missile velocity obtained by using the Tornado Type III curve for 240 mph tornado in Figure 16.3.1 from Wind Effects on Structures: Fundamentals and Applications to Design to the maximum horizontal missile velocity corresponding to a 200 mph tornado event when parameter C_DA/m equals 0.0048 m^2/kg.

A. Pertinent Data Per Figure 16.3.1

Per Figure 16.3.1 shown on Sheet A-8, the approximate corresponding maximum horizontal missile velocities, based on Tornado Type II and III curves when C_DA/m equals 0.0048 m^2/kg, are as follows:

Curve	Associated Tornado Velocity	V_H^{max}
Type II	300 mph	45.5 m/sec
Type III	240 mph	24.5 m/sec

B. Correlation Power Factor to Convert Maximum Horizontal Missile Velocity Associated With 300 Mph Tornado to Horizontal Missile Velocity Value Associated With 240 Mph Tornado

1. General Form for Relationship

Let the general form for the relationship of converting a known maximum horizontal missile velocity associated with a known higher tornado event to a maximum horizontal missile velocity corresponding to a known lower tornado event be as follows:

$$(V_H^{max})_{\text{lower tornado event}} = \left(\frac{V_{lower}}{V_{higher}}\right)^N (V_H^{max})_{\text{higher tornado event}}$$

where

V_{lower} = Lower tornado wind velocity event (mph) where corresponding maximum horizontal missile velocity is required for a specific C_DA/m parameter.

V_{higher} = Higher tornado wind velocity event (mph) where corresponding maximum horizontal wind velocity is defined by Figure 16.3.1 for a specific C_DA/m parameter.

N = Correlation Power Factor

$(V_H^{max})_{higher}$ = Maximum horizontal missile velocity for the higher tornado wind velocity event for a specific C_DA/m parameter.

$(V_H^{max})_{lower}$ = Maximum horizontal missile velocity for the lower tornado wind velocity event for a specific C_DA/m parameter.

2. Determine Correlation Power Factor (N) Using Pertinent Data From Section A

$$24.5 \text{ m/sec} = \left(\frac{240 \text{ mph}}{300 \text{ mph}}\right)^N (45.5 \text{ m/sec}) \quad \text{or}$$

$$(0.8)^N = 0.538$$

Therefore, $N = 2.78$

C. Use this Correlation Power Factor, i.e., 2.78, to convert corresponding maximum horizontal missile velocity associated with 240 mph tornado to horizontal missile velocity value associated with 200 mph tornado when parameter C_DA/m equals 0.0048 m^2/kg.

3. Check Kinetic Energy for Manhole Cover

$$E_s = \frac{M_m V_s^2}{2} = \frac{(11.62 \text{ lbs-sec}^2/\text{ft})(53 \text{ ft/sec})^2}{2} = 16{,}320 \text{ ft-lbs} < E_{s\,hyp} \text{ (i.e., 148.49 ft-k)}$$

ok

4. Check Local Effect Ratio for Concrete Targets

$$LERCT_{Hazard\ 2} = \frac{15.5\ W^{0.4}\ Vs^{0.5}}{D^{0.2}} = \frac{(15.5)(374)^{0.4}(53)^{0.5}}{(7.23)^{0.2}} = 812.47 > LERCT_{hyp} \text{ (i.e., 469.08)}$$

5. Check Local Effect Ratio for Steel Targets

$$LERST_{Hazard\ 2} = \frac{E_k^{2/3}}{D} = \frac{(16{,}320 \text{ ft-lbs})^{2/3}}{7.23} = 88.99 < LERST_{hyp} \text{ (i.e., 143.76)}$$ ok

6. Conclusion About Missile Hazard 2 (Circular Steel Access Manhole Covers)

   Since this missile hazard will induce more local damage than the design basis hypothetical missiles striking a concrete target, this missile hazard shall be anchored to prevent detachment and becoming a more severe missile hazard than the design basis hypothetical missiles.

C. Evaluation of Missile Hazard 3 (Rectangular Cast Iron Access Manhole Covers)

1. As identified in Section II.C, the rectangular cast iron manhole cover (lid), Neenah Type R6665-3FP, can become a tornado-induced missile. Per Attachment B and Table 2, the design characteristics for this specific cover are as follows:

   a. Weight

   m = (229 lbs) (1 kilogram/2.204622 lbs) = 103.9 kg

   b. Dimensions: 32" x 22" x 1.25"

   c. Areas

$$A_1 = (32")(22")\left[\frac{1 \text{ ft}^2}{144 \text{ in}^2}\right]\left[\frac{1 \text{ m}^2}{10.763910 \text{ ft}^2}\right] = 0.454 \text{ m}^2$$

$$A_2 = (32")(1.25")\left[\frac{1\ ft^2}{144\ in^2}\right]\left[\frac{1\ m^2}{10.763910\ ft^2}\right] = 0.026\ m^2$$

$$A_3 = (22")(1.25")\left[\frac{1\ ft^2}{144\ in^2}\right]\left[\frac{1\ m^2}{10.763910\ ft^2}\right] = 0.018\ m^2$$

d. Missile Mass

$$M_m = (229\ lbs)/(32.2\ ft/sec^2) = 7.11\ lbs\text{-}sec^2/ft$$

e. Equivalent Missile Diameter for Local Effects

To maximize local effects, use smallest area, i.e., $A = (22\ in.)(1.25") = 27.5\ in^2$

$$D = [(4)(27.5\ in^2)/\pi]^{0.5} = 5.92\ inches$$

2. Determine Maximum Horizontal Missile Velocity Per Section I.B.8

a. Parameter C_DA

$$C_DA = c\,(C_{D1}A_1 + C_{D2}A_2 + C_{D3}A_3)$$

$$C_DA = (0.5)\,[(2)(0.454\ m^2) + (2)(0.026\ m^2) + (2)(0.018\ m^2)] = 0.50\ m^2$$

b. Parameter C_DA/m

$$C_DA/m = (0.50\ m^2)/(103.9\ kg) = 0.0048\ m^2/kg$$

c. Maximum Horizontal Missile Velocity

Using $C_DA/m = 0.0048\ m^2/kg$ and correlation factor for 200 mph tornado wind as developed per Sheet C-3,

$$V_s = V_H^{max} = (24.5\ m/sec)\,[(3.280840\ ft)/(1\ m)]\,(200\ mph/240\ mph)^{2.78}$$

$$V_s \approx 48.4\ ft/sec$$

3. Check Kinetic Energy for Missile Hazard 3

$$E_s = \frac{M_m V_s^2}{2} = \frac{(7.11\ lbs\text{-}sec^2/ft)(48.4\ ft/sec)^2}{2} = 8{,}328\ ft\text{-}lbs < E_{s\ hyp}\ (\text{i.e., } 148.49\ ft\text{-}k)$$

ok

4. Check Local Effect Ratio for Concrete Targets

$$LERCT_{Hazard\ 3} = \frac{15.5\ W^{0.4}\ Vs^{0.5}}{D^{0.2}} = \frac{(15.5)\ (229)^{0.4}\ (48.4)^{0.5}}{(5.92)^{0.2}} = 664.15 > LERCT_{hyp}\ \text{(i.e., 469.08)}$$

5. Check Local Effect Ratio for Steel Targets

$$LERST_{Hazard\ 3} = \frac{E_k^{2/3}}{D} = \frac{(8{,}328\ \text{ft-lbs})^{2/3}}{5.92} = 69.42 < LERST_{hyp}\ \text{(i.e., 143.76)}\ \underline{\text{ok}}$$

6. Conclusion About Missile Hazard 3 (Rectangular Cast Iron Access Manhole Covers)

Since this missile hazard will induce more local damage than the design basis hypothetical missiles striking a concrete target, this missile hazard shall be anchored to prevent detachment and becoming a more severe missile hazard than the design basis hypothetical missiles.

D. Evaluation of Missile Hazard 4 (Another Rectangular Cast Iron Access Manhole Cover Size)

1. As identified in Section II.C, this rectangular cast iron manhole cover (lid) can become a tornado-induced missile. Per Table 2, the design characteristics for this specific cover are as follows:

a. Weight

$$m = (332\ \text{lbs})\ (1\ \text{kilogram}/2.204622\ \text{lbs}) = 150.6\ \text{kg}$$

b. Dimensions: 49" x 26" x 1"

c. Areas

$$A_1 = (49")\ (26")\ \left[\frac{1\ ft^2}{144\ in^2}\right]\left[\frac{1\ m^2}{10.763910\ ft^2}\right] = 0.822\ m^2$$

$$A_2 = (49")\ (1.00")\ \left[\frac{1\ ft^2}{144\ in^2}\right]\left[\frac{1\ m^2}{10.763910\ ft^2}\right] = 0.032\ m^2$$

$$A_3 = (26")\ (1.00")\ \left[\frac{1\ ft^2}{144\ in^2}\right]\left[\frac{1\ m^2}{10.763910\ ft^2}\right] = 0.017\ m^2$$

ATTACHMENT

5-1

file copy

69-20132 04/10/00

NUCLEAR POWER GENERATION
CF3.ID4
ATTACHMENT 7.2

INDEX No. 402
BINDER No. 2004

umt 11/9/01

TITLE: Determination of Thermal and Shrinkage Values for the ISFSI Concrete Pad Design

Unit(s): 1&2 File No.: 52.27

Responsible Group: NCFC Calculation No.: 52.27.100.701

No. of Pages ~~58~~ 59 Design Calculation YES ☒ NO GK 10/16/01

System No. 42C GK 11/8/01 Quality Classification X Q GK 11/8/01

Structure, System or Component: ISFSI Foundation Pad -Thermal and Shrinkage Values

Subject: Thermal and Shrinkage Values for the ISFSI concrete pad design.

Electronic calculation YES ☐ NO X

Computer Model	Computer ID	Program Location	Date of Last Change
NA			
NA			

Registered Engineer Stamp: Complete A or B

A. Insert PE Stamp or Seal Below

REGISTERED PROFESSIONAL ENGINEER
ANTON D PIRTZ
Anton D Pirtz
35282
CIVIL
STATE OF CALIFORNIA

Expiration Date: 9/20/03

B. Insert stamp directing to the PE stamp or seal

REGISTERED ENGINEERS' STAMPS AND EXPIRATION DATES ARE SHOWN ON DWG 063618.

NOTE 1: Update DCI promptly after approval.

NOTE 2: Forward electronic calculation file to CCTG for uploading to EDMS.

CF3.ID4
ATTACHMENT 7.2

TITLE: Determination of Thermal and Shrinkage Values for the ISFSI Concrete Pad Design

RECORD OF REVISIONS

CALC No. 52.27.100.701

Rev No.	Status	Reason for Revision	Prepared By:	LBIE Screen	LBIE	Check Method*	LBIE Approval		Checked	Supervisor	Registered Engineer
		Remarks	Initials/ LAN ID/ Date	Yes/ No/ NA	Yes/ No/ NA		PSRC Mtg. No.	PSRC Mtg. Date	Initials/ LAN ID/ Date	Initials/ LAN ID/ Date	Signature/ LAN ID/ Date
0	F	Provide Thermal and Shrinkage Values for ISFSI concrete Pad design	[signature] ADP2 5/7/01	☐ Yes ☒ No ☐ NA	☐ Yes ☐ No ☒ NA	☐ A ☐ B ☐ C	NA	NA	CFK1 [signature] 5/7/01	DAW1 [signature] 5/8/01	[signature] ADP2 5/8/01
1	F	Provide aggregate properties, early compressive strength values and thermal expansion value See Shts 48,49,50	[signature] ADP2 10/11/01	☐ Yes ☒ No ☐ NA	☐ Yes ☐ No ☒ NA	☐ A ☐ B ☐ C	NA	NA	[signature] CFK1 10/11/2001	[signature] DAW1 10/11/01	[signature] ADP2 10/11/01
2	F	Added Shrinkage/Depth of Concrete Curve & Temperature at Pad Surface See sht 51 thru 59	[signature] ADP2 11/8/01	☐ Yes ☒ No ☐ NA	☐ Yes ☐ No ☒ NA	☒ A ☐ B ☐ C	NA	NA	[signature] CFK1 11/8/01	[signature] DAW1 11/8/01	[signature] ADP2 11/8/01
				☐ Yes ☐ No ☐ NA	☐ Yes ☐ No ☐ NA	☐ A ☐ B ☐ C					
				☐ Yes ☐ No ☐ NA	☐ Yes ☐ No ☐ NA	☐ A ☐ B ☐ C					

*Check Method: A: Detailed Check, B: Alternate Method (note added pages), C: Critical Point Check

SUBJECT Determination of Thermal and Shrinkage Values for the ISFSI Concrete Pad Design

MADE BY ADP DATE 5/7/01 CHECKED BY Carl Knifton DATE 5/7/01

DETERMINATION OF SHRINKAGE AND THERMAL VALUES FOR THE DCPP ISFSI CONCRETE PAD DESIGN

PURPOSE:

The purpose of this calculation is to document the determination of thermal and shrinkage values for the ISFSI Concrete Pad design. The requested physical properties of hardened concrete for the ISFSI Foundation Pad are:

- Expected shrinkage values of pad concrete
- Expected heat rise of pad
  - At 0.5' intervals of the pad
  - At concrete/rock interface
  - At concrete surface
- Expected heat rise of rock below pad
  - At 0.5' intervals to a depth of 4 feet

BACKGROUND:

To obtain the expected shrinkage and heat rise values of hardened concrete for the ISFSI Foundation Pad, a concrete mix to be use is required. TES Report # 420DC-96.160 "DIABLO CANYON POWER PLANT - ASW BYPASS PROJECT THRUST BLOCK "Q" CLASS CONCRETE MIX DESIGNS - Using Type II Cement, Santa Margarita Granite Aggregates and SP Milling's Standard Admixtures" was used to develop the requested values. The TES report was issued January 13, 1997. The values from this report will be referred to as 'Thrust Block Values' subsequently in this calculation.

IMPACT OF OTHER DCPP DOCUMENTS:

No impact of other DCPP documents.

REFERENCES:

1. TES REPORT 420DC-96.160
   Included as Appendix A.

SUBJECT Determination of Thermal and Shrinkage Values for the ISFSI Concrete Pad Design

MADE BY ADP DATE 5/7/01 CHECKED BY Carl Knifton DATE 5/7/01

ASSESSMENT:

Concrete Mix Design Determination

Several assumptions are required to determine the concrete mix.

1. The concrete materials to be used:

   Cement: Type II
   Pozzolan: Fly Ash, Class F
   Fine Aggregate: Crushed granite, Santa Margarita Quarry
   Coarse Aggregate: 1-1/2" MSA Crushed granite, Santa Margarita Quarry
   Admixtures:
   Water reducer: WRDA-55, Grace Construction Products
   Air Entraining: DAREX II AEA, Grace Construction Products

   The cement, pozzolan, fine and coarse aggregates and admixtures are the same type as used for the 'Thrust Block Values'. The maximum size of coarse aggregate to be used for the pad is 1-1/2". The change from ¾" to 1-1/2" MSA will change the water requirement for the mix insignificantly.

2. The desired slump at the site is 4 inches (+/- 1 inch).

3. Based on the exposure conditions entrained air content of 6% (+/- 1%) is desirable.

4. The specified compressive strength is 5000 psi for this mix design, at an age of 90 days. It was agreed to use the 90-day age for the compressive strength determination due to the fact that the storage casks will not be placed on the pad immediately upon completion of the pad. As required by ACI 318 the required average compressive strength for the mix will be increased by 600 psi. This increase will ensure that the probability of test cylinders will not be below the specified compressive strength. Therefore this concrete will be designed for a compressive strength of 5600 psi, at an age of 90 days.

Selecting and adjusting the concrete mix design proportions was conducted in accordance with ACI 211 "Standard Practice for Selecting Proportions for Normal, Heavyweight and Mass Concrete". The method used for selecting and adjusting the concrete mix design proportions is based on the absolute volume occupied by the concrete ingredients. The mix design selection took into consideration the requirements for placeability, consistency, strength and durability

SUBJECT Determination of Thermal and Shrinkage Values for the ISFSI Concrete Pad Design

MADE BY ADP DATE 5/7/01 CHECKED BY Carl Knifton DATE 5/7/01

To reduce the heat generated the flyash percentage was increased from 22.7% to 25% by weight of cement. A value of 25% flyash by weight of cement is normally the maximum used in typical applications.

Using the 'Thrust Block Values' to obtain the required compressive strength the cement quantity will be required to increase and the water to cementitious (w/c) ratio will be required to decrease. The simplest solution to obtain the required compressive strength would be to simply increase the cement quantity. But this solution would increase the heat generated significantly.

Using data from Table 1 and Figure 1 (TES Report) of the 'Thrust Block Values' a w/c ratio of 0.45 is necessary. The air content of the Thrust Block mix design was 3%, the pad desired air content is 6%. This 3% increase in air content will reduce the compressive strength significantly. Due to the increased air content the w/c will need to be decreased by 0.02 to increase the compressive strength. Thus a w/c ratio of 0.43 is required. From past experience with the crushed granite aggregates a w/c of 0.45 is the minimum that can be practically obtained. Therefore a w/c of 0.45 will be used, this will require a slight increase in the cement content.

The increase in cement content will be determined using data from the 'Thrust Block Values', mix design "THR-A Trial", which has a w/c of 0.46. This mix design has the lowest and closest w/c to that to be used for the ISFSI pad. Since no additional data is available an approximation will be used, compressive strength per pound of cement will be used to calculate the additional cement required. Since the fly ash content for each mix will be similar and the flyash will not significantly effect the 28-day compressive strength, only the cement content will be used to calculate the required increase. "THR-A Trial" contains 562 lbs. of cement and had a compressive strength of 4870 psi at 28 days. The required compressive strength of at 28 days for the ISFSI pad is 5100 psi.

Concrete Mix Design

Increase weight of cement

4870 psi / 562 lbs. of cement = 8.66 psi/ lb. of cement

5100 psi - 4870 psi = 230 psi

230 psi / 8.66 psi/ lb. of cement = 26.5 lbs. of cement

562 lbs. of cement + 26.5 lbs. of cement = 588.5 lbs. of cement

Use 590 lbs. of cement

Use 25% flyash by weight of cement

SUBJECT Determination of Thermal and Shrinkage Values for the ISFSI Concrete Pad Design

MADE BY ADP DATE 5/7/01 CHECKED BY Carl Knifton DATE 5/7/01

590 lbs. cement * 0.25 = 147.5 lbs flyash

Use 148 lbs. of flyash

Weight of water use 0.45 w/c

(590 lbs. cement + 148 lbs. of flyash) * 0.45 = 332.1 lbs water

Use 332 lbs of water

Absolute Volume of material

Weight of material / (Specific Gravity * Unit weight of water)

= material volume, cu. ft.

Volume of cement

590 lbs / (3.15 * 62.4) = 3.00 cu. ft.

Volume of flyash

148 lbs / (2.30 * 62.4) = 1.03 cu. ft.

Volume of water

332 lbs / (1.00 * 62.4) = 5.32 cu. ft.

Volume of air

0.06 % air * 27 cu. ft./ cu. yd. = 1.62 cu. ft.

Volume of (cement + flyash + water + air)

3.00 + 1.03 + 5.32 +1.62 = 10.97 cu. ft.

Aggregate volume

27 cu. ft. - 10.97 cu. ft. = 16.03 cu. ft.

From the 'Thrust Block Values' the ratio of fine aggregate to total aggregate was 0.46

Volume of fine aggregate

16.03 cu. ft. * 0.46 = 7.37 cu. ft.

7.37 cu. ft. * (2.60 * 62.4) = 1195.7 lbs

Use 1195 lbs fine aggregate

Volume of coarse aggregate

Aggregate volume - Volume of fine aggregate = Volume of coarse aggregate

16.03 cu. ft. - 7.37 cu. ft. = 8.66 cu. ft.

SUBJECT Determination of Thermal and Shrinkage Values for the ISFSI Concrete Pad Design

MADE BY ADP DATE 5/7/01 CHECKED BY Carl Knifton DATE 5/7/01

8.66 cu. ft. * (2.62 * 62.4) = 1415.8 lbs

Use 1415 lbs coarse aggregate

Use nearly equal amounts of 3/4 " and 1-1/2" coarse aggregate

1415 lbs / 2 = 707.5 lbs

Use 705 lbs of 3/4" Fine Aggregate

Use 710 lbs of 1-1/2" Coarse Aggregate

Water reducing Admixture

The 'Thrust Block' mix used 13 oz / 100 lbs of cementitious material this mix should require a slightly greater amount, use 15 oz / 100 lbs of cementitious material. Trial mixes should determine the final dosage, this dose will provide a sufficient starting point.

15 oz. * (590 lbs. cement + 148 lbs flyash) / 100 = 110.7 oz. / cu. yd.

Use 111 oz. Water reducing Admixture / cu. yd.

Air Entraining Admixture

The 'Thrust Block' mix used 1.1 oz / 100 lbs of cementitious material. The air content of the Thrust Block mix design was 3%, the pad desired air content is 6%. To achieve the required air content the manufacture recommends the use of 2.5 oz. / 100 lbs of cementitious material. Trial mixes should determine the final dosage, this dose will provide a sufficient starting point.

2.5 oz. * (590 lbs. cement + 148 lbs flyash) / 100 = 18.5 oz. / cu. yd.

Use 19 oz. Air Entraining Admixture / cu. yd.

The estimated compressive strength vs. age for this mix design is shown on Figure 1. Table 1 below shows the Thrust Block and ISFSI Pad mix design. These mix designs meet the requirements of ACI 318.

SUBJECT Determination of Thermal and Shrinkage Values for the ISFSI Concrete Pad Design

MADE BY ADP DATE 5/7/01 CHECKED BY Carl Knifton DATE 5/7/01

Table 1
Mix Design Summary

Material	Specific Gravity	Thrust Block	ISFSI Pad	ISFSI Pad Volume
Cement, lbs	3.15	550	590	3.00
Flyash, lbs	2.3	125	148	1.03
Water, lbs	1	327	332	5.32
Santa Margarita Fine Agg. lbs	2.6	1295	1195	7.37
Santa Margarita 3/4" Agg. lbs	2.62	1520	705	4.31
Santa Margarita 1-1/2" Agg. lbs	2.62	0	710	4.34
WRA, oz. (WRDA 55)		84.4	111	
AEA, oz. (DAREX II)		7.4	19	
Weight per CU. YD.		3824	3680	
Sacks per Yard		5.85	6.28	
Water/Cementitious Ratio		0.48	0.45	
Fine Agg./Total Agg.		0.46	0.46	
Properties				
Slump, in		4	4	
Air, % (+/-1)		3	6	
Compressive Strength, psi		4200	5600	

SUBJECT Determination of Thermal and Shrinkage Values for the ISFSI Concrete Pad Design

MADE BY ADP DATE 5/7/01 CHECKED BY Carl Knifton DATE 5/7/01

Drying Shrinkage Values Determination

The drying shrinkage for the ISFSI pad concrete will be similar to that of the Thrust Block concrete. The mixes have similar materials and proportions.

- Factors affecting drying shrinkage
  - Water / Cement Ratio
    - Major effect – decrease in W/C will decrease shrinkage
  - Total Aggregate Content
    - Very Major effect – decrease in aggregate content will increase shrinkage
  - Maximum size of aggregate
    - Major effect – increase in MSA will decrease shrinkage
  - Total volume of cementitious material
    - Major effect – increase in cementitious material will increase shrinkage
  - Water content
    - Very minor effect - water content very similar
  - Total volume of aggregate material
    - Minor effect - volume of aggregate similar

The effect of Water/Cement Ratio will decrease the shrinkage and the effect of Total Aggregate Content will increase the shrinkage. Based on the graph of w/c ratio and aggregate content verses shrinkage, "Properties of Concrete" by A. M. Neville", the combined effect will increase the shrinkage by 14.2%.

Increase in shrinkage due to w/c ratio and aggregate content = 14.2%

The effect of maximum size of aggregate will decrease the shrinkage. Based on literature review and engineering judgment this effect will reduce the shrinkage by approximately 7% to 15%.

Decrease in shrinkage due maximum size of aggregate = 11%

The effect of total volume of cementitious material increase will increase the shrinkage in a linear manner, at a 10 to 1 ratio (for each 10% increase in cementitious material the shrinkage will increase 1%). The percentage increase in cementitious material will relate directly to an increase in shrinkage.

Volume of cementitious for Thrust Block
550 lbs cement + 125 lbs flyash = 675 lbs
Volume of cementitious for ISFSI pad
590 lbs cement + 148 lbs flyash = 738 lbs
Increase in cementitious material for ISFSI pad
(738 lbs - 675 lbs) * 100 / 675 lbs
Increase in cementitious material = 9.3%
Increase in shrinkage due to an increase in cementitious material
9.3% / 10 = 0.93%

SUBJECT Determination of Thermal and Shrinkage Values for the ISFSI Concrete Pad Design

MADE BY ADP DATE 5/7/01 CHECKED BY Carl Knifton DATE 5/7/01

The effect of water content and total volume of aggregate material will be neglected since their effect in minor.

Their combined effect to the shrinkage will be.
+14.2% - 11% + 0.9% = 4.1 %

The drying shrinkage for the ISFSI pad concrete will be increased by 4.1% to that of the Thrust Block concrete. The calculated shrinkage results for the ISFSI pad are shown on Figure 2.

Thermal Values Determination

Problem

Determine the expected heat rise for the concrete ISFSI Foundation Pad.

1. Calculate and plot the heat rise of pad at 0.5 foot intervals.
2. Calculate and plot the heat rise of pad at concrete/rock interface.
3. Calculate and plot the heat rise of the rock below the pad at 0.5 foot intervals to a depth of 4 feet.
4. Calculate and plot the heat rise of pad at concrete surface.

Solution

To determine the heat rise due to cement hydration at a given location in a mass of concrete the actual temperature gradients need to be determined. The Schmidt's method (Rawhouser 1945) (ACI 207.1R – Mass Concrete) has proven to be a reliable and useful method to determine actual temperature gradients. The Schmidt's method is based on the theorem that if the body under question is considered to be divided into a number of equal elements, and if a number of physical limitations are satisfied simultaneously, the temperature for a given increment at the end of an interval of time is the average of the temperature of the two neighboring elements at the beginning of that time interval. The necessary physical relationship is

$$\Delta t = (\Delta x)^2 / 2h^2$$

Where Δt is the time interval, Δx is the length of element, and h^2 is the diffusivity constant. Unit of Δt and Δx must be consistent with units in which h^2 is expressed. Stated mathematically, θ_p, θ_q and θ_r are the temperatures of three successive elements at time t, then at time t_2

$$\theta_q + \Delta\theta_q = \tfrac{1}{2}(\theta_p + \theta_r)$$

ISFSI Slab and Rock Heat Rise Determination

The one-dimensional case can be used for this analysis. To determine temperature rise throughout a lift of concrete using this method the $\Delta\theta$ is required. The $\Delta\theta$ is determined from the adiabatic

SUBJECT Determination of Thermal and Shrinkage Values for the ISFSI Concrete Pad Design

MADE BY ADP DATE 5/7/01 CHECKED BY Carl Knifton DATE 5/7/01

temperature rise results of a given concrete mix. Adiabatic temperature rise results for this concrete mix are not available. To obtain the adiabatic temperature information required, data from the TES report will be used:

> "To obtain an approximation of the heat rise of the thrust blocks, a four-foot concrete cube test specimen was cast. The results of temperature rise above ambient of the center of the 4 ft. concrete cube test specimen are shown in Figure 5 (TES Report)1. This test cube was insulated from ambient temperature variations. The concrete at three separate locations 1 inch in the concrete from the surface, varied +/- 1.9 degrees F. in temperature for the duration of the test (8 days)."

To determine temperature rise throughout a lift of concrete and the rock below the diffusivity of each material needs to be determined. Using the Schmidt's method for both the trial and error method to determine the adiabatic temperature rise result and then using these adiabatic temperature rise results to determine the heat rise of the ISFSI pad, the diffusivity value for both evaluations does not need to be determined to obtain accurate results. For this analysis a value of 1.0 ft^2/day will be used for the concrete diffusivity. Based on literature review of the rock type at the ISFSI site, a rock diffusivity value of 1.0 ft^2/day will be used.

Determination Adiabatic Temperature Rise Curve from the Thrust Block Data

A trial and error method will be used to determine the adiabatic temperature rise result. The results of the temperature rise above ambient of the center of the 4 ft. concrete cube test specimen will be used. From the insulated cube and the known temperature at the center the required information can be determined using the Schmidt's method.

For this is analysis the values to be used will be:

$\Delta x = 0.5$ ft
$h = 1.0$ ft^2/day for the concrete
$h = 1.0$ ft^2/day for the rock

$\Delta t = (\Delta x)^2 / 2h^2$
$\Delta t = (0.5)^2 / (2 * 1.0\ ft^2/day^2)$
$\Delta t = 0.125$ days

The calculations required were performed in an Excel spreadsheet. The spreadsheet works well because the calculations are simple and repetitive in nature. Once the thickness, 4 foot, for the 'Thrust Block' test specimen and the first time period 0.125 days calculations are completed, the first time period formulas can be copied to the next time period and so on until the maximum required time period is reached.

SUBJECT Determination of Thermal and Shrinkage Values for the ISFSI Concrete Pad Design

MADE BY ADP DATE 5/7/01 CHECKED BY Carl Knifton DATE 5/7/01

Table 2 below shows the results for the first half day of the 4-foot test cube. The columns are labeled with letters and the rows are labeled with numbers. A location in the spreadsheet will be denoted by the column then the row, 'B1' is column B row 1. Row '1' is the time in days. Row '2' is the trial temperature rise, values shown are the final results. Values were placed in Row '2' initial using engineering judgment on what the final heat rise curve should look like. Row '2' values were varied to achieve a match at the center, 2-foot results to those of the 'Thrust Block' test cube. The 'B3' value 'Factor' is used to multiply the Row '2' values to obtain large corrections to the trail temperature rise values. Row '4' is the final incremental temperature rise, it is obtained by multiplying row '2' by 'Factor'. The adiabatic temperature rise at a given time is calculated by summing the previous incremental temperature rise values. Column 'A' rows '7' to '15' are the cube depths in feet, 4 ft. being the top.

Table 2

Spreadsheet for the 4-Foot Test Cube

	A	B	C	D	E	F	G	H	I	J
1	Time, days	0	0.13		0.25		0.38		0.50	
2	Trial Temperature Rise		5.00		11.00		10.00		9.00	
3	Factor	1.2191								
4	Temperature Rise		6.10		13.41		12.19		10.97	
5										
6	Cube depth									
7	4.00	0.00	0.00			0.00	0.00			0.00
8	3.50	0.00	6.10	3.05	16.46			15.09	26.06	
9	3.00	0.00	6.10			17.98	30.17			33.98
10	2.50	0.00	6.10	6.10	19.51			30.93	41.91	
11	2.00	0.00	6.10			19.51	31.70			41.91
12	1.50	0.00	6.10	6.10	19.51			30.93	41.91	
13	1.00	0.00	6.10			17.98	30.17			33.98
14	0.50	0.00	6.10	3.05	16.46			15.09	26.06	
15	0.00	0.00	0.00			0.00	0.00			0.00

SUBJECT Determination of Thermal and Shrinkage Values for the ISFSI Concrete Pad Design

MADE BY ADP DATE 5/7/01 CHECKED BY Carl Yrafton DATE 5/7/01

Column 'B' rows '7' to '15' are the initial temperatures of the cube, the ambient temperature was subtracted from the test results since the test specimen was insulated therefore the adiabatic temperature rise is not affected significantly by ambient temperature. The temperature at the cube surface is the ambient temperature, therefore it is always '0'. Rows '7' and '15' are the cubes surface, these will always have values of '0'.
For the first time interval the temperature is equal to the incremental temperature rise value, column 'C' rows '8' to '14', the value is 6.10.

The value at;	'D8' = (C7+C9)/2	= 3.05	= ½ ($\theta_p + \theta_r$)
	'D10' = (C9+C11)/2	= 6.10	= ½ ($\theta_p + \theta_r$)
	'D12' = (C11+C13)/2	= 6.10	= ½ ($\theta_p + \theta_r$)
	'D14' = (C13+C15)/2	= 3.05	= ½ ($\theta_p + \theta_r$)
	'E4'	= 13.41	incremental temperature rise at 0.25 days
	'E8' = E4+D8	= 16.46	= + the $\Delta\theta_q$ for the element
	'E10' = E4+D10	= 19.51	= + the $\Delta\theta_q$ for the element
	'E12' = E4+D12	= 19.51	= + the $\Delta\theta_q$ for the element
	'E14' = E4+D14	= 16.46	= + the $\Delta\theta_q$ for the element
	'F7' = 0	= concrete surface	
	'F9' = (E8+E10)/2	= 17.98	= ½ ($\theta_p + \theta_r$)
	'F11' = (E10+E12)/2	= 19.51	= ½ ($\theta_p + \theta_r$)
	'F13' = (E12+E14)/2	= 17.98	= ½ ($\theta_p + \theta_r$)
	'F15' = 0	= concrete surface	
	'G7' = 0	= concrete surface	
	'G4'	= 12.19	incremental temperature rise at 0.38 days
	'G9' = G4+F9	= 30.17	= + the $\Delta\theta_q$ for the element
	'G11' = G4+F11	= 31.70	= + the $\Delta\theta_q$ for the element
	'G13' = G4+F13	= 30.17	= + the $\Delta\theta_q$ for the element
	'G15' = 0	= concrete surface	

With these formulas entered and checked columns 'D' to 'G' row '7' to '15' can be copied and pasted to the following time intervals until the required maximum time period is reached. The complete spreadsheet is shown in appendix B. The calculated adiabatic temperature rise curve from the thrust block data is plotted below on Figure 3.

Determination Adiabatic Temperature Rise Curve for the ISFSI Pad

SUBJECT Determination of Thermal and Shrinkage Values for the ISFSI Concrete Pad Design

MADE BY ADP DATE 5/7/01 CHECKED BY Carl Knifton DATE 5/7/01

Since the ISFSI pad concrete mix design is different than the Thrust Block mix design the adiabatic temperature rise result will need to be modified. This modification will be linear due to fast similar materials are used in each mix. The main factor in the adiabatic temperature rise is the quantity of cement. The ISFSI pad concrete mix design has more cementitious material than the Thrust Block mix design, thus the adiabatic temperature rise result will be increased.

The increase to the adiabatic temperature rise due to an increase in cementitious material will be linear. The Type F used will have ½ the impact in the heat rise as the cement.

Increase in the weight of cement
590 lbs cement - 550 lbs cement = 40 lbs cement
Increase in the weight of flyash
148 lbs flyash - 125 lbs flyash = 23 lbs flyash
23 lbs flyash / 2 = 11.5 lbs cement - equivalent due to heat rise
Increase in cementitious material for ISFSI pad
40 lbs cement + 11.5 lbs cement = 51.5 lbs cement
Percentage increase in adiabatic temperature rise due to increase in cementitious material
51.5 lbs cement * 100 / 550 lbs cement = 9.36%

The values of the calculated adiabatic temperature rise curve for the thrust block will be multiplied by 9.36% to obtain the adiabatic temperature rise curve for the ISFSI pad concrete.
Adiabatic temperature rise at 8 days for thrust block
98.1 degrees
Adiabatic temperature rise at 8 days for ISFSI pad
98.1 degrees * 1.0936 = 107.3

The calculated adiabatic temperature rise curve corrected for the ISFSI pad concrete mix design is plotted on Figure 4.

Determination of Temperature Rise for the ISFSI Pad

The calculated adiabatic temperature rise curve corrected for the ISFSI pad concrete mix design was used to calculate the expected heat rise of the pad:
At 0.5 foot intervals of pad
At concrete/rock interface
And heat rise of the rock below the pad at 0.5 foot intervals to a depth of 4 feet

The calculations required were performed in an Excel spreadsheet. The same format and calculations were used for this calculation as the calculation to determine Thrust Block heat rise. The 'B3' value 'Factor' which is used to multiply the Row '2' values to obtain large corrections was increased by 9.36% to obtain the adiabatic temperature rise curve for the ISFSI pad concrete. Row '4' is the final incremental temperature rise, it is obtained by multiplying row '2' by 'Factor'.

Value of 'B3' 'Factor'
1.2191 for the 4-foot Test Cube
1.2191 * 1.0936 = 1.3332
Value of 'B3' 'Factor'
1.3332 for the ISFSI pad concrete

The thickness of concrete was increased to 8-foot and the thickness of rock was increased to 4-feet. Once the changes were made and first time period calculations were completed and checked, the first time period formulas were copied to the next time period and so on until the maximum required time period is reached.

The results are summarized in Table 3. The complete spreadsheet is shown in appendix B. The maximum concrete temperature of 87.13 degrees in the slab occurred at 2.375 days at a depth of 3-feet (5-feet from the surface).

<u>Expected heat rise of pad at concrete surface</u>
The Schmidt's method used to determine the temperature rise assumes that surface temperature is the ambient temperature, therefore it is always '0'. But this is not precisely true. At early ages when the incremental heat rise is comparatively large the surface will be greater than '0'. The greatest incremental heat rise occurs at 0.5 days. Therefore it is assumed that the greatest pad surface temperature will occur at 0.5 days. Upon examination of the thermal gradient at 0.5 days it appears that the pad surface temperature will be very nearly the temperature at 0.5 foot (slab thickness of 7.5 feet), which is 28.5 degrees. The pad surface will reduce after 0.5 days and approach the ambient temperature.

SUBJECT Determination of Thermal and Shrinkage Values for the ISFSI Concrete Pad Design

MADE BY ADP DATE 5/7/01 CHECKED BY Carl Knifton DATE 5/7/01

Table 3

THE CONCRETE TEMPERATURE

Time, Days / Depth,ft	0.000	0.125	0.250	0 375	0.500	0.625	0.750	0.875	1.000	1.125	1.250	1.375	1.500
7.5	0.00	6.67	18.00		28.50		25.79		21.36		18.05		15.26
7	0.00	6.67		33 00		38.24		33.39		29.43		25.84	
6.5	0.00	6.67	21.33		29.33		30.33		29.50		28.31		26.69
6	0.00	6.67		34 66		47.33		49.66		49.95		48.72	
5.5	0.00	6.67	21.33		46.66		58.33		62.41		63.80		63.20
5	0 00	6.67		34 66		55.99		65.82		70.99		73.01	
4.5	0.00	6.67	21.33		46.66		62.66		71.57		76 88		79.27
4	0.00	6.67		34.66		55.99		67.99		76.10		80.87	
3.5	0 00	6.67	21.33		46.66		62.66		72.63		79.54		83.56
3	0.00	6.67		34.66		55.99		67.94		76.31		81.59	
2.5	0.00	6.67	21.33		46.66		62.55		71.98		78.31		81.97
2	0.00	6.67		34.66		55.78		66.70		73.64		77.68	
1.5	0.00	6.67	21.33		46.24		60.18		67.30		71.71		73.95
1	0.00	6.67		33.83		51.24		58.56		63.12		65.55	
0.5	0.00	6.67	19.66		37.58		46.29		50.95		54.06		55.77
0	0.00	3.33		17.33		28.00		34.00		38.33		41.33	
-0.5	0.00	0.00	1.67		9 08		16.37		21.71		25.93		29.22
-1	0.00	0.00		0.83		4.75		9.43		13.53		17.10	
-1.5	0.00	0.00	0.00		0 42		2.48		5.36		8.27		11.04
-2	0.00	0.00		0.00		0.21		1.29		3.02		4.98	
-2.5	0.00	0.00	0.00		0 00		0.10		0.67		1.68		2.95
-2	0.00	0.00		0.00		0.00		0.05		0.35		0.93	
-3.5	0.00	0.00	0.00		0.00		0.00		0.03		0.18		0.51
-4	0.00	0.00		0.00		0.00		0.00		0.01		0.09	

SUBJECT Determination of Thermal and Shrinkage Values for the ISFSI Concrete Pad Design

MADE BY ADP DATE 5/7/01 CHECKED BY Carl Knifton DATE 5/7/01

Table 3 (Cont.)

THE CONCRETE TEMPERATURE

Time, Days / Depth,ft	1.625	1.750	1.875	2.000	2.125	2 250	2.375	2.500	2.625	2.750	2.875	3.000	3.125
7.5		13.15		11.64		10.66		9.75		8.85		8.34	
7	22.97		20.61		18.91		17.63		16.36		15.35		14.56
6.5		25.14		23 79		22.74		21.65		20.51		19.71	
6	46.95		44.91		43.08		41.43		39.69		38.09		36.69
5.5		61.76		59.96		58.25		56.40		54.35		52.59	
5	73.24		72.34		71.02		69.51		67.67		65.76		63.91
4.5		79.99		79.68		78.90		77.61		75.84		74.16	
4	83.42		84.34		84.38		83.84		82.68		81.22		79.64
3.5		85.76		86.68		86.92		86 42		85.26		84.05	
3	84.76		86.36		87.05		87.13		86.52		85.55		84.41
2.5		84.03		85.02		85.47		85.29		84.51		83.69	
2	79.96		81.02		81.49		81.58		81.16		80.50		79.73
1.5		75.07		75.55		75.83		75.71		75.16		74.71	
1	66.86		67.43		67.77		67.97		67.83		67.58		67.31
0.5		56.84		57.58		58.24		58.61		58.66		58.85	
0	43.49		45.06		46.32		47.38		48.16		48.79		49.32
-0.5		31.81		33.87		35.59		37.05		38.25		39.27	
-1	20.13		22.69		24.85		26.71		28.34		29.75		30.97
-1.5		13.56		15.83		17.84		19.63		21.24		22.68	
-2	7.00		8 96		10.82		12.55		14.14		15.61		16.94
-2.5		4.37		5.82		7.26		8.65		9.97		11.20	
-2	1.73		2.68		3.71		4.76		5.80		6.80		7.76
-3.5		0 99		1.59		2.25		2.94		3.63		4.31	
-4	0.26		0.50		0.79		1.12		1.47		1.82		2.15

Pacific Gas and Electric Company
Engineering - Calculation Sheet
Project: Diablo Canyon Unit ( )1 ( )2 (X) 1&2

CALC. NO. 52.27.100.701
REV. NO. ~~0~~ 1 10/16/01
SHEET NO 16 OF 47

SUBJECT Determination of Thermal and Shrinkage Values for the ISFSI Concrete Pad Design

MADE BY ADP DATE 5/7/01 CHECKED BY Carl Knifton DATE 5/7/01

Table 3 (Cont.)

THE CONCRETE TEMPERATURE

Time, Days / Depth,ft	3.250	3 375	3.500	3.625	3.750	3.875	4.000	4.125	4.250	4.375	4.500	4.625	4.750
7.5	7.81		7.14		6.56		6.19		5.91		5.68		5.49
7		13.75		12.72		11.98		11.42		10.97		10.57	
6.5	18.88		17.89		16.99		16.26		15.63		15.06		14.54
6		35.25		33.59		32.12		30.85		29.72		28.69	
5.5	50.83		48.88		46.85		45.04		43.41		41.92		40.55
5		61.97		59.72		57.56		55.57		53.72		52.00	
4.5	72.31		70.17		67.87		65.69		63.63		61.69		59.87
4		77.83		75.62		73.41		71.29		69.26		67.33	
3.5	82.56		80.67		78.56		76.49		74.49		72.57		70.72
3		82.98		81.10		79.17		77.30		75.47		73.71	
2.5	82.60		81.12		79.39		77.70		76.05		74.45		72.90
2		78.73		77.29		75.82		74.40		73.02		71.70	
1.5	74.06		73.06		71.84		70.70		69.60		68.54		67.52
1		66.85		66.00		65.17		64.40		63.67		62.95	
0.5	58.85		58.54		58.10		57.71		57.33		56.95		56.56
0		49.70		49.81		49.85		49 86		49.83		49.77	
-0.5	40.15		40.88		41.40		41.81		42.13		42.39		42.59
-1		32.05		32.99		33.76		34 40		34.95		35.41	
-1.5	23.96		25.10		26.12		27.00		27.76		28.42		29.00
-2		18.15		19.25		20.24		21.12		21.90		22.59	
-2.5	12.35		13.40		14.37		15.25		16.04		16.75		17.37
-2		8.65		9.48		10.25		10.95		11.59		12.16	
-3.5	4.96		5.56		6.13		6.66		7.14		7.58		7.98
-4		2.48		2.78		3.07		3.33		3 57		3.79	

Pacific Gas and Electric Company
Engineering - Calculation Sheet
Project· Diablo Canyon Unit ( )1 ( ) 2 (X) 1&2

CALC NO 52.27.100.701
REV. NO. ~~0~~ 1 10/16/01
SHEET NO. 17 OF 47

SUBJECT Determination of Thermal and Shrinkage Values for the ISFSI Concrete Pad Design

MADE BY ADP DATE 5/7/01 CHECKED BY Carl Crifton DATE 5/7/01

Table 3 (Cont.)

THE CONCRETE TEMPERATURE

Time, Days Depth,ft	4.875	5.000	5.125	5.250	5.375	5.500	5.625	5.750	5.875	6.000	6.125	6.250	6.375
7.5		5.31		5.14		5.00		4.86		4.73		4.61	
7	10.21		9.89		9.59		9.31		9.06		8.81		8.59
6.5		14.07		13.64		13.23		12.86		12.50		12.17	
6	27.74		26.87		26.06		25.31		24.60		23.94		23.32
5.5		39.28		38.09		36.99		35.95		34.98		34.07	
5	50.41		48.91		47.51		46.20		44.96		43.79		42.69
4.5		58.15		56.53		55.00		53.56		52.20		50.91	
4	65.49		63.75		62.10		60.53		59.05		57.64		56.30
3.5		68.95		67.26		65.66		64.13		62.67		61.28	
3	72.01		70.38		68.82		67.32		65.89		64.53		63.22
2.5		71.41		69.97		68.59		67.26		65.98		64.75	
2	70.41		69.17		67.96		66.80		65.67		64.58		63.52
1.5		66.53		65.55		64.61		63.68		62.78		61.89	
1	62.24		61.54		60.85		60.16		59.48		58.80		58.13
0.5		56.16		55.74		55.32		54.88		54.43		53.97	
0	49.67		49.54		49.39		49.20		48.98		48.74		48.48
-0.5		42.73		42.83		42.88		42.88		42.85		42.79	
-1	35.79		36.11		36 37		36.57		36.72		36.83		36.90
-1.5		29.49		29.91		30.27		30.57		30.81		31.01	
-2	23.19		23.71		24.17		24.56		24.89		25.18		25.41
-2.5		17.93		18.42		18 85		19.22		19.55		19.82	
-2	12.68		13.13		13.53		13.89		14.20		14.47		14.70
-3.5		8.33		8.65		8.93		9.18		9.39		9.58	
-4	3.99		4.17		4.32		4.46		4.59		4.70		4.79

SUBJECT Determination of Thermal and Shrinkage Values for the ISFSI Concrete Pad Design

MADE BY ADP DATE 5/7/01 CHECKED BY Carl Knifton DATE 5/7/01

Table 3 (Cont.)

THE CONCRETE TEMPERATURE

Time, Days / Depth,ft	6.500	6.625	6.750	6.875	7.000	7.125	7.250	7.375	7.500	7.625	7.750	7.875	8.000
7.5	4.49		4.39		4.29		4.19		4.11		4.02		3.94
7		8.38		8.18		7.99		7.81		7.64		7.48	
6.5	11.86		11.57		11.29		11.03		10.78		10.55		10.32
6		22.73		22.18		21.65		21.16		20.69		20.25	
5.5	33.20		32.39		31.62		30.89		30.20		29.55		28.93
5		41.65		40.66		39.73		38.84		38.00		37.21	
4 5	49.69		48.54		47.44		46.40		45.41		44.46		43.56
4		55.03		53.82		52.66		51.57		50 52		49.52	
3 5	59.96		58.69		57.49		56.34		55.24		54.19		53.18
3		61.96		60.76		59.61		58.51		57.45		56.43	
2 5	63.57		62.43		61.33		60.28		59.26		58.28		57.33
2		62.50		61.51		60.55		59.61		58.71		57.83	
1.5	61.03		60.18		59.36		58.55		57.76		56.99		56.24
1		57.47		56.81		56.15		55.51		54.87		54.24	
0.5	53.51		53.03		52.55		52.07		51.58		51.08		50.59
0		48.20		47.90		47.58		47.24		46.90		46.54	
-0.5	42.69		42.56		42.40		42.22		42.02		41.80		41.56
-1		36.92		36.91		36.87		36.80		36.70		36.58	
-1.5	31.16		31.26		31.34		31.37		31.38		31.36		31.31
-2		25.61		25.76		25.88		25.96		26.01		26.03	
-2.5	20.06		20.26		20.42		20.54		20.64		20.71		20.76
-2		14.90		15.07		15.21		15.33		15 42		15.48	
-3 5	9.75		9.89		10.01		10.11		10.19		10.26		10.31
-4		4.87		4.94		5.00		5.05		5.10		5.13	

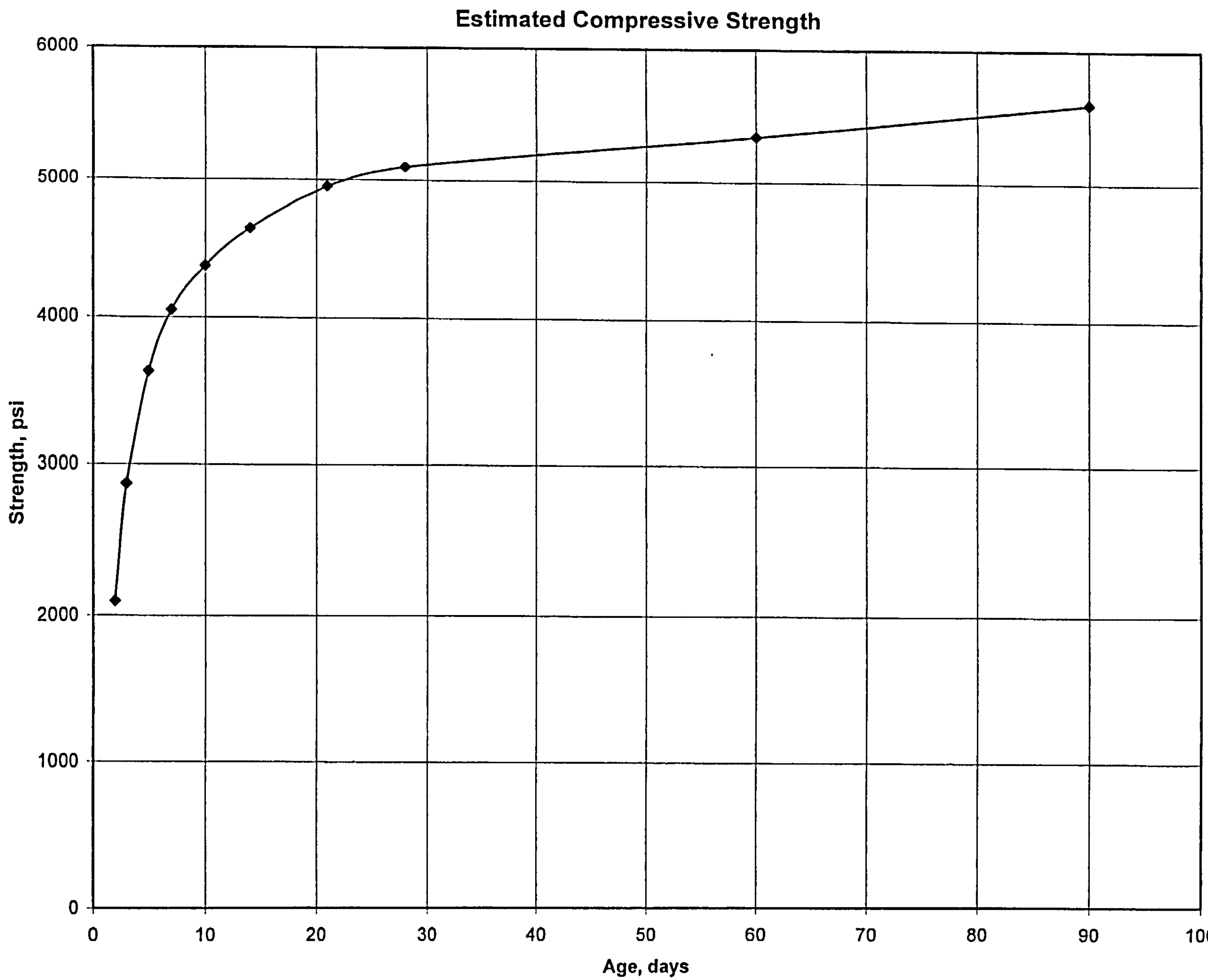

Calc. No. 52.27.100.701
Rev. No 0 10/16/01
Thermal and Shrinkage Values for the ISFSI Concrete Pad Design

Figure 1

Calculated Shrinkage
For 5600 psi Concrete with 1-1/2" aggregate

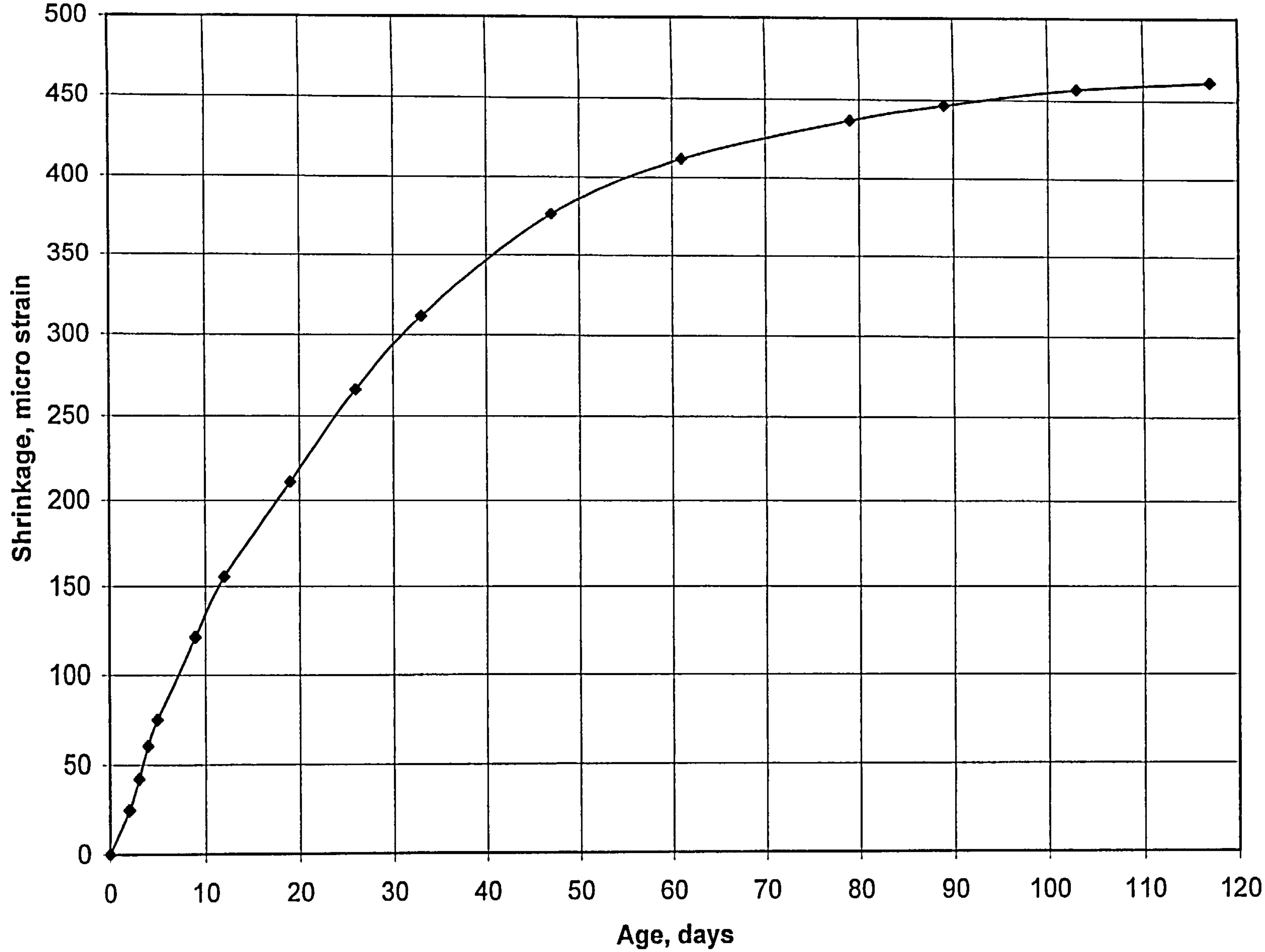

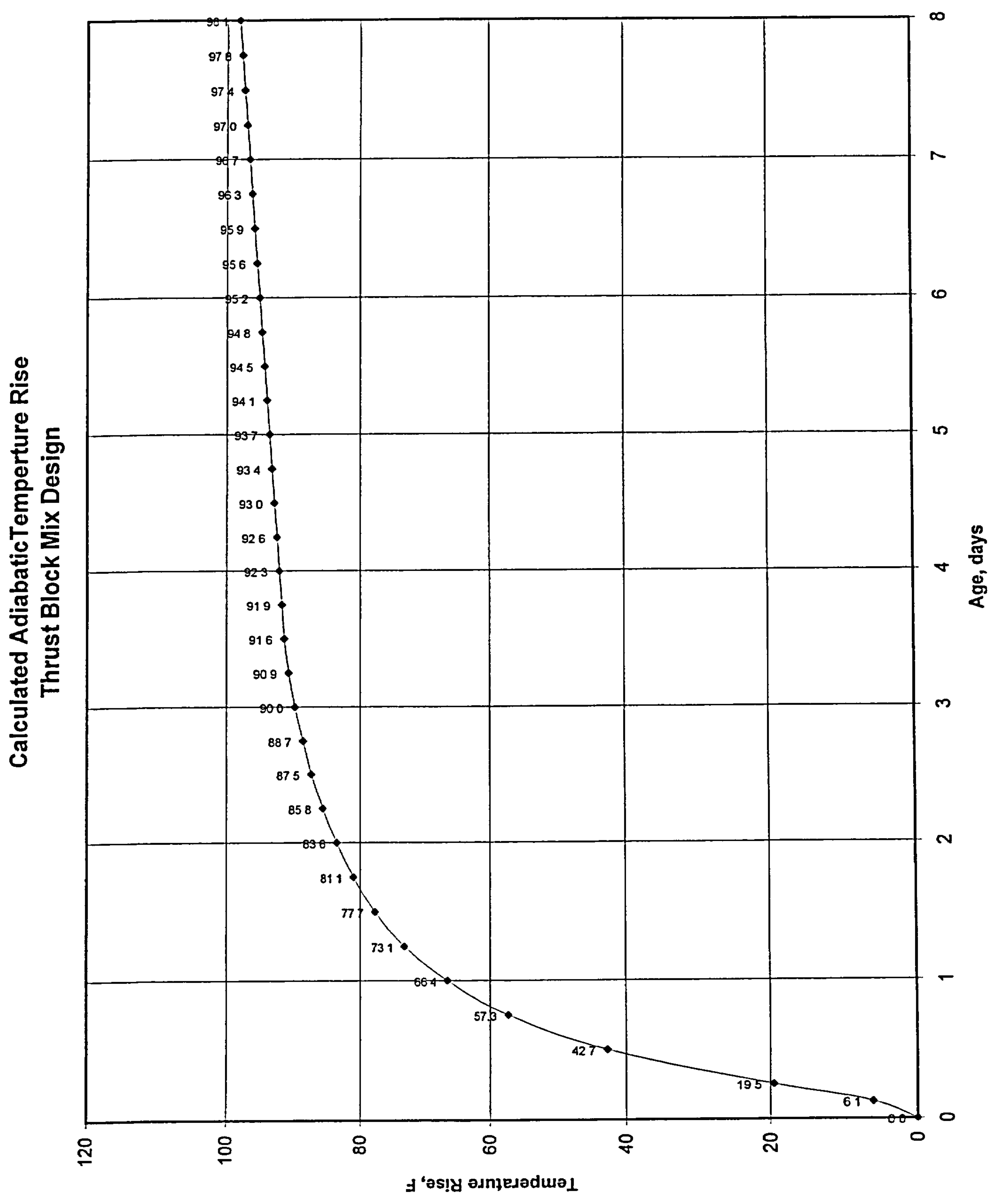
Calculated Adiabatic Temperture Rise
Thrust Block Mix Design
Temperature Rise, F
Age, days
0
20
40
60
80
100
120
0
1
2
3
4
5
6
7
8
0 0
6 1
19 5
42 7
57.3
66 4
73 1
77 7
81 1
83 6
85 8
87 5
88 7
90 0
90 9
91 6
91 9
92 3
92 6
93 0
93 4
93 7
94 1
94 5
94 8
95 2
95 6
95 9
96 3
96 7
97 0
97 4
97 8

Thermal and Shrinkage Values for the ISFSI Concrete Pad Design

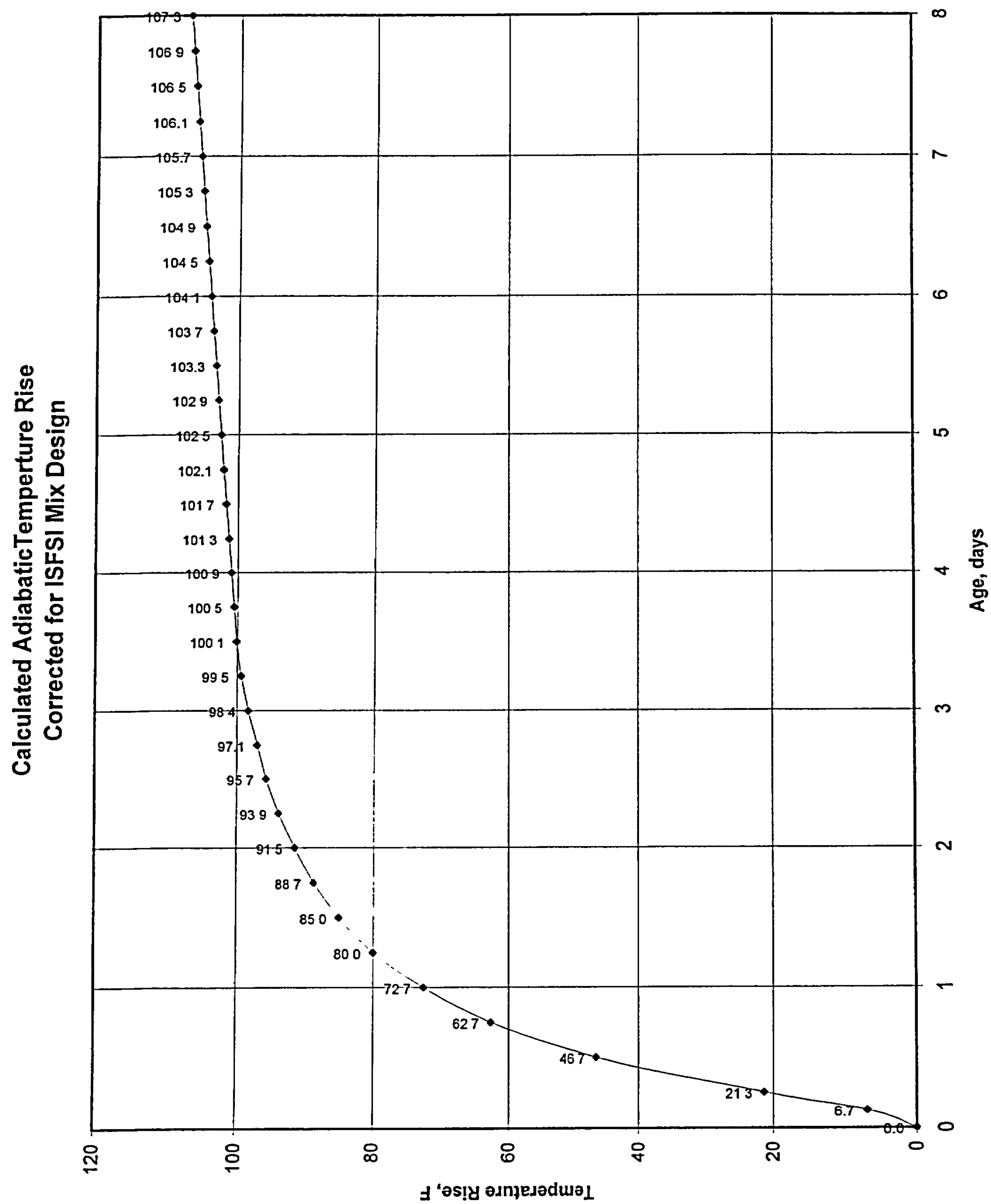

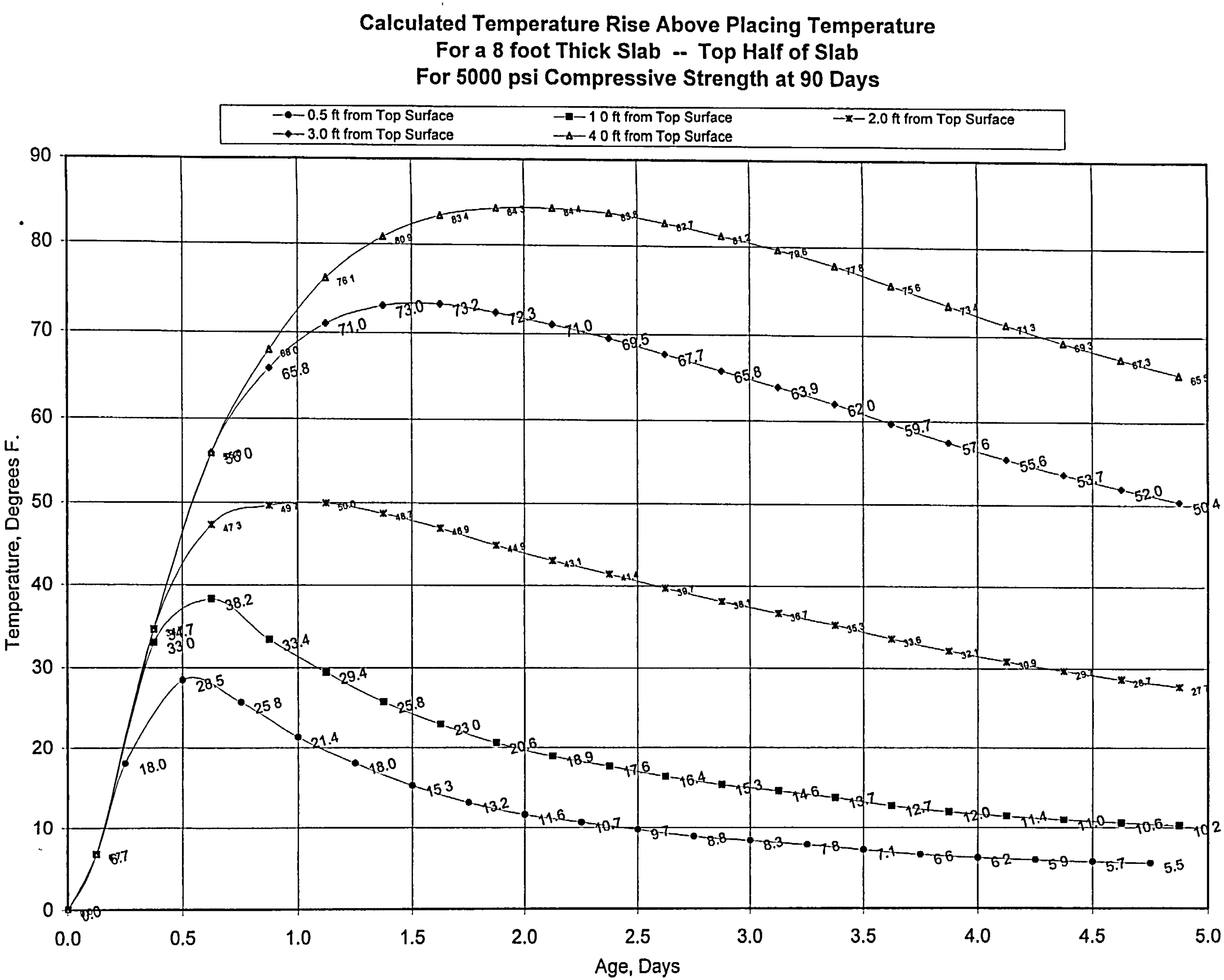

Calc. No. 52.27.100.701
Rev. No. 4 0 10/16/01
Thermal and Shrinkage Values for the ISFSI Concrete Pad Design

Figure 5

Page 23 of 47

Calculated Temperature Rise Above Placing Temperature
For a 8 foot Thick Slab -- Bottom Half of Slab
For 5000 psi Compressive Strength at 90 Days

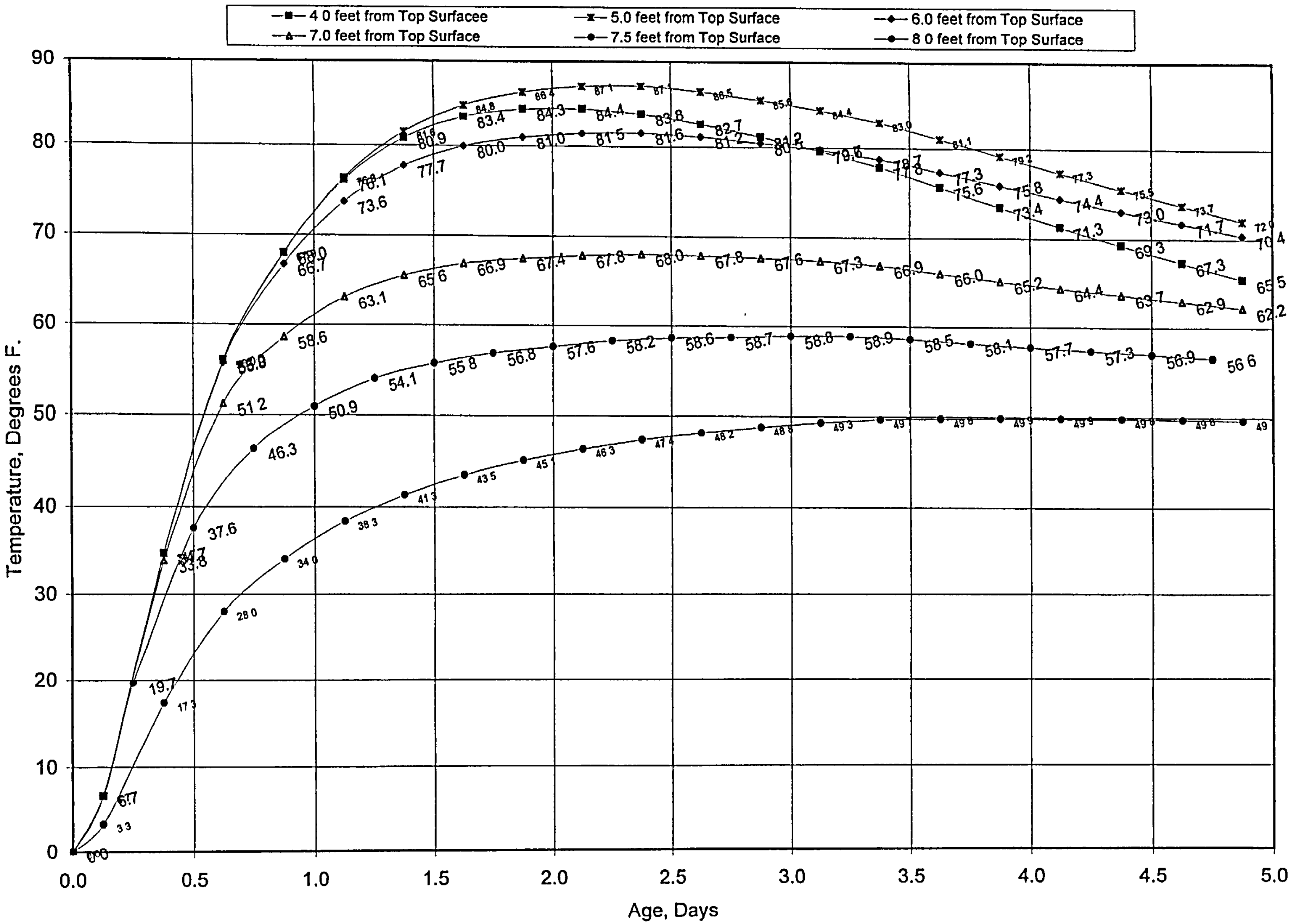

Calculated Temperature Rise Above Placing Temperature
For a 8 foot Thick Slab -- Concrete/Rock and Rock
For 5000 psi Compressive Strength at 90 Days

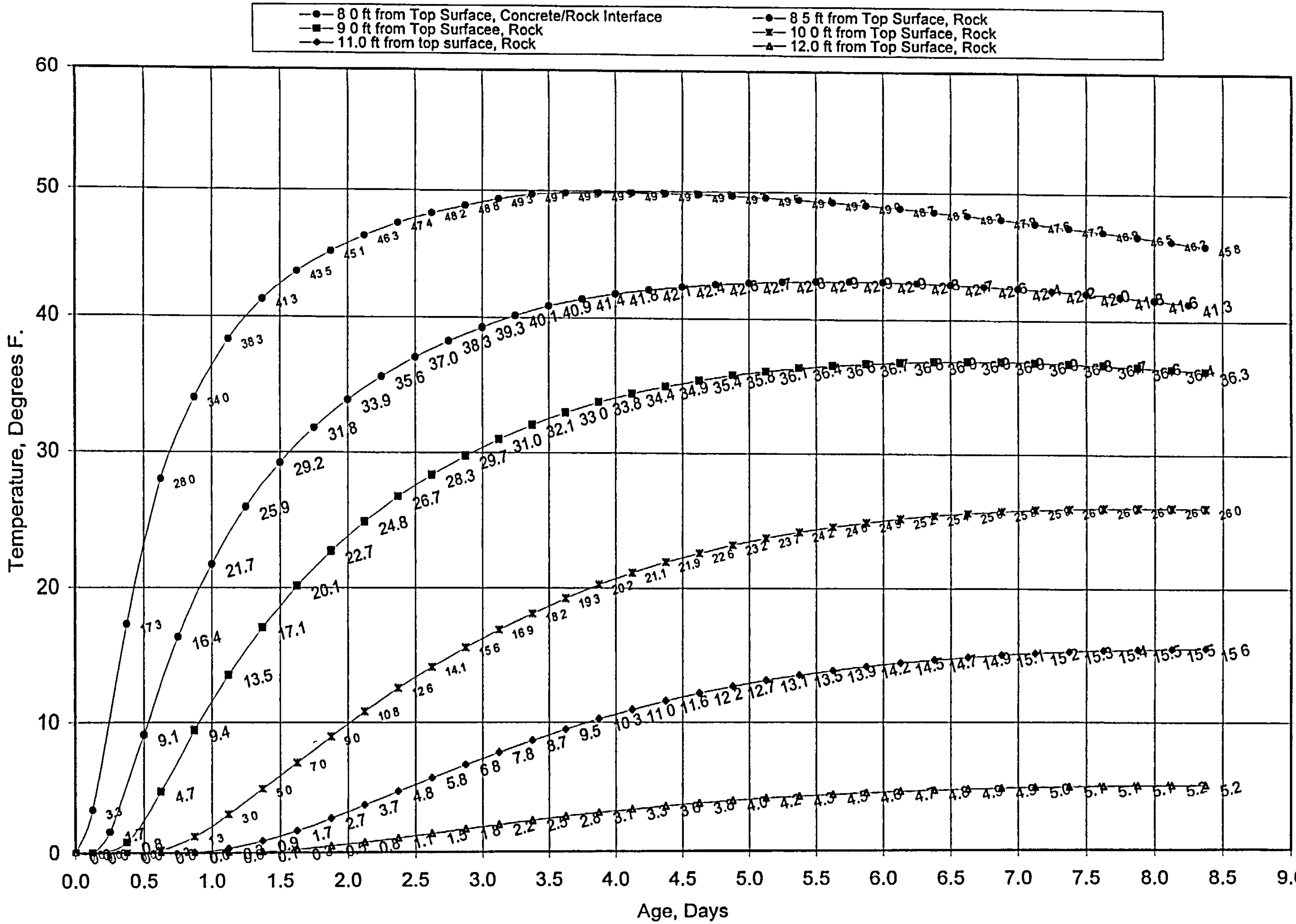

Appendix A

Report Issued: October 16, 1996
Revised: January 13, 1997

Report # 420DC-96.160

Pacific Gas and Electric Company
Laboratory Test Report
Technical and Ecological Services
3400 Crow Canyon Road
San Ramon, CA 94583

SUBJECT: DIABLO CANYON POWER PLANT - ASW BYPASS PROJECT
THRUST BLOCK "Q" CLASS CONCRETE MIX DESIGNS
Using Type II Cement, Santa Margarita Granite Aggregates and
SP Milling's Standard Admixtures

Tests and analysis of concrete and concrete materials obtained from Southern Pacific Milling Company, located in San Luis Obispo were performed to determine mix designs for the use in the production of "Q" class for the ASW Bypass Project Thrust Block concrete at Diablo Canyon Power Plant. The mix design given is for Thrust Block concrete only.

Selecting and adjusting the concrete mix design proportions was conducted in accordance with ACI 211 "Standard Practice for Selecting Proportions for Normal, Heavyweight and Mass Concrete". The method used for selecting and adjusting the concrete mix design proportions is based on the absolute volume occupied by the concrete ingredients. The mix design selection took into consideration the requirements for placeability, consistency, strength and durability. This mix design meets the requirements of ACI 318-89.

The concrete materials were sampled from SP Milling's plant. The materials used were:

Cement:		Type II, Kaiser Permanente Mill, San Jose
Pozzolan:		Fly Ash, Class F, Navajo Fly Ash Page Arizona
Fine Aggregate:		Crushed granite, Santa Margarita Quarry
Coarse Aggregate:		3/4" Crushed granite, Santa Margarita Quarry
Admixtures:		
	Water reducer:	WRDA-55, Grace Construction Products
	Air Entraining:	DAREX II AEA, Grace Construction Products

The specified compressive strength is 3000 psi is required for this mix design, with maximum size aggregate of 3/4 inch. The required average compressive strength for the mix is 4200 psi, as required by ACI 318. The required slump at the site is 3-1/2 inches (+/- 1 inch). Based on the exposure conditions air entrainment is not required. An air

Distribution: SKFlaten
AXSudhakar
AFTafoya
Nuclear Indexer

Date: January 13,1997

Tested by: Lorin Lienau/Tom Voss

Approved by: Anton Pirtz

content of 3% (+/- 1%) is desirable. The air content is recommended to decrease the water/cementitious ratio, which in return will increase durability. The air content will not significantly effect the compressive strength. The lubrication effect of the entrained air bubbles on the mixture and because of the size and grading of the air voids, air-entrained concrete usually contains up to 10 percent less water than non-entrained concrete of equal slump.

To provide an acceptable record, two cubic yard field mixes were batched at SP Milling and tested. All concrete tested was purchased in accordance with DCPP Specification No. 2105. The mix proportions given are from these field mixes. For these mixes the slump is within 0.75 inches and the air content is within 0.5% of that specified. Prior to making these field mixes several trial field mixes for each of the specific mix designs were made. These trial field mixes had differing water/cementitious ratios and cement contents.

The "THRUST BLOCK" concrete mix proportions submitted for "Q" class for the ASW Bypass Project Thrust Block concrete to be used at DCPP are shown on Table 1. This concrete mix and its properties meet the requirements of ACI 318. The final water/cementitious ratio is 0.485, see figure 2. The final mix contains 550 pounds of cement with 22.5 percent flyash. The adjusted trial batch mix proportions are also shown on Table 1. The trial batch mix proportions are adjusted for actual weight of material batched, additional water or other material added to obtain a volume of one cubic yard. Two compressive strength specimens were tested at each age. Figure 1 shows the compressive strength vs. age relationship. Figure 2 shows the 28-day compressive strength vs. water/cementitious ratio relationship. The drying shrinkage results are shown in Figure 3. The drying shrinkage values were obtained in accordance ASTM-C157 "Length Change Of Hardened Hydraulic - Cement And Concrete". The results of test for estimating concrete strength by the maturity method are shown in Figure 4, these values were obtained in accordance ASTM-C1074. Compressive strengths vs. maturity values were determined at 2, 3, 5 and 7 days. To obtain an approximation of the heat rise of the thrust blocks, a four-foot concrete cube test specimen was cast. The results of temperature rise above ambient of the center of the 4 ft. concrete cube test specimen are shown in Figure 5. This test cube was insulated from ambient temperature variations. The concrete at three separate locations 1 inch in the concrete from the surface, varied +/- 1.9 degrees F. in temperature for the duration of the test (7 days).

The results of the rapid chloride permeability tests are 4320 and 3870 coulombs for specimens tested at 28 and 90 days respectively. The permeability values were obtained in accordance ASTM-C1202 "Electrical Indication Of Concrete's Ability To Resist Chloride Ion Penetration". The 28-day results indicate chloride ion penetrability in the high range. The 90-day results indicate a chloride ion penetrability in the moderate range. A correlation between chloride ion penetration and long-term chloride ponding has not been conducted for this mix. Since this mix contains flyash these results should be used with caution.

Considering other similar proportioned mixes that use the same materials this mix will be pumpable. Recommended proportions from ACI 304.2R "Placing Concrete by Pumping Methods" were followed. There is no recognized laboratory apparatus to test pumpability of a mix in the laboratory.

Table 1

MIX DESIGNS - ASW BYPASS PROJECT
THRUST BLOCK "Q" CLASS CONCRETE

Mix #	THRUST BLOCK	THR-A Trial	THR-B Trial	THR-C Trial
Specified Compressive Strength	3000 PSI	3000 PSI	3000 PSI	3000 PSI
Required Average Compressive Strength	4200 PSI	4200 PSI	4200 PSI	4200 PSI
Maximum Aggregate Size	3/4	3/4	3/4	3/4
Material				
Cement, lbs	550	562	548	531
Flyash, lbs	125	115	127	115
Water, lbs	327	311	317	323
Santa Margarita Fine Agg., lbs	1295	1319	1319	1296
Santa Margarita 3/4" Agg., lbs	1520	1530	1526	1539
WRA, oz. (WRDA 55)	84.4	100.2	87.7	71.1
AEA, oz. (DAREX II)	7.4	7.5	7.4	7.1
Weight per CU. YD.	3824	3836	3837	3804
Sacks per Yard	5.85	5.98	5.83	5.65
Water/Cementitious	0.485	0.46	0.48	0.50
Fine Agg./Total Agg.	0.46	0.46	0.46	0.46
Measured Values				
Slump, in		3	3-3/4	3-1/2
Air, % (+/-1)		3.2	2.9	3.4
Unit Weight, lbs/cuft		142.0	142.2	140.8
	Projected			
Compressive Strength, psi	Values			
Age 2 day	1820	2100	1880	1640
3 day	2350	2870	2490	1950
5 day	2680	3620	2790	2360
7 day	2940	4000	3050	2600
10 day	3350	4210	3460	3020
14 day	3770	4440	3890	3410
21 day	4020	4650	4110	3750
28 day	4270	4870	4370	3980

FIGURE 1

MIX DESIGNS - ASW BYPASS PROJECT
THRUST BLOCK "Q" CLASS CONCRETE

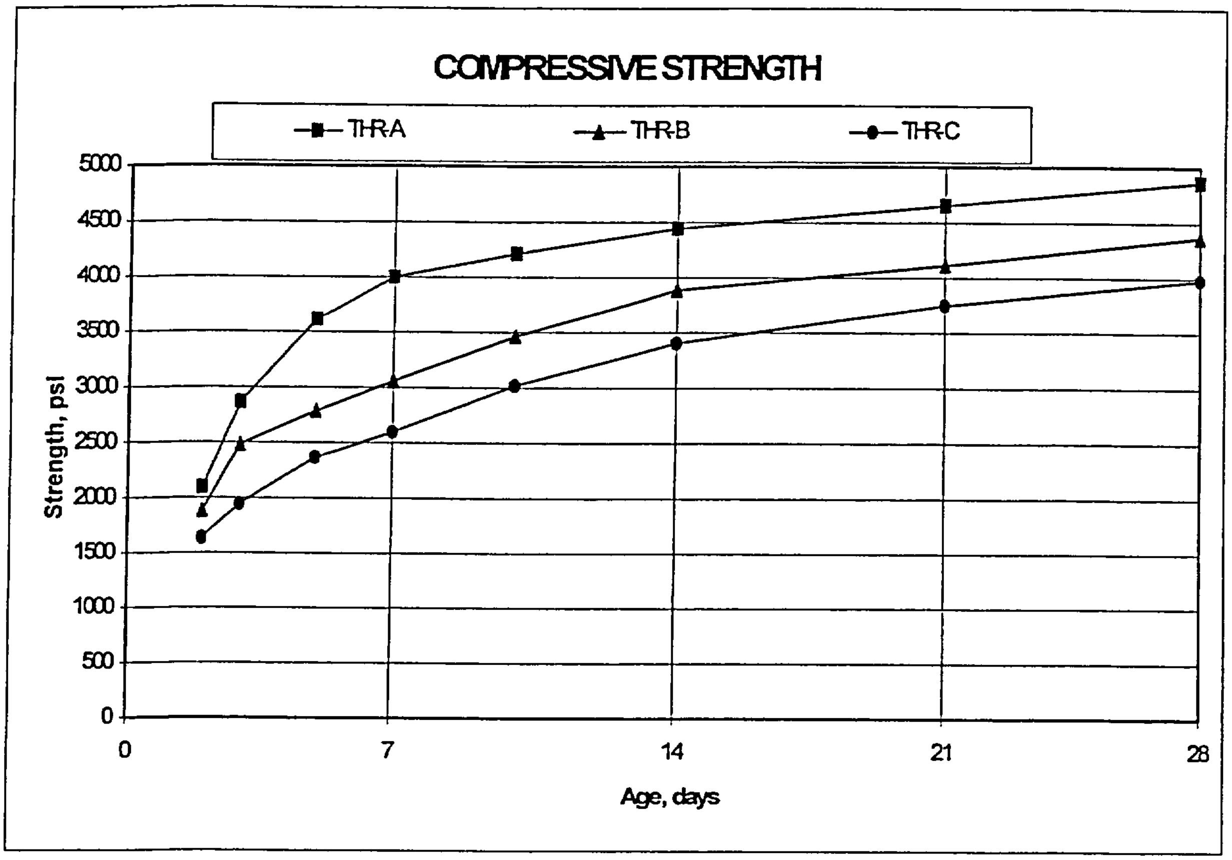

FIGURE 2

MIX DESIGNS - ASW BYPASS PROJECT
THRUST BLOCK "Q" CLASS CONCRETE

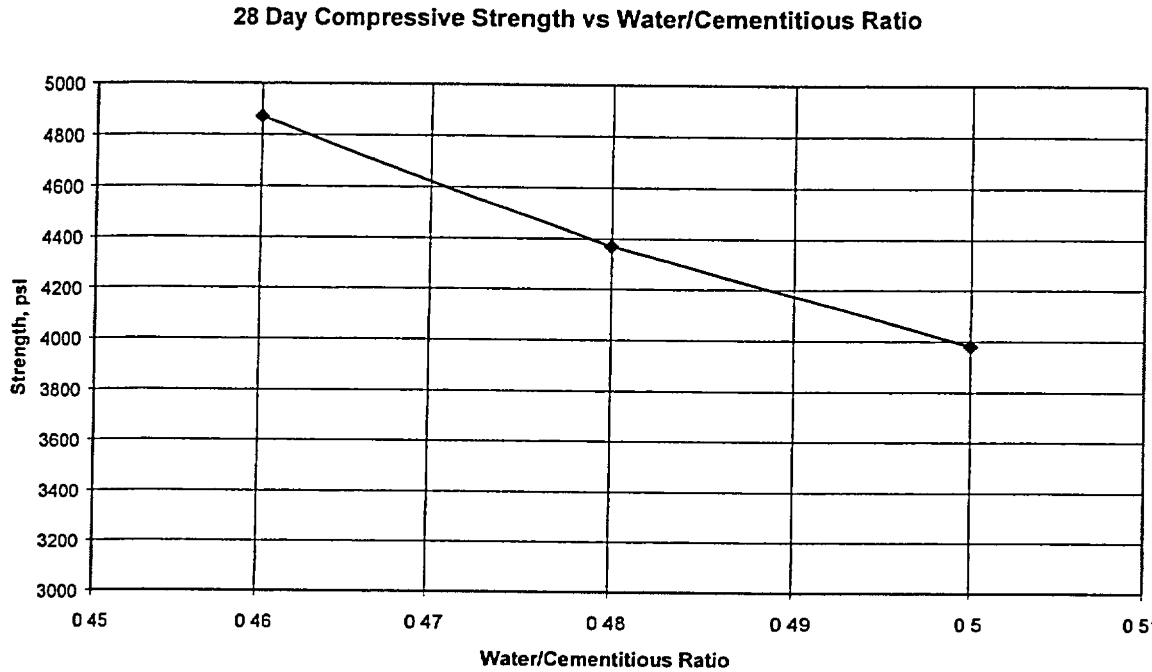

FIGURE 3

MIX DESIGNS - ASW BYPASS PROJECT
THRUST BLOCK "Q" CLASS CONCRETE

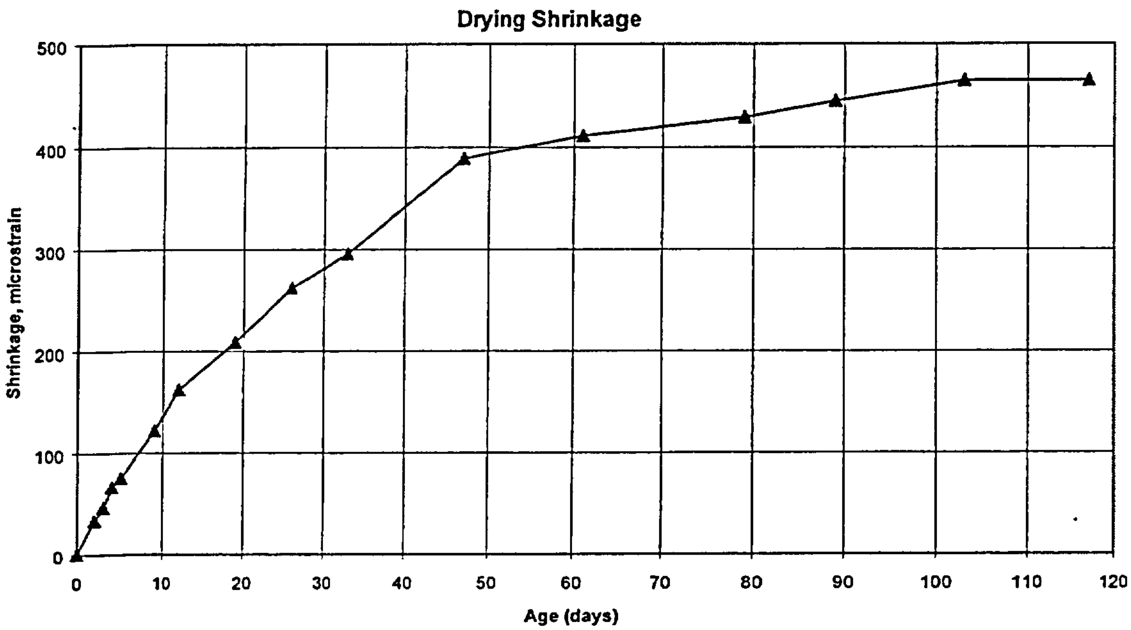

FIGURE 4

MIX DESIGNS - ASW BYPASS PROJECT
THRUST BLOCK "Q" CLASS CONCRETE

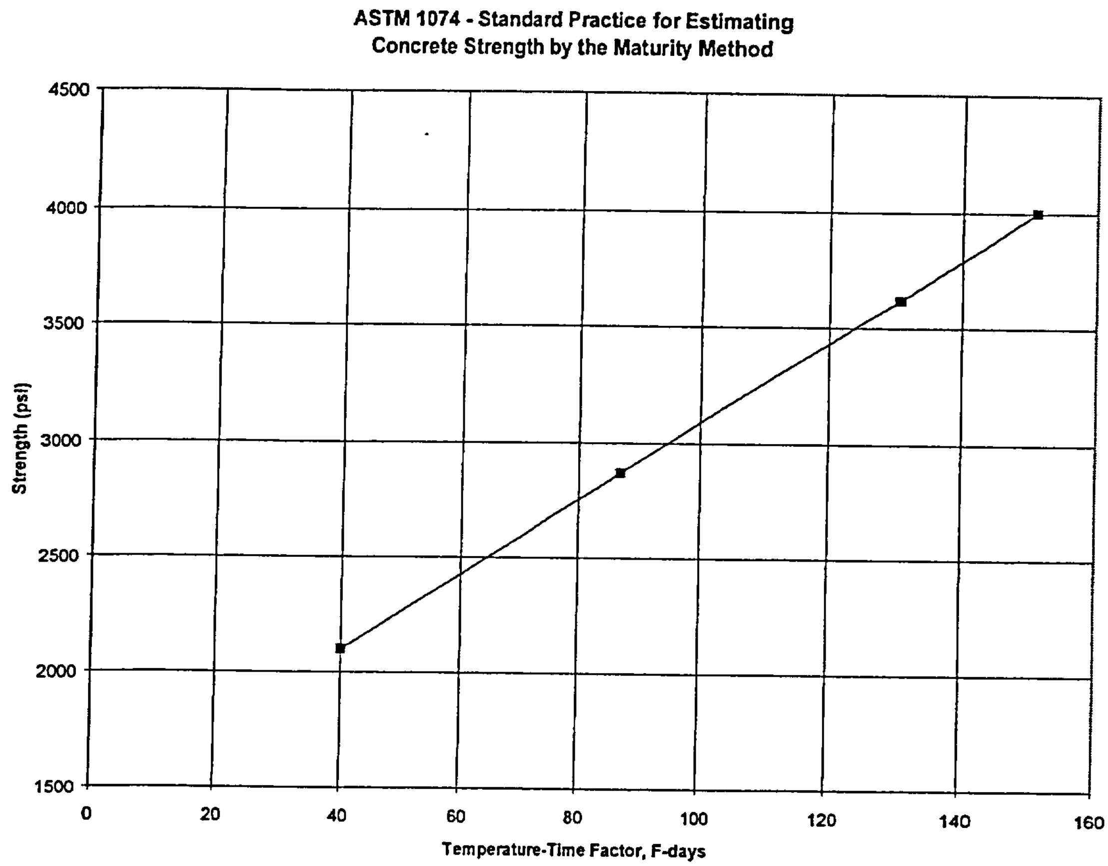

FIGURE 5

MIX DESIGNS - ASW BYPASS PROJECT
THRUST BLOCK "Q" CLASS CONCRETE

Temperature Rise Of Center

Of 4 Ft. Concrete Cube

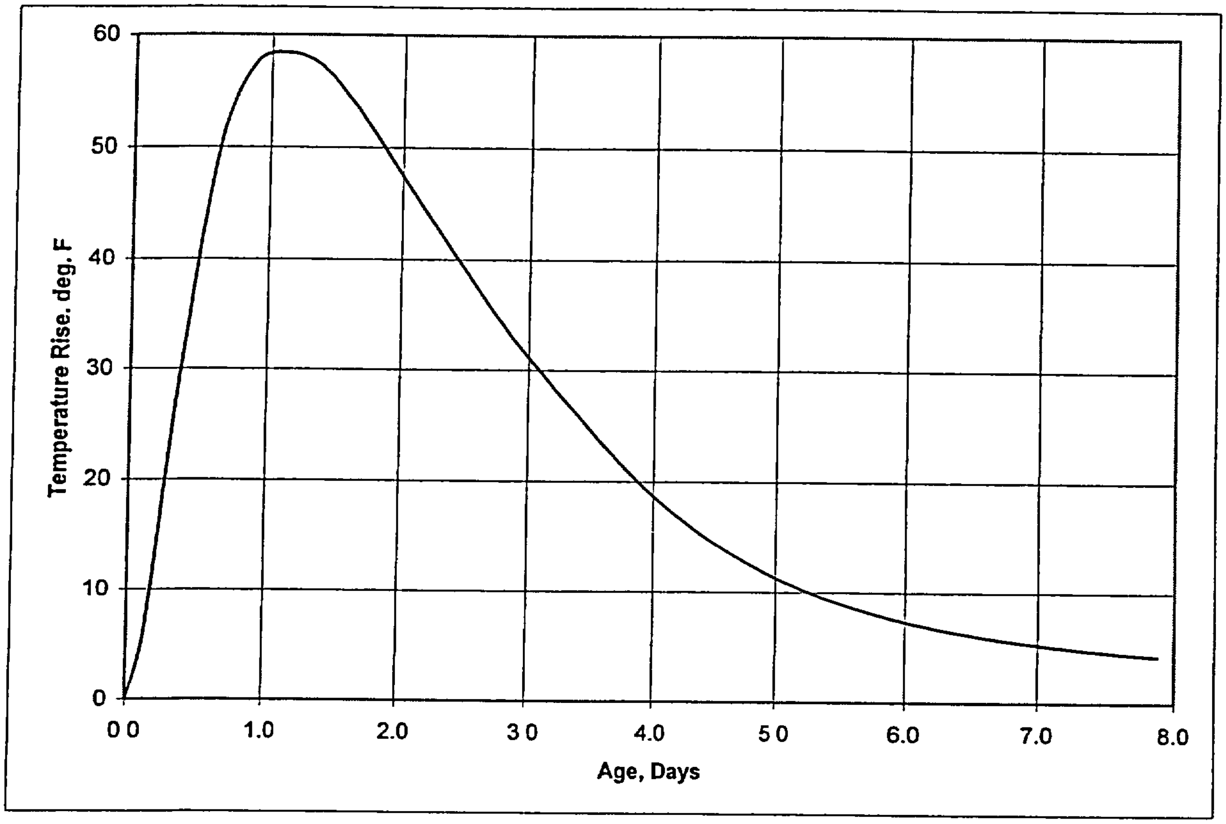

SUBJECT Determination of Thermal and Shrinkage Values for the ISFSI Concrete Pad Design

MADE BY ADP DATE CHECKED BY DATE

Appendix B

Determination of Thermal and Shrinkage Values for the ISFSI Concrete Pad Design

Calculated Adiabatic Temperature Rise Curve from the Thrust Block Data

4 Foot Test Cube

1 21910		0.13		0.25		0 38		0.50		0.63		0.75		0 88		1.00		1.13		1.25		1.38		1.50	
		5 00		11.00		10 00		9.00		7.00		5.00		4 00		3.00		3 00		3.00		2.00		1.75	
		6.10		13.41		12.19		10 97		8.53		6 10		4.88		3 66		3.66		3 66		2 44		2.13	
4.00	0 00	0 00			0 00	0 00			0 00	0 00			0.00	0 00			0 00	0.00			0 00	0 00			0 00
3 50	0 00	6.10	3 05	16 46			15.09	26.06			21.26	27.35			22.42	26 08			22.05	25.71			21.38	23.51	
3 00	0 00	6.10			17.98	30.17			33 98	42.52			39 96	44.84			40.44	44.10			40.32	42.76			37.86
2.50	0.00	6.10	6.10	19.51			30.93	41.91			46.48	52.57			51.15	54.80			51.28	54.94			50.07	52.20	
2.00	0.00	6.10			19.51	31.70			41.91	50.44			52 57	57.45			54.80	58 46			54.94	57.37			52.20
1.50	0 00	6.10	6.10	19.51			30 93	41.91			46 48	52.57			51.15	54.80			51 28	54.94			50 07	52.20	
1.00	0 00	6 10			17.98	30.17			33 98	42.52			39.96	44 84			40 44	44.10			40 32	42.76			37.86
0.50	0 00	6.10	3.05	16.46			15 09	26 06			21.26	27.35			22 42	26.08			22 05	25.71			21.38	23.51	
0 00	0 00	0.00			0 00	0 00			0 00	0.00			0 00	0.00			0.00	0.00			0 00	0 00			0.00

Determination of Thermal and Shrinkage Values for the ISFSI Concrete Pad Design

Calculated Adiabatic Temperature Rise Curve from the Thrust Block Data

1.63		1.75		1 88		2.00		2 13		2 25		2.38		2.50		2 63		2.75		2 88		3 00		3.13	
1 50		1 25		1.10		1 00		0 90		0.90		0 70		0.70		0.50		0 50		0 50		0 50		0.40	
1 83		1.52		1 34		1.22		1.10		1 10		0 85		0 85		0 61		0 61		0 61		0 61		0 49	
0 00			0 00	0.00			0 00	0.00			0 00	0.00			0 00	0 00			0.00	0 00			0 00	0.00	
	19.84	21.37			18.11	19.33			16.43	17.52			14 85	15.70			13 28	13 89			11.85	12 46			10 59
39 69			34 87	36.21			31 76	32 85			28 85	29.70			25.96	26.57			23.10	23.71			20 69	21.18	
	46 86	48.38			42 97	44.19			39.07	40.17			35.36	36.21			31 69	32 30			28 31	28.92			25 29
54.03			48.38	49.72			44 19	45 28			40.17	41.02			36 21	36.82			32 30	32.91			28 92	29 41	
	46 86	48 38			42.97	44 19			39.07	40.17			35 36	36 21			31.69	32.30			28.31	28.92			25 29
39.69			34 87	36 21			31.76	32 85			28 85	29.70			25 96	26 57			23.10	23.71			20 69	21.18	
	19.84	21.37			18.11	19 33			16 43	17.52			14 85	15.70			13.28	13.89			11 85	12.46			10.59
0 00			0 00	0 00			0 00	0 00			0.00	0.00			0 00	0 00			0 00	0.00			0.00	0.00	

Determination of Thermal and Shrinkage Values for the ISFSI Concrete Pad Design

Calculated Adiabatic Temperature Rise Curve from the Thrust Block Data

3 25		3 38		3 50		3.63		3 75		3 88		4 00		4.13		4.25		4 38		4.50		4 63		4.75	
0 40		0 30		0 20		0 15		0.15		0.15		0 15		0.15		0 15		0 15		0.15		0.15		0 15	
0 49		0.37		0 24		0 18		0.18		0 18		0 18		0.18		0 18		0 18		0.18		0 18		0.18	
	0 00	0 00			0 00	0 00			0 00	0 00			0 00	0 00			0 00	0 00			0 00	0 00			0.00
11.08			9.40	9 64			8.18	8 36			7.14	7 32			6 25	6.43			5.50	5.68			4.85	5 03	
	18.43	18 80			16.18	16 36			14 09	14.27			12 32	12.50			10 81	10 99			9.52	9.70			8.42
25 78			22 47	22 72			19 63	19 81			17.13	17 32			15 00	15.18			13 18	13.36			11.62	11.81	
	25.78	26 15			22 72	22 90			19 81	20 00			17.32	17.50			15 18	15.37			13.36	13 54			11.81
25.78			22 47	22.72			19 63	19.81			17.13	17.32			15 00	15 18			13.18	13.36			11.62	11.81	
	18 43	18.80			16.18	16.36			14.09	14 27			12.32	12.50			10 81	10 99			9 52	9.70			8 42
11.08			9 40	9 64			8 18	8.36			7.14	7.32			6 25	6.43			5.50	5 68			4 85	5 03	
	0 00	0.00			0.00	0.00			0 00	0 00			0 00	0 00			0 00	0.00			0.00	0 00			0.00

CALC. NO. 52.27.100 701
REV. NO. ~~X~~ 0 GK 10/16/01

Determination of Thermal and Shrinkage Values for the ISFSI Concrete Pad Design

Calculated Adiabatic Temperature Rise Curve from the Thrust Block Data

4,88		5.00		5.13		5.25		5.38		5.50		5.63		5.75		5.88		6.00		6.13		6 25		6 38		6.50		6 63		6 75
0.15		0.15		0.15		0.15		0.15		0.15		0.15		0.15		0.15		0.15		0.15		0.15		0.15		0.15		0.15		0.15
0.18		0.18		0.18		0.18		0.18		0.18		0.18		0.18		0,18		0.18		0.18		0.18		0.18		0.18		0.18		0.18
0.00			0.00	0.00			0.00	0.00			0.00	0 00			0 00	0.00			0.00	0.00			0.00	0.00			0.00	0 00		
	4.30	4.48			3.83	4.01			3 43	3.61			3.09	3.27			2.80	2.98			2.55	2.73			2.34	2.52			2.15	2.34
8.60			7.48	7.66			6 68	6.86			6.00	6.18			5.41	5.60			4 91	5.10			4.49	4.67			4.13	4.31		
	10.30	10 48			9.16	9.35			8.20	8.38			7.37	7.55			6.67	6 85			6.06	6.25			5.55	5.73			5.11	5.30
11.99			10 48	10 66			9.35	9.53			8.38	8.56			7.55	7.74			6.85	7.03			6.25	6.43			5.73	5.92		
	10 30	10.48			9.16	9.35			8 20	8.38			7.37	7 55			6 67	6.85			6.06	6 25			5.55	5.73			5 11	5 30
8 60			7.48	7.66			6 68	6.86			6 00	6.18			5.41	5 60			4.91	5.10			4.49	4 67			4.13	4.31		
	4.30	4.48			3 83	4 01			3 43	3 61			3.09	3 27			2 80	2.98			2.55	2.73			2.34	2.52			2.15	2.34
0 00			0.00	0.00			0.00	0.00			0.00	0 00			0.00	0.00			0.00	0 00			0.00	0.00			0.00	0.00		

CALC. NO. 52.27.100.701
REV. NO. 0 GC 10/16/01

Determination of Thermal and Shrinkage Values for the ISFSI Concrete Pad Design

Calculated Adiabatic Temperature Rise Curve from the Thrust Block Data

	6 88		7.00		7.13		7.25		7.38		7.50		7.63		7.75		7.88		8.00		8.13
	0.15		0.15		0.15		0.15		0.15		0.15		0.15		0.15		0.15		0.15		0.15
	0.18		0.18		0.18		0.18		0.18		0.18		0.18		0.18		0.18		0.18		0.18
0 00	0.00			0.00	0.00			0.00	0.00			0 00	0.00			0 00	0.00			0 00	0.00
		2.00	2.18			1.87	2.05			1.75	1 94			1.66	1.84			1.58	1.76		
3.82	4.00			3.55	3.74			3.33	3.51			3.13	3.32			2 97	3.15			2.83	3.01
		4.74	4.92			4.42	4.60			4.15	4.33			3.92	4.10			3.72	3 90		
5.30	5.48			4.92	5.11			4.60	4.79			4.33	4.51			4.10	4.28			3.90	4.08
		4.74	4.92			4.42	4 60			4.15	4.33			3.92	4.10			3.72	3.90		
3.82	4 00			3 55	3.74			3.33	3.51			3.13	3.32			2.97	3.15			2.83	3.01
		2.00	2.18			1.87	2.05			1.75	1.94			1.66	1.84			1.58	1.76		
0 00	0.00			0.00	0.00			0.00	0 00			0.00	0 00			0 00	0.00			0.00	0.00

Pacific Gas and Electric Company
Engineering - Calculation Sheet
Project: Diablo Canyon Unit ( )1 ( )2 (X) 1&2

CALC. NO. 52.27.100.701
REV NO ~~X~~ 0 10/16/01
SHEET NO. 41 OF 47

SUBJECT Determination of Thermal and Shrinkage Values for the ISFSI Concrete Pad Design

MADE BY ADP DATE CHECKED BY DATE

Appendix C

Determination of Thermal and Shrinkage Values for the ISFSI Concrete Pad Design

Calculated Temperature Rise for the ISFSI Pad

ISFSI Pad, 8.0 foot thick, 4 feet into the rock

1.33315		0.13		0.25		0.38		0.50		0 63		0 75		0.88		1.00		1.13		1.25		1.38		1.50
		5.00		11.00		10.00		9 00		7.00		5 00		4 00		3.50		3.00		2.50		2 00		1.75
		6.67		14.66		13.33		12.00		9.33		6.67		5.33		4.67		4 00		3.33		2.67		2.33
8.00	0 00	0.00			0 00	0.00			0 00	0.00			0.00	0 00			0.00	0 00			0 00	0 00		
7.50	0 00	6 67	3.33	18.00			16.50	28.50			19.12	25.79			16.70	21.36			14.71	18 05			12.92	15.26
7.00	0.00	6.67			19.66	33.00			28 91	38.24			28 06	33.39			25.43	29.43			23.18	25.84		
6.50	0.00	6.67	6.67	21.33			17.33	29.33			23.66	30.33			24.83	29.50			24.98	28.31			24.36	26.69
6.00	0.00	6 67			21.33	34.66			37.99	47.33			44.33	49.66			45.95	49.95			46.06	48.72		
5 50	0.00	6.67	6.67	21.33			34 66	46 66			51.66	58.33			57.74	62.41			60.47	63.80			60.87	63.20
5 00	0.00	6.67			21.33	34 66			46.66	55 99			60.49	65 82			66.99	70.99			70.34	73.01		
4.50	0.00	6 67	6 67	21.33			34 66	46.66			55.99	62.66			66.91	71.57			73.55	76 88			76.94	79.27
4.00	0.00	6 67			21.33	34.66			46 66	55.99			62.66	67.99			72.10	76.10			78.21	80 87		
3.50	0 00	6 67	6.67	21.33			34 66	46.66			55.99	62 66			67.96	72.63			76.20	79.54			81.23	83.56
3.00	0 00	6 67			21.33	34.66			46.66	55.99			62.61	67.94			72.31	76.31			78.92	81.59		
2.50	0.00	6.67	6.67	21.33			34.66	46.66			55.89	62.55			67.32	71.98			74.97	78.31			79.63	81.97
2.00	0.00	6 67			21.33	34 66			46.45	55.78			61.37	66.70			69.64	73 64			75.01	77.68		
1.50	0.00	6.67	6.67	21.33			34.25	46.24			53.51	60.18			62 63	67.30			68 38	71.71			71.61	73 95
1.00	0.00	6 67			20.50	33.83			41.91	51.24			53 23	58 56			59.12	63.12			62 89	65.55		
0.50	0.00	6 67	5.00	19 66			25.58	37.58			39.62	46.29			46 28	50.95			50.72	54.06			53.44	55.77
0.00	0.00	3 33			10.67	17.33			23.33	28.00			31.33	34.00			36.33	38.33			39.99	41.33		
-0.50	0 00	0 00	1.67	1.67			9.08	9 08			16.37	16 37			21.71	21.71			25.93	25.93			29 22	29.22
-1.00	0.00	0.00			0.83	0.83			4.75	4.75			9 43	9.43			13 53	13 53			17.10	17.10		
-1.50	0 00	0.00	0 00	0 00			0 42	0.42			2.48	2.48			5.36	5.36			8.27	8.27			11.04	11.04
-2.00	0 00	0 00			0.00	0.00			0 21	0.21			1.29	1.29			3.02	3 02			4.98	4 98		
-2.50	0.00	0.00	0.00	0.00			0 00	0.00			0.10	0.10			0.67	0.67			1.68	1.68			2.95	2 95
-3.00	0.00	0 00			0 00	0.00			0 00	0.00			0 05	0 05			0.35	0 35			0.93	0 93		
-3.50	0.00	0.00	0 00	0.00			0.00	0.00			0.00	0 00			0 03	0.03			0.18	0.18			0.51	0.51
-4.00	0 00	0.00			0.00	0.00			0 00	0.00			0.00	0.00			0.01	0 01			0.09	0.09		

CALC. NO. 52.27.100.701
REV. NO. ✗ 0 GK 10/16/01

Determination of Thermal and Shrinkage Values for the ISFSI Concrete Pad Design

Calculated Temperature Rise for the ISFSI Pad

	1.63		1.75		1.88		2.00
	1.50		1.25		1.10		1.00
	2.00		1.67		1.47		1.33
0.00	0.00	11.49	13.15	0.00	0.00	10.31	11.64
20.97	22.97	23.47	25.14	19.15	20.61	22.46	23.79
44.95	46.95	60.09	61.76	43.45	44.91	58.63	59.96
71.24	73.24	78.33	79.99	70.88	72.34	78.34	79.68
81.42	83.42	84.09	85.76	82.88	84.34	85.35	86.68
82.76	84.76	82.36	84.03	84.89	86.36	83.69	85.02
77.96	79.96	73.41	75.07	79.55	81.02	74.22	75.55
64.86	66.86	55.18	56.84	65.96	67.43	56.24	57.58
42.49	43.49	31.81	31.81	44.33	45.06	33.87	33.87
20.13	20.13	13.56	13.56	22.69	22.69	15.83	15.83
7.00	7.00	4.37	4.37	8.96	8.96	5.82	5.82
1.73	1.73	0.99	0.99	2.68	2.68	1.59	1.59
0.26	0.26			0.50	0.50		

	2.13		2.25		2.38		2.50
	0.90		0.90		0.70		0.70
	1.20		1.20		0.93		0.93
0.00	0.00	9.46	10.66	0.00	0.00	8.82	9.75
17.72	18.91	21.54	22.74	16.70	17.63	20.71	21.65
41.88	43.08	57.05	58.25	40.49	41.43	55.47	56.40
69.82	71.02	77.70	78.90	68.57	69.51	76.67	77.61
83.18	84.38	85.72	86.92	82.91	83.84	85.48	86.42
85.85	87.05	84.27	85.47	86.19	87.13	84.35	85.29
80.29	81.49	74.63	75.83	80.65	81.58	74.78	75.71
66.57	67.77	57.04	58.24	67.04	67.97	57.68	58.61
45.72	46.32	35.59	35.59	46.92	47.38	37.05	37.05
24.85	24.85	17.84	17.84	26.71	26.71	19.63	19.63
10.82	10.82	7.26	7.26	12.55	12.55	8.65	8.65
3.71	3.71	2.25	2.25	4.76	4.76	2.94	2.94
0.79	0.79			1.12	1.12		

	2.63		2.75		2.88		3.00
	0.50		0.50		0.50		0.50
	0.67		0.67		0.67		0.67
0.00	0.00	8.18	8.85	0.00	0.00	7.67	8.34
15.70	16.36	19.84	20.51	14.68	15.35	19.05	19.71
39.02	39.69	53.68	54.35	37.43	38.09	51.93	52.59
67.00	67.67	75.17	75.84	65.09	65.76	73.49	74.16
82.01	82.68	84.60	85.26	80.55	81.22	83.39	84.05
85.85	86.52	83.84	84.51	84.89	85.55	83.03	83.69
80.50	81.16	74.49	75.16	79.83	80.50	74.04	74.71
67.16	67.83	57.99	58.66	66.91	67.58	58.18	58.85
47.83	48.16	38.25	38.25	48.46	48.79	39.27	39.27
28.34	28.34	21.24	21.24	29.75	29.75	22.68	22.68
14.14	14.14	9.97	9.97	15.61	15.61	11.20	11.20
5.80	5.80	3.63	3.63	6.80	6.80	4.31	4.31
1.47	1.47			1.82	1.82		

	3.13
	0.40
	0.53
0.00	0.00
14.03	14.56
36.15	36.69
63.37	63.91
79.10	79.64
83.87	84.41
79.20	79.73
66.78	67.31
49.06	49.32
30.97	30.97
16.94	16.94
7.76	7.76
2.15	2.15

Determination of Thermal and Shrinkage Values for the ISFSI Concrete Pad Design

Calculated Temperature Rise for the ISFSI Pad

	3.25		3.50		3.75		4.00		4.25		4.50		4.75
	0.40		0 20		0.15		0.15		0.15		0.15		0.15
	0 53		0 27		0.20		0.20		0.20		0 20		0.20
7.28	7.81	6 87	7.14	6.36	6 56	5.99	6.19	5.71	5.91	5.48	5.68	5.29	5 49
18.34	18.88	17.63	17.89	16.79	16.99	16 06	16.26	15 43	15.63	14.86	15.06	14.34	14.54
50 30	50.83	48 61	48.88	46.65	46.85	44.84	45.04	43 21	43.41	41.72	41.92	40.35	40.55
71.77	72.31	69.90	70.17	67.67	67.87	65.49	65.69	63.43	63.63	61.49	61.69	59 67	59.87
82.02	82.56	80.40	80 67	78 36	78.56	76.29	76 49	74.29	74.49	72.37	72.57	70.52	70.72
82.07	82.60	80 85	81.12	79.19	79.39	77.50	77.70	75.85	76.05	74.25	74.45	72.70	72.90
73.52	74.06	72.79	73.06	71 64	71.84	70.50	70.70	69.40	69 60	68.34	68 54	67.32	67 52
58.32	58 85	58.28	58 54	57.90	58.10	57.51	57.71	57.13	57.33	56.75	56.95	56.36	56.56
40.15	40.15	40 88	40 88	41.40	41.40	41.81	41.81	42.13	42.13	42.39	42.39	42.59	42.59
23.96	23.96	25.10	25.10	26.12	26.12	27.00	27.00	27.76	27.76	28 42	28.42	29.00	29 00
12.35	12.35	13 40	13.40	14.37	14 37	15 25	15.25	16.04	16.04	16.75	16.75	17.37	17.37
4.96	4.96	5 56	5.56	6.13	6.13	6.66	6 66	7.14	7.14	7.58	7.58	7.98	7.98

	3.38		3.63		3 88		4.13		4.38		4.63
	0.30		0.15		0.15		0.15		0.15		0.15
	0.40		0.20		0 20		0.20		0.20		0 20
0 00	0.00	0.00	0.00	0.00	0 00	0.00	0 00	0.00	0.00	0 00	0.00
13.35	13.75	12.52	12.72	11.78	11.98	11.22	11.42	10.77	10 97	10.37	10.57
34.85	35.25	33.39	33.59	31.92	32.12	30 65	30.85	29.52	29.72	28.49	28 69
61.57	61.97	59.52	59.72	57.36	57.56	55.37	55.57	53.52	53.72	51.80	52.00
77.43	77.83	75.42	75.62	73 21	73.41	71.09	71.29	69.06	69 26	67.13	67.33
82.58	82.98	80.90	81.10	78.97	79.17	77.10	77.30	75.27	75.47	73.51	73.71
78.33	78.73	77.09	77.29	75.62	75.82	74.20	74.40	72.82	73 02	71.50	71.70
66.45	66.85	65 80	66.00	64 97	65.17	64.20	64 40	63.47	63 67	62.75	62.95
49.50	49.70	49.71	49.81	49.75	49 85	49.76	49.86	49.73	49.83	49.67	49.77
32.05	32.05	32 99	32.99	33.76	33.76	34.40	34.40	34 95	34.95	35.41	35.41
18.15	18.15	19.25	19 25	20.24	20.24	21.12	21.12	21.90	21.90	22.59	22.59
8.65	8 65	9.48	9.48	10.25	10.25	10 95	10 95	11.59	11.59	12.16	12.16
2.48	2 48	2.78	2.78	3.07	3.07	3 33	3 33	3 57	3.57	3.79	3.79

Determination of Thermal and Shrinkage Values for the ISFSI Concrete Pad Design

Calculated Temperature Rise for the ISFSI Pad

	4 88		5.00		5.13		5.25		5.38		5.50		5.63		5.75		5.88		6.00		6.13		6.25		6.38
	0.15		0.15		0.15		0.15		0.15		0.15		0.15		0.15		0.15		0.15		0.15		0.15		0.15
	0.20		0.20		0.20		0.20		0.20		0.20		0.20		0.20		0 20		0 20		0.20		0 20		0 20
0 00	0.00			0 00	0.00			0.00	0.00			0 00	0.00			0.00	0 00			0.00	0.00			0.00	0.00
		5.11	5 31			4.94	5.14			4.80	5.00			4.66	4.86			4.53	4.73			4.41	4.61		
10.01	10.21			9 69	9 89			9.39	9.59			9.11	9.31			8.86	9.06			8.61	8.81			8.39	8.59
		13.87	14.07			13.44	13.64			13 03	13.23			12 66	12.86			12.30	12.50			11.97	12.17		
27.54	27.74			26 67	26.87			25 86	26.06			25.11	25.31			24.40	24.60			23 74	23.94			23.12	23.32
		39.08	39.28			37.89	38.09			36.79	36.99			35.75	35.95			34.78	34.98			33.87	34.07		
50 21	50.41			48.71	48 91			47.31	47.51			46.00	46.20			44.76	44.96			43.59	43.79			42.49	42.69
		57.95	58.15			56.33	56 53			54.80	55.00			53.36	53 56			52.00	52.20			50.71	50.91		
65 29	65 49			63.55	63.75			61.90	62.10			60.33	60.53			58.85	59.05			57.44	57.64			56.10	56.30
		68.75	68.95			67.06	67.26			65.46	65.66			63.93	64 13			62.47	62.67			61.08	61.28		
71.81	72.01			70.18	70 38			68.62	68 82			67.12	67.32			65.69	65.89			64.33	64.53			63.02	63 22
		71.21	71.41			69.77	69.97			68 39	68 59			67.06	67.26			65.78	65.98			64.55	64.75		
70.21	70.41			68.97	69.17			67.76	67.96			66.60	66.80			65.47	65 67			64.38	64 58			63.32	63 52
		66.33	66.53			65 35	65.55			64.41	64.61			63.48	63 68			62.58	62.78			61.69	61.89		
62.04	62.24			61.34	61.54			60 65	60.85			59 96	60.16			59.28	59.48			58 60	58 80			57.93	58 13
		55.96	56.16			55.54	55.74			55.12	55.32			54 68	54.88			54.23	54.43			53.77	53.97		
49.57	49.67			49.44	49.54			49 29	49.39			49.10	49.20			48 88	48 98			48 64	48.74			48.38	48.48
		42.73	42.73			42.83	42 83			42.88	42.88			42.88	42.88			42.85	42.85			42.79	42.79		
35.79	35 79			36.11	36.11			36.37	36.37			36.57	36.57			36.72	36.72			36.83	36.83			36.90	36 90
		29.49	29.49			29 91	29.91			30.27	30 27			30.57	30 57			30.81	30.81			31.01	31.01		
23.19	23.19			23.71	23.71			24.17	24.17			24.56	24 56			24.89	24.89			25.18	25.18			25.41	25.41
		17.93	17.93			18 42	18.42			18 85	18 85			19.22	19.22			19.55	19.55			19.82	19 82		
12.68	12 68			13.13	13.13			13 53	13.53			13.89	13.89			14 20	14.20			14.47	14.47			14.70	14.70
		8.33	8.33			8.65	8.65			8 93	8.93			9.18	9.18			9.39	9.39			9 58	9.58		
3.99	3 99			4.17	4.17			4 32	4.32			4.46	4.46			4.59	4.59			4.70	4.70			4.79	4.79

Determination of Thermal and Shrinkage Values for the ISFSI Concrete Pad Design

Calculated Temperature Rise for the ISFSI Pad

	6.50		6.63		6.75		6.88		7.00		7.13		7.25		7.38		7.50		7.63		7.75		7.88		8.00
	0.15		0.15		0.15		0.15		0.15		0.15		0.15		0.15		0.15		0.15		0.15		0.15		0.15
	0.20		0.20		0.20		0.20		0.20		0.20		0.20		0.20		0.20		0.20		0.20		0.20		0.20
		0.00	0.00			0.00	0.00			0.00	0.00			0.00	0.00			0.00	0.00			0.00	0.00		
4.29	4.49			4.19	4.39			4.09	4.29			3.99	4.19			3.91	4.11			3.82	4.02			3.74	3.94
		8.18	8.38			7.98	8.18			7.79	7.99			7.61	7.81			7.44	7.64			7.28	7.48		
11.66	11.86			11.37	11.57			11.09	11.29			10.83	11.03			10.58	10.78			10.35	10.55			10.12	10.32
		22.53	22.73			21.98	22.18			21.45	21.65			20.96	21.16			20.49	20.69			20.05	20.25		
33.00	33.20			32.19	32.39			31.42	31.62			30.69	30.89			30.00	30.20			29.35	29.55			28.73	28.93
		41.45	41.65			40.46	40.66			39.53	39.73			38.64	38.84			37.80	38.00			37.01	37.21		
49.49	49.69			48.34	48.54			47.24	47.44			46.20	46.40			45.21	45.41			44.26	44.46			43.36	43.56
		54.83	55.03			53.62	53.82			52.46	52.66			51.37	51.57			50.32	50.52			49.32	49.52		
59.76	59.96			58.49	58.69			57.29	57.49			56.14	56.34			55.04	55.24			53.99	54.19			52.98	53.18
		61.76	61.96			60.56	60.76			59.41	59.61			58.31	58.51			57.25	57.45			56.23	56.43		
63.37	63.57			62.23	62.43			61.13	61.33			60.08	60.28			59.06	59.26			58.08	58.28			57.13	57.33
		62.30	62.50			61.31	61.51			60.35	60.55			59.41	59.61			58.51	58.71			57.63	57.83		
60.83	61.03			59.98	60.18			59.16	59.36			58.35	58.55			57.56	57.76			56.79	56.99			56.04	56.24
		57.27	57.47			56.61	56.81			55.95	56.15			55.31	55.51			54.67	54.87			54.04	54.24		
53.31	53.51			52.83	53.03			52.35	52.55			51.87	52.07			51.38	51.58			50.88	51.08			50.39	50.59
		48.10	48.20			47.80	47.90			47.48	47.58			47.14	47.24			46.80	46.90			46.44	46.54		
42.69	42.69			42.56	42.56			42.40	42.40			42.22	42.22			42.02	42.02			41.80	41.80			41.56	41.56
		36.92	36.92			36.91	36.91			36.87	36.87			36.80	36.80			36.70	36.70			36.58	36.58		
31.16	31.16			31.26	31.26			31.34	31.34			31.37	31.37			31.38	31.38			31.36	31.36			31.31	31.31
		25.61	25.61			25.76	25.76			25.88	25.88			25.96	25.96			26.01	26.01			26.03	26.03		
20.06	20.06			20.26	20.26			20.42	20.42			20.54	20.54			20.64	20.64			20.71	20.71			20.76	20.76
		14.90	14.90			15.07	15.07			15.21	15.21			15.33	15.33			15.42	15.42			15.48	15.48		
9.75	9.75			9.89	9.89			10.01	10.01			10.11	10.11			10.19	10.19			10.26	10.26			10.31	10.31
		4.87	4.87			4.94	4.94			5.00	5.00			5.05	5.05			5.10	5.10			5.13	5.13		

Determination of Thermal and Shrinkage Values for the ISFSI Concrete Pad Design

Calculated Temperature Rise for the ISFSI Pad

	8.13		8 25		8.38
	0.15		0.15		0.15
	0 20		0 20		0.20
0 00	0 00			0.00	0.00
		3 67	3 87		
7.13	7.33			6.99	7.19
		9.91	10.11		
19 62	19.82			19 22	19.42
		28 13	28 33		
36.25	36 45			35.52	35.72
		42.51	42.71		
48 37	48 57			47 46	47.66
		52 01	52 21		
55.26	55 46			54.32	54.52
		56.22	56.42		
56.78	56 98			55.96	56.16
		55.30	55 50		
53.41	53 61			52.80	53 00
		49 89	50.09		
46.07	46.17			45 70	45 80
		41 30	41.30		
36 43	36 43			36 27	36.27
		31.23	31 23		
26.03	26.03			26.01	26.01
		20.78	20.78		
15.53	15 53			15.56	15.56
		10.34	10.34		
5.15	5.15			5.17	5.17

Pacific Gas and Electric Company
Engineering - Calculation Sheet
Project: Diablo Canyon Unit ( )1 ( ) 2 (X) 1&2

CALC. NO. 52.27.100.701
REV. NO 1
SHEET NO 48 OF

SUBJECT Determination of Thermal and Shrinkage Values for the ISFSI Concrete Pad Design

MADE BY ADP DATE 10/11/2001 CHECKED BY Carl Knifton DATE 10/11/2001

Rev. #1 added sheets 48, 49 and 50. Note sheets 1 to 47 should have Rev. # 0 on each sheet.

Reason for Revision

Additional Information has been requested:

- Physical Properties of Aggregate for the ISFSI Foundation Pad.
- Physical properties of hardened concrete for the ISFSI Foundation Pad.
  - Expected Compressive Strength Values at early ages (0.25, 0.50 days)
  - Expected Thermal Expansion

Physical Properties of Aggregate for the ISFSI Foundation Pad.

The ISFSI Foundation Pad concrete mix is based on the use of Granite fine and coarse aggregates from the Santa Margarita Quarry. This aggregate is a crushed material with angular particle shape. The surface texture of this aggregate is rough.

Physical properties of hardened concrete for the ISFSI Foundation Pad.

Expected Compressive Strength Values at early ages (0.25, 0.50, etc. days) 1

The specified compressive strength is 5000 psi for this mix design, at an age of 90 days. This concrete will be designed for a compressive strength of 5600 psi, at an age of 90 days. The estimated compressive strength curve is shown in Figure 1 (page 19 rev.0). The TES Report # 420DC-96.160 was used to develop the estimated compressive strength curve. The first value of estimated compressive strength is at the age of two days. To estimate the compressive at ages early then 2 days it is assumed that the strength gain from zero time to 2 days is linear.

The 2-day Compressive Strength is 2100 psi.

Therefore

Compressive strength = 1050 * Age in days

= 262.5 psi at 0.25 days

= 525 psi at 0.5 days

= 787.5 psi at 0.75 days

= 1050 psi at 1.0 days

SUBJECT Determination of Thermal and Shrinkage Values for the ISFSI Concrete Pad Design

MADE BY ADP ADP DATE 10/11/2001 CHECKED BY Carl Knifton DATE 10/11/2001

The table below shows the Specified Compressive Strength and the required Mix Design Average Compressive Strength to the age of 90 days.

Age, days	Specified Compressive Strength, psi	Mix Design Average Compressive Strength, psi
0	0	0
0.25	234	262.5
0.5	469	525
0.75	703	787.5
1	937	1050
2	1875	2100
3	2562	2870
5	3232	3620
7	3616	4050
10	3902	4370
14	4143	4640
21	4420	4950
28	4554	5100
60	4777	5350
90	5000	5600

1

Physical properties of hardened concrete for the ISFSI Foundation Pad.

Expected Thermal Expansion

Prediction of the coefficient of thermal expansion for concrete is given in section 2.9.2 of "ACI 209R-92 - Prediction of Creep, Shrinkage and Temperature Effects in Concrete Structures". There are no test results for the thermal coefficient of expansion using this aggregate, therefore the equation in section 2.9.2 will be used. In the absence of specific data from local materials and environmental conditions, the values given by the following equation may be used for the thermal coefficient of expansion.

Pacific Gas and Electric Company
Engineering - Calculation Sheet
Project: Diablo Canyon Unit ( )1 ( )2 (X) 1&2

CALC NO. 52.27.100.701
REV NO 1
SHEET NO 50 OF

SUBJECT Determination of Thermal and Shrinkage Values for the ISFSI Concrete Pad Design

MADE BY ADP ADP DATE 10/11/2001 CHECKED BY Carl Yrifton DATE 10/11/2001

Coefficient of thermal expansion for concrete = $e_{mc} + 1.72 * 10^{-6} + 0.72\, e_a$

e_{mc} from Table 2.9.1 for Mass concrete = $0.72 * 10^{-6}$

$1.72 * 10^{-6}$ is the thermal expansion of hydrated cement

(The 10^{-6} factor in this equation for hydrated cement in ACI 209 is missing)

e_a from Table 2.9.2 for granite aggregate = $3.8 * 10^{-6}$ degrees F.

Coefficient of thermal expansion for concrete $= 0.72 * 10^{-6} + 1.72 * 10^{-6} + 0.72 * 3.8 * 10^{-6}$

$= 5.18 * 10^{-6}$ degrees F.

1

Pacific Gas and Electric Company
Engineering - Calculation Sheet
Project: Diablo Canyon Unit ( )1 ( )2 (X) 1&2

CALC. NO. 52.27.100.701
REV. NO 2
SHEET NO 51 OF

SUBJECT Determination of Thermal and Shrinkage Values for the ISFSI Concrete Pad Design

MADE BY ADP GDP DATE 11/08/2001 CHECKED BY Carl Knifton DATE 11/8/01

Reason for Revision
Additional Information has been requested:

Relationship of Shrinkage vs. Depth of Concrete
Temperature of the Surface of the Pad

Relationship of Shrinkage vs. Depth of Concrete.

Non-uniform shrinkage with a thick concrete member will occur. Moisture loss takes place at the surface so that a moisture gradient is established in the concrete, which is thus subject to differential shrinkage. The progress of shrinkage extends gradually from the drying surface into the interior of the concrete but does so extremely slowly. Desiccation has been observed to reach the depth of 3 inches in one month but only 2 feet after 10 years, "Properties of Concrete, Third Edition 1981", by A. M. Neville page 385.

2

Information on the progress of shrinkage with time as a function of distance from drying surface was obtained from the "Properties of Concrete, Third Edition 1981", by A. M. Neville, page 385. See Figure 8 for the shrinkage vs. distance from the surface. Results are given for concrete, mix design unknown, which had a shrinkage value of 320 micro-strain at an age of 225 days at the surface. With no drying possible in directions other than the surface the shrinkage at a depth of 1.64 feet (500 mm) was 18 micro-strain. The pad concrete has an estimated shrinkage of 463 micro-strain at 117 days (see page 20, Figure 2), Figure 9 shows the Pad and Neville shrinkage values. The higher shrinkage of the pad concrete can be attributed to many factors. Not knowing the mix design or the materials for the Neville concrete mix a comparison cannot be made. The most probable reason for the increased shrinkage for the pad concrete is greater cement content. The drying of the surface of each concrete should be similar.

The values obtained from Neville for 90 and 225 day shrinkage values were extended from 1.64 feet to 8 feet, using an exponential curve fit on the Neville data then forecasting forward. The Neville values for 90 and 225 day were used to develop a curve of shrinkage vs. distance from the surface of a concrete at the age of 117 days, by linear interpolation using the ratio of;

$$\text{Ratio} = (117 - 90) / (225 - 90)$$
$$= 0.2$$

The shrinkage values at various depths of the developed curve of shrinkage vs. distance from the surface of a concrete at the age of 117 days was linear interpolated to obtain a shrinkage curve at various depths for a shrinkage maximum value of 463 micro-strain at the age of 117 days. See the table below or Figure 10 for the relationship of shrinkage vs. depth of concrete calculated for a 463 micro-strain shrinkage at 117 days.

Pacific Gas and Electric Company
Engineering - Calculation Sheet
Project: Diablo Canyon Unit ( )1 ( )2 (X) 1&2

CALC. NO. 52.27.100.701
REV. NO. 2
SHEET NO. 52 OF

SUBJECT Determination of Thermal and Shrinkage Values for the ISFSI Concrete Pad Design

MADE BY ADP ADP DATE 11/08/2001 CHECKED BY Carl Knifton DATE 11/8/01

Relationship of Shrinkage vs. Depth of Concrete

Distance from the Surface, ft	Neville Shrinkage at 225 days, micro-strain	Neville Shrinkage at 90 days, micro-strain	Calculated Neville Shrinkage at 117 days, micro-strain	Calculated Pab Shrinkage at 117 days, micro-strain
0	318	237	253	463
.5	131	55	70	128
1	54	10.5	19	35
1.5	22	-4	1.2	2.2
2	9	-10.5	-6.6	-12
2.5	3.7	-13	-9.6	-17
3	1.5	-16	-12.5	-23
3.5	.6	-17	-13.5	-25
4	.3	-17	-13.5	-25
4.5	.1	-17	-13.5	-25
5	0	-17	-13.6	-25
5.5	0	-17	-13.6	-25
6	0	-17	-13.6	-25
6.5	0	-17	-13.6	-25
7	0	-17	-13.6	-25
7.5	0	-17	-13.6	-25
8	0	-17	-13.6	-25

2

SUBJECT Determination of Thermal and Shrinkage Values for the ISFSI Concrete Pad Design

MADE BY ADP DATE 11/08/2001 CHECKED BY Carl Knifton DATE 11/8/01

FIGURE 8
Shrinkage vs. Depth At Various Ages
from "Properties of Concrete", A. M. Neville

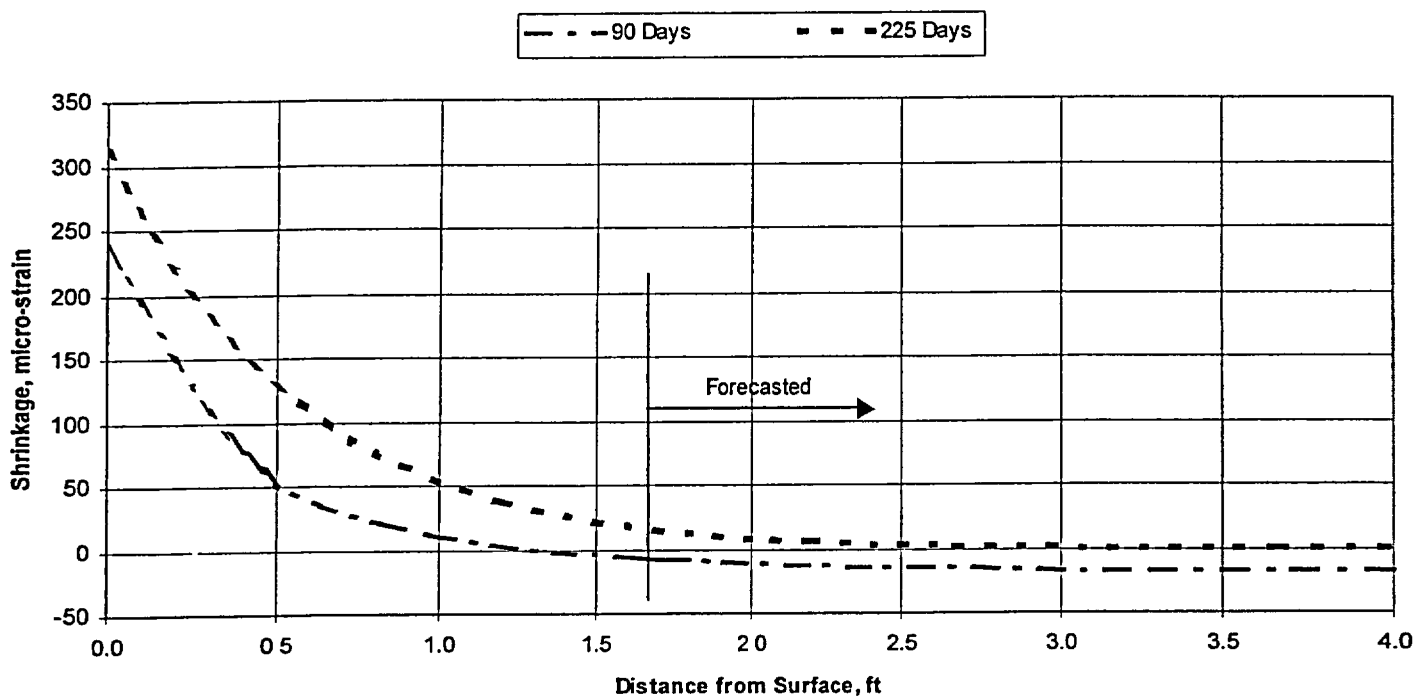

2

SUBJECT Determination of Thermal and Shrinkage Values for the ISFSI Concrete Pad Design

MADE BY ADP *ADPto* DATE 11/08/2001 CHECKED BY *Carl Knifton* DATE *11/8/01*

FIGURE 9
Shrinkage

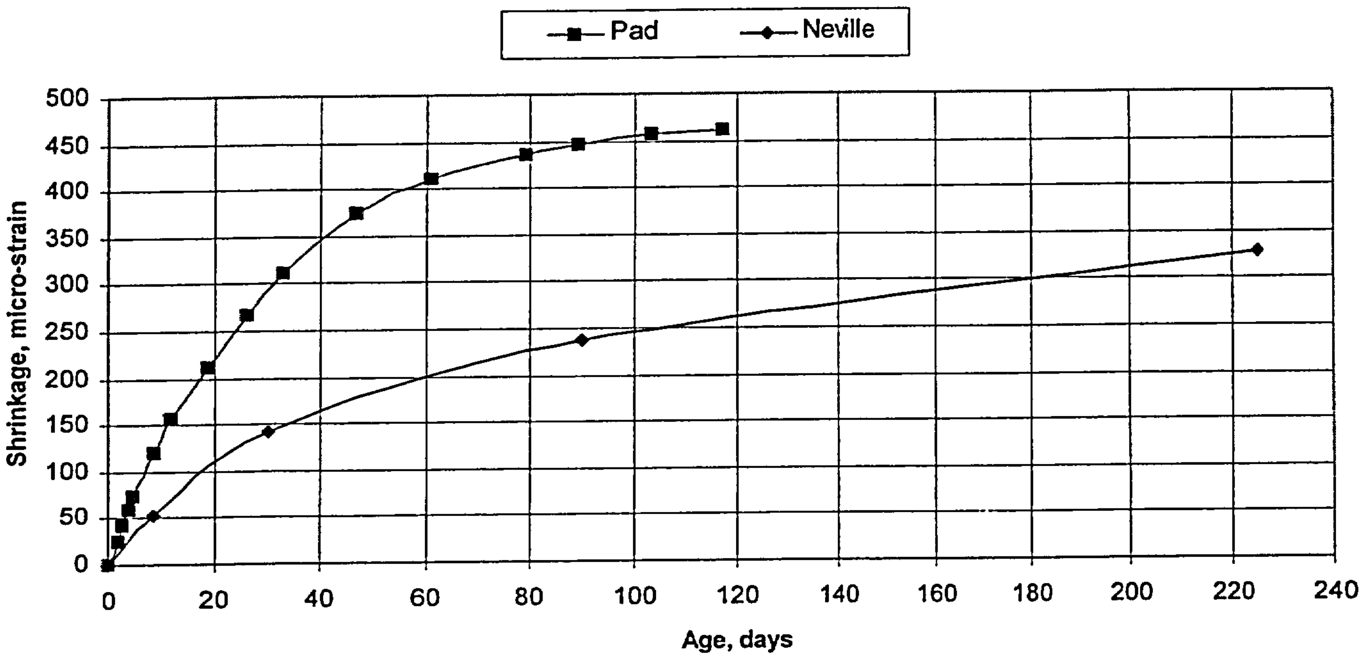

2

Pacific Gas and Electric Company
Engineering - Calculation Sheet
Project: Diablo Canyon Unit ( )1 ( )2 (X) 1&2

CALC NO 52.27.100.701
REV NO 2
SHEET NO. 55 OF

SUBJECT Determination of Thermal and Shrinkage Values for the ISFSI Concrete Pad Design

MADE BY ADP GDB DATE 11/08/2001 CHECKED BY Carl Knifton DATE 11/8/01

Figure 10
Pad Shrinkage Vs Depth @ 117 days

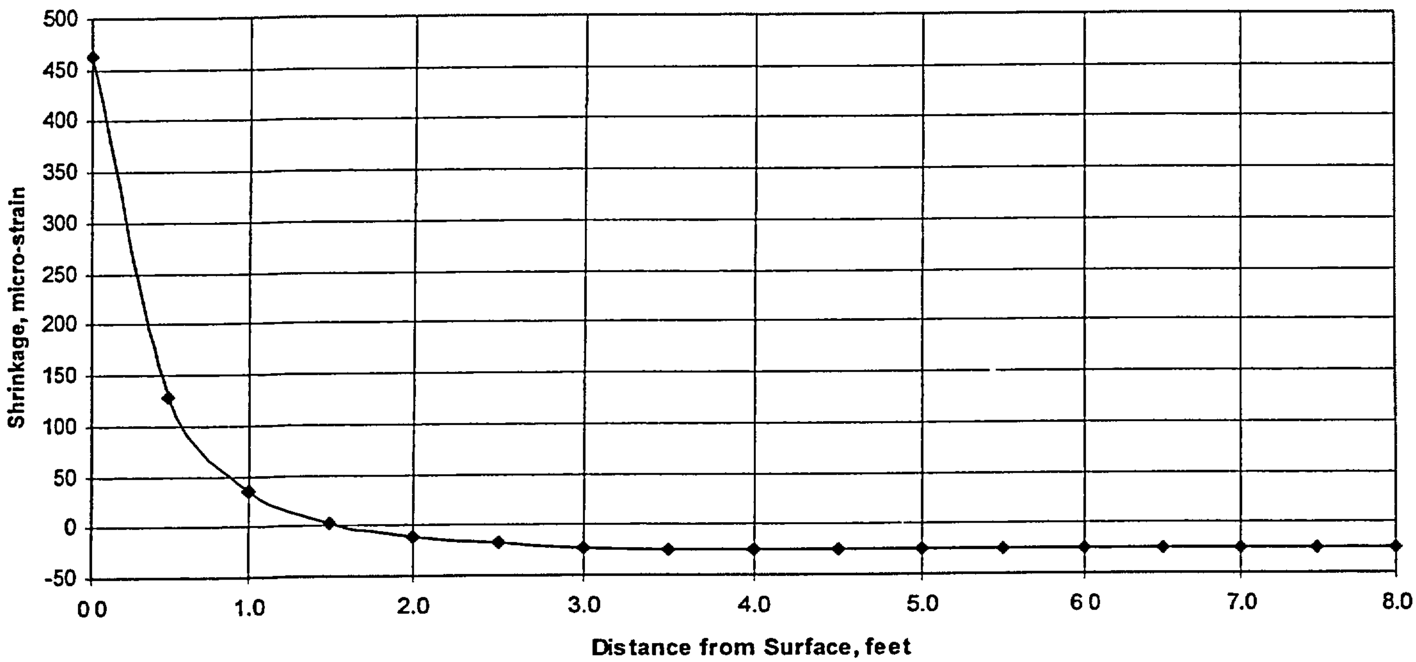

2

SUBJECT Determination of Thermal and Shrinkage Values for the ISFSI Concrete Pad Design

MADE BY ADP *ADP* DATE 11/08/2001 CHECKED BY *Carl Knifton* DATE *11/8/01*

Temperature of the Surface of the Pad

The surface temperature of the pad is equal to the heat dissipation of the temperature at 0.5 feet depth to the surface plus the rate of heat generation in the top 0.5 foot concrete thickness.

Heat dissipation of the temperature at 0.5 feet depth to the surface

The heat dissipation computation from ACI 207.1, section 5.4.1 was used to calculate the heat dissipation of the temperature at 0.5 feet depth to the surface.

Time, days, t = 0.125
Diffusivity, ft^2 per day, h^2 = 1 (Assumed)
Thickness of section, ft, D = 0.5
Initial temperature, degrees F. θ_o = Element temperature
Surface temperature, degrees F. θ_m = unknown

$h^2 t / D^2$ was calculated for each interval then Figure 5.4.1 was used to determine θ_m / θ_o, θ_m was then calculated for each interval

Rate of heat generation in the top 0.5 foot concrete thickness

The heat generated in the top 0.5 foot element for each time interval was determined from Appendix C or Figure 4 (page 22) - The calculate adiabatic temperature rise curve.

Determination of the Temperature at the surface of the pad at 0.125 days

Heat dissipation of the temperature at 0.5 feet depth to the surface of the pad at 0.125 days

$$\frac{h^2 t}{D^2} = \frac{1 * 0.125}{0.5^2} = 0.5$$

Use Figure 5.4.1 (see Appendix D), use Slab curve to determine θ_m / θ_o using $h^2 t / D^2$

$\theta_m / \theta_o = 0.02$

Solve for θ_m

θ_o = 6.67 obtained from Appendix C or Figure 5 (page 23)
θ_m = 0.02 * 6.67
θ_m = .13 degrees F.

SUBJECT Determination of Thermal and Shrinkage Values for the ISFSI Concrete Pad Design

MADE BY ADP *ADP* DATE 11/08/2001 CHECKED BY *Carl Knifton* DATE *11/8/01*

Rate of heat generation in the top 0.5 foot concrete thickness at 0.125 days.

At the age of 0.125 the heat generated in the top 0.5 foot element as determined from Appendix C = 6.67 degrees F.

Surface temperature of the pad at 0.125 days	=	Heat dissipation of the temperature at 0.5 feet depth to the surface of the pad at 0.125 days	+	Rate of heat generation in the top 0.5 foot concrete thickness at 0.125 days.
	=	.13 degrees F.	+	6.67 degrees F.
	=	6.80 degrees F.		

The surface temperature of the pad was calculated for each time interval (0.125 days) to the age of 8 days. The calculated surface temperatures are shown on the following figure.

Pacific Gas and Electric Company
Engineering - Calculation Sheet
Project: Diablo Canyon Unit ( )1 ( )2 (X) 1&2

CALC NO 52.27.100.701
REV. NO. 2
SHEET NO. 58 OF

SUBJECT Determination of Thermal and Shrinkage Values for the ISFSI Concrete Pad Design

MADE BY ADP *ADPt* DATE 11/08/2001 CHECKED BY *Carl Knifton* DATE *11/8/01*

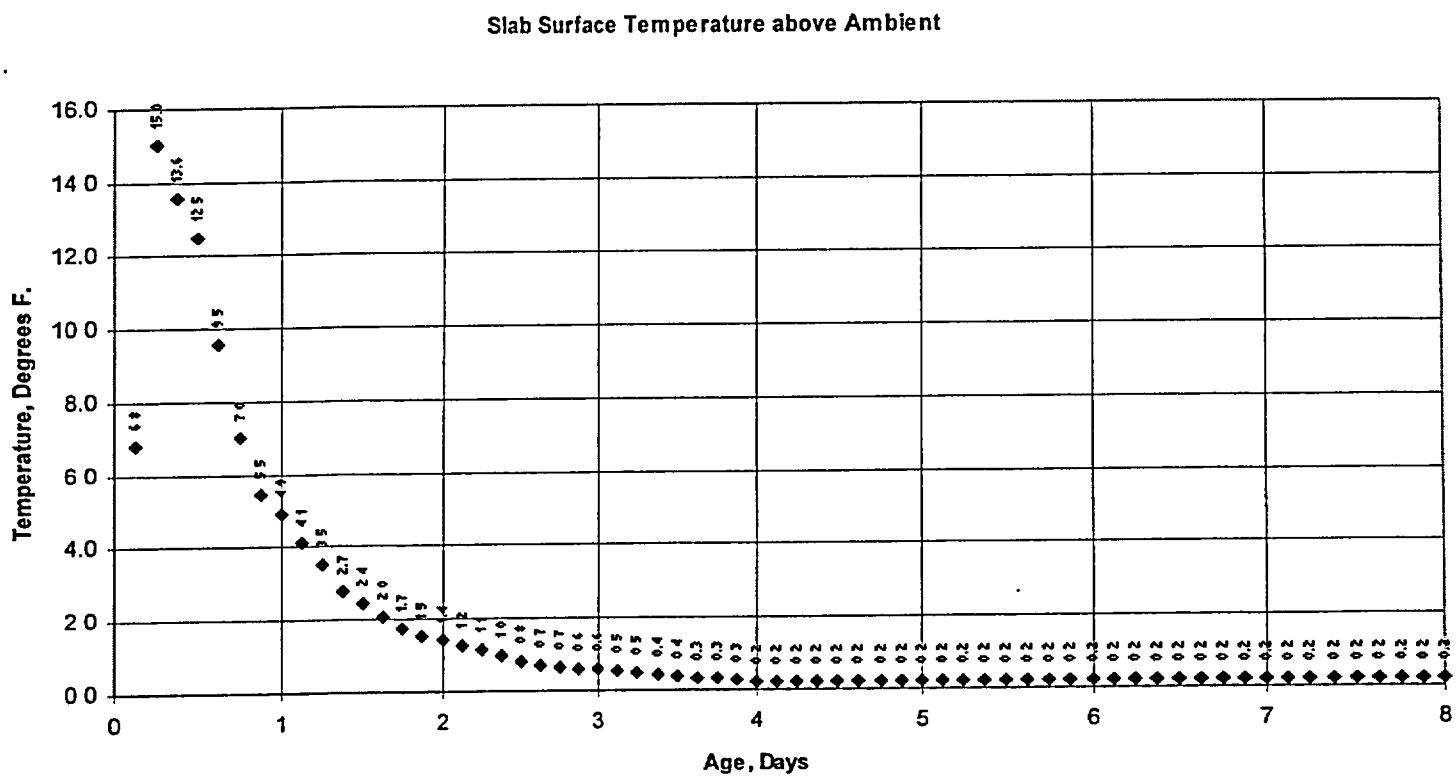

2

Pacific Gas and Electric Company
Engineering - Calculation Sheet
Project: Diablo Canyon Unit ( )1 ( )2 (X) 1&2

CALC. NO. 52.27.100.701
REV. NO. 2
SHEET NO. 59 OF

SUBJECT Determination of Thermal and Shrinkage Values for the ISFSI Concrete Pad Design

MADE BY ADP DATE 11/08/2001 CHECKED BY DATE 11/8/01

Appendix D

ACI 207.1

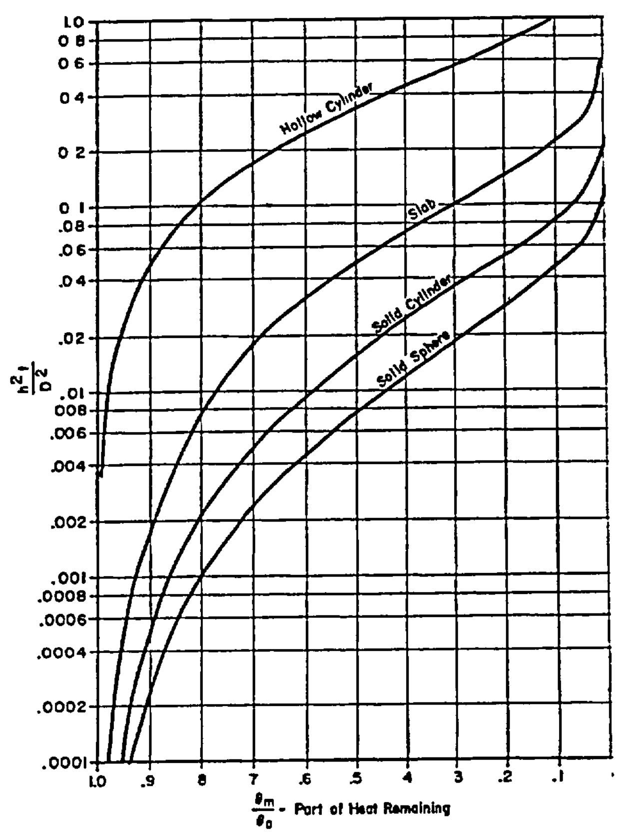

Fig. 5.4.1—Heat loss from solid bodies

2

REFERENCE MATERIAL

NOT PART OF CALCULATION

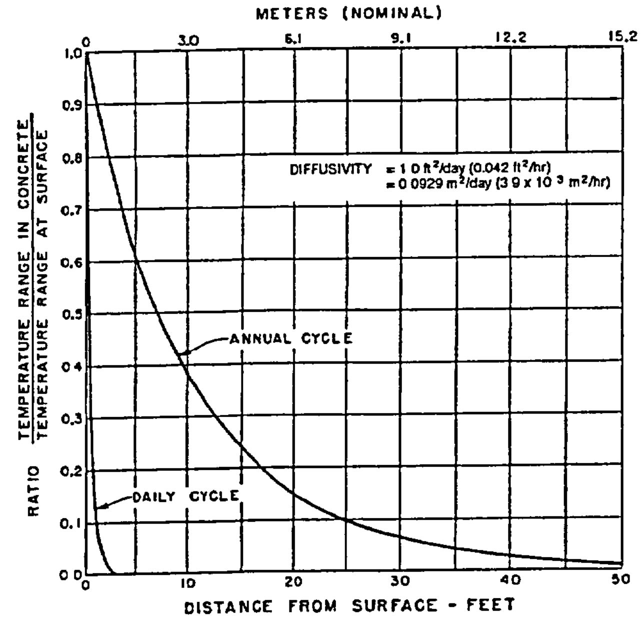

Fig. 5.3.5—Temperature variation with depth

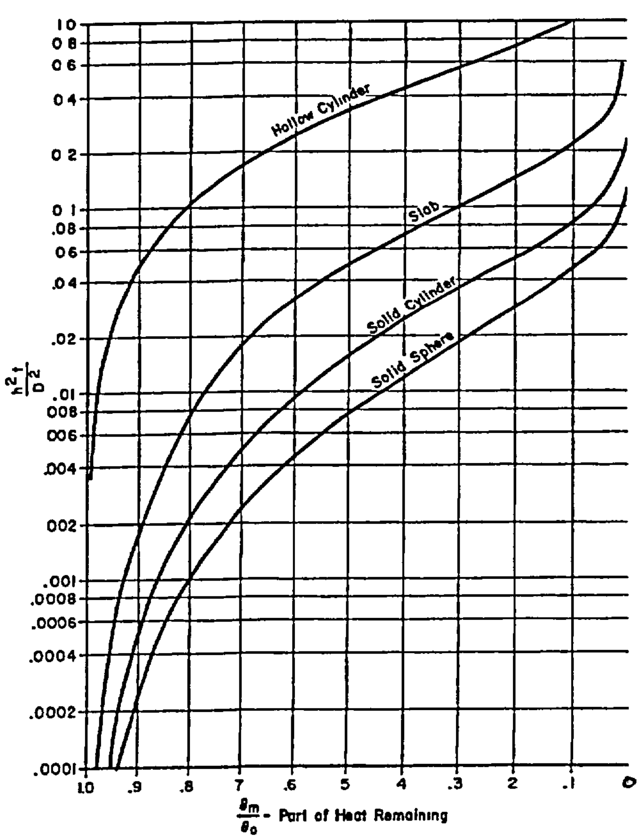

Fig 5.4.1—Heat loss from solid bodies

use of Fig 5.4.1. For simplicity of presentation the examples are in inch-pound units only; Appendix A presents the examples worked in SI (metric) units In the examples below and Fig 5.4.1, the following notation is followed:

t = time, days
h^2 = diffusivity, ft^2 per day (m^2/day)
D = thickness of concrete section, ft (m)
θ_o = initial temperature difference between concrete and ambient material, F (C)
θ_m = final temperature difference between concrete and ambient material, F (C)

Example 1 (See Appendix A for examples worked in SI units)

At a certain elevation an arch dam is 70 ft thick and has a mean temperature of 100 F. If exposed to air at 65 F, how long will it take to cool to 70 F? Assume h^2 = 1.20 ft^2/day.

Initial temperature difference, θ_o = 100 - 65 = 35 F

Final temperature difference, θ_m = 70 - 65 = 5 F

The portion of the original heat remaining is

$$\frac{\theta_m}{\theta_o} = \frac{5}{35} = 0.142$$

From Fig. 5.4.1, using the slab curve

$$\frac{h^2 t}{D^2} = 0.18$$

Then

$$t = \frac{0.18D^2}{h^2} = \frac{0.18(70)^2}{1.20} = 740 \text{ days}$$

Example 2

A mass concrete bridge pier has a horizontal cross section of 25 x 50 ft, and is at a mean temperature of 80 F. Determine the mean temperature at various times up to 200 days if the pier is exposed to water at 40 F and if the diffusivity is 0.90 ft^2/day. For a prismatic body such as this pier, where heat is moving towards each of four pier faces, the part of original heat remaining may be computed by finding the part remaining in two infinite slabs of respective thickness equal to the two horizontal dimensions of the pier, and multiplying the two quantities so obtained to get the total heat remaining in the pier. For this two-dimensional use, it is better to find for various times the heat losses associated with each direction and then combine them to find the total heat loss of the pier.

Initial temperature difference, θ_o = 80 - 40 = 40 F

For the 25-ft dimension

$$\frac{h^2 t}{D^2} = \frac{0.90t}{(25)^2} = 0.00144t$$

and for the 50-ft dimension

$$\frac{h^2 t}{D^2} = \frac{0.90t}{(50)^2} = 0.00036t$$

Then calculate numerical values of 0.00144t and 0.00036t for times from 10 to 200 days. See Table 5.4.1. These values can be used with Fig. 5.4.1 to obtain the θ_m/θ_o ratios for both 25-ft and 50-ft slabs. The product of these ratios indicates the

Neville
Properties of Concrete

curing on the magnitude of shrinkage is small though rather complex. As far as neat cement paste is concerned, the greater the quantity of hydrated cement the smaller is the volume of unhydrated cement grains which restrain the shrinkage: thus prolonged curing leads to greater shrinkage[6.18] but the paste becomes stronger with age and is able to attain a larger fraction of its shrinkage tendency without cracking. If, however, cracking takes place, e.g. around aggregate particles, the overall shrinkage, measured on a concrete specimen, apparently decreases. Well-cured concrete shrinks more rapidly[6.72] and therefore the relief of shrinkage stresses by creep is smaller; also, the concrete, being stronger, has an inherent low creep capacity. These factors may outweigh the higher tensile strength of well-cured concrete and may lead to cracking. In view of this it is not surprising that contradictory results on the effects of curing on shrinkage have been reported, but in general the length of the curing period is not an important factor in shrinkage. (*See* p. 387.)

The magnitude of shrinkage is largely independent of the rate of drying except that transferring concrete directly from water to a very low humidity can lead to fracture. Rapid drying out does not allow a relief of stress by creep and may lead to more pronounced cracking. However, neither wind nor forced convection have any effect on the rate of drying of hardened concrete (except during very early stages) because the moisture conductivity of concrete is so low that only a very small rate of evaporation is possible: the rate cannot be increased by movement of air.[6.90] This has been confirmed experimentally.[6.91] (*See* p. 308 for evaporation from fresh concrete.)

The relative humidity of the medium surrounding the concrete greatly affects the magnitude of shrinkage, as shown for instance in Fig. 6.20. The same figure illustrates also the greater absolute magnitude of shrinkage compared with swelling in water: swelling is about six times smaller than shrinkage in air of relative humidity of 70 per cent or eight times smaller than shrinkage in air at 50 per cent.

We see thus that concrete placed in "dry" (unsaturated) air shrinks, but it swells in water or air with a relative humidity of 100 per cent. This would indicate that the vapour pressure within the cement paste is always less than the saturated vapour pressure, and it is logical to expect that there is an intermediate humidity at which the paste would be in hygral equilibrium. In fact, Lorman[6.31] found this humidity to be 94 per cent, but in practice equilibrium is possible only in small and practically unrestrained specimens.

In the shrinkage test prescribed in BS 1881: Part 5: 1970 the specimens are dried for a specified period under prescribed conditions of temperature and humidity. The shrinkage occurring under these conditions is of the same order as that after a long exposure to air with a relative humidity of approximately 65 per cent,[6.19] and is therefore in excess of the shrinkage met with outdoors in the British Isles. The magnitude of shrinkage can be

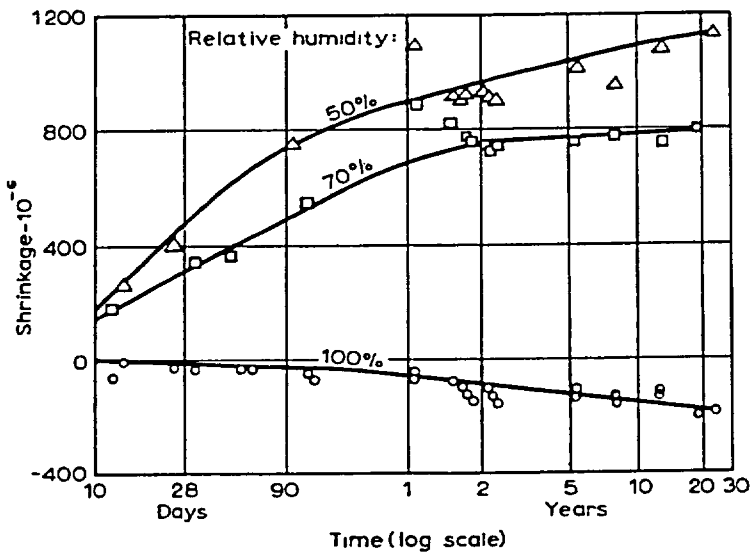

Fig. 6.20. *Relation between shrinkage and time for concretes stored at different relative humidities*[6 24]
Time reckoned since end of wet curing at the age of 28 days

determined using a measuring frame fitted with a micrometer gauge or a dial gauge reading to 10^{-5} strain, or by means of an extensometer or strain gauges.

BS 2028:1968 prescribes maximum shrinkage of precast blocks as—

500×10^{-6} to 600×10^{-6} for general use concrete blocks;
700×10^{-6} to 900×10^{-6} for load-bearing lightweight concrete blocks; and
800×10^{-6} to 900×10^{-6} for non-load-bearing lightweight concrete.

In each case, the particular limit within the range depends on strength or density. The higher limit for lightweight aggregate concrete is due to its inherently higher shrinkage; in the case of precast concrete this can be reduced by drying during the process of manufacture.[6 19]

Differential Shrinkage

In addition to internal restraints – aggregate and reinforcement – some restraint arises also from non-uniform shrinkage within the concrete member itself. Moisture loss takes place at the surface so that a moisture gradient is established in the concrete specimen, which is thus subject to differential shrinkage. This shrinkage is compensated by strains due to internal stresses, tensile near the surface and compressive in the core. When drying takes place in an unsymmetrical manner, warping can result.

The progress of shrinkage extends gradually from the drying surface into the interior of the concrete but does so only extremely slowly. Desiccation was observed to reach the depth of 75 mm (3 in.) in one month but only 600mm (2ft) after 10 years.[6.14] Data[6.100] of L'Hermite are shown in Fig. 6.21; initial swelling in the interior can be seen. Ross[6.32] found the

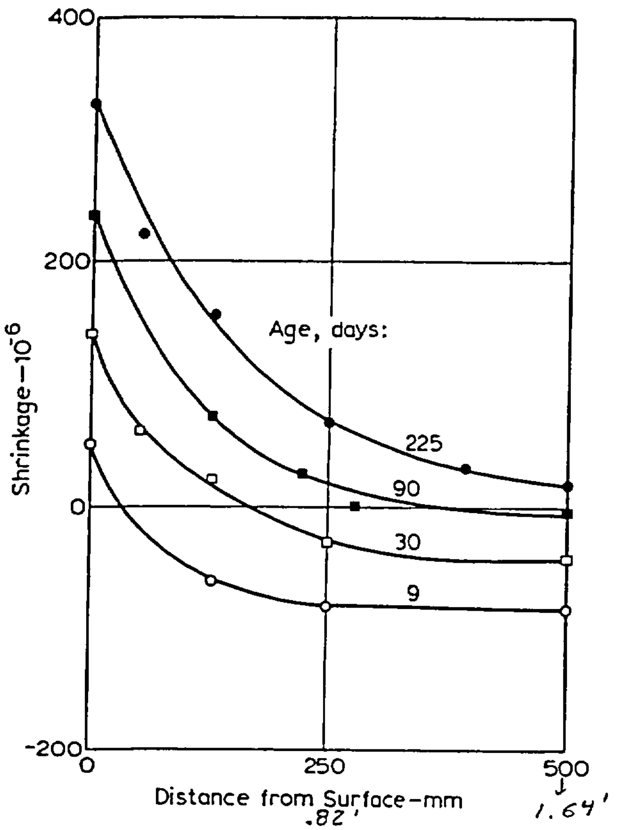

Fig. 6.21. *Progress of shrinkage with time as a function of distance from drying surface (no drying possible in other directions). (Shrinkage values corrected for temperature differences)*[6.100]

difference between shrinkage in a mortar slab at the surface and at depth of 150 mm (6 in.) to be 470×10^{-6} after 200 days. If the modulus of elasticity of mortar is 21 GPa (3×10^6 psi) the differential shrinkage would induce a stress of 10 MPa (1400 psi); since the stress arises gradually it is relieved by creep, but even so surface cracking may result. Increasing the volume of aggregate would considerably restrain the shrinkage so that the technical advantage of using concrete rather than neat cement paste or mortar is clear.

Because drying takes place at the surface of concrete, the magnitude of shrinkage varies considerably with the size and shape of the specimen, being a function of the surface/volume ratio.[6 32] A part of the size effect may also be due to the pronounced carbonation of small specimens. Thus for practical purposes shrinkage cannot be considered as purely an inherent property of concrete without reference to the size of the concrete member.

Many investigations have in fact indicated an influence of the size of the specimen on shrinkage. The observed shrinkage decreases with an increase in the size of the specimen but above some value the size effect is small initially but pronounced later (Fig. 6.22). The shape of the specimen also

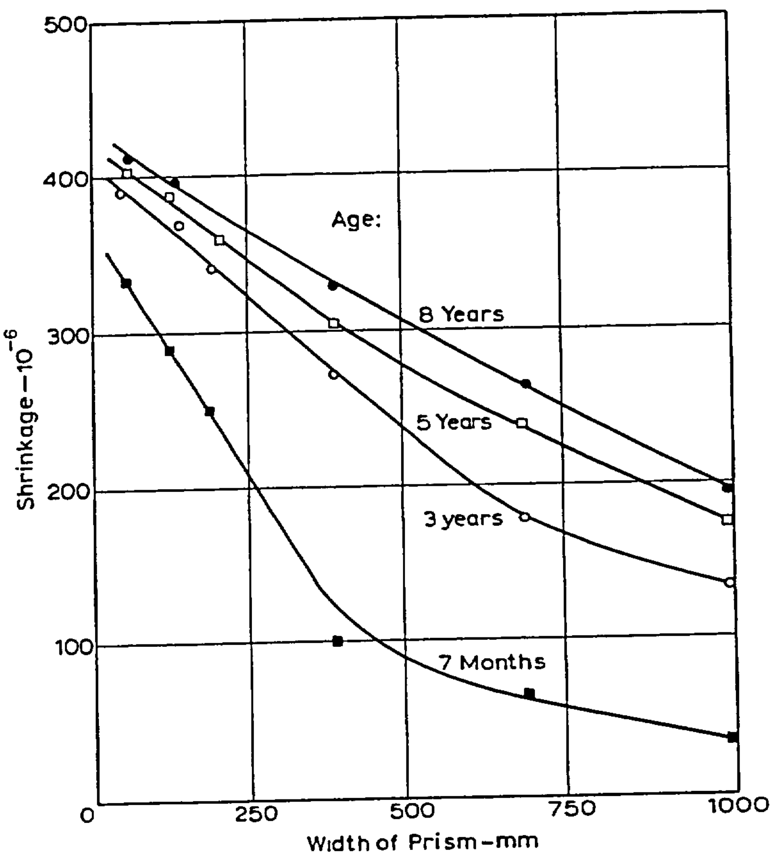

Fig. 6.22. *Relation between axial shrinkage and width of concrete prisms of square cross-section and length/width of 4 (drying allowed at all surfaces)*[6 100]

appears to enter the picture but as a first approximation shrinkage can be expressed as a function of the volume/surface ratio of the specimen. There appears to be a linear relation between this ratio and the logarithm of shrinkage[6 92] (Fig. 6.23). Furthermore, the ratio is linearly related to the

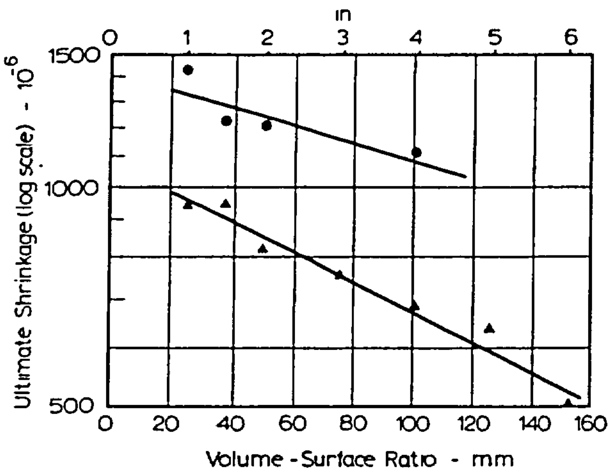

Fig. 6.23. *Relation between ultimate shrinkage and volume/surface ratio*[6.92]

logarithm of time required for half the shrinkage to be achieved. The latter relation applies to concretes made with different aggregates, so that, while the magnitude of shrinkage is affected by the type of aggregate used, the rate at which the final value of shrinkage is reached is not influenced.[6.92] Hobbs[6.120] argued that theoretically the ultimate shrinkage is independent of the size of the concrete element but, for realistic periods, it must be accepted that shrinkage is smaller in larger elements.

The effect of shape is secondary. I-shaped specimens exhibit less shrinkage than cylindrical ones of the same volume/surface ratio, the difference being 14 per cent on the average.[6.92] The difference, which can be explained in terms of variation in the mean distance that the water has to travel to the surface, is thus not significant for design purposes.

Shrinkage-induced Cracking

As mentioned in connection with differential shrinkage, the importance of shrinkage in structures is largely related to cracking. Strictly speaking, we are concerned with the cracking tendency as the advent or absence of cracking depends not only on the potential contraction but also on the extensibility of concrete, its strength and its degree of restraint to the deformation that may lead to cracking.[6.93] Restraint in the form of reinforcing bars or a gradient of stress increases extensibility in that it allows concrete to develop strain well beyond that corresponding to maximum stress.

A high extensibility of concrete is generally desirable because it permits concrete to withstand greater volume changes. The Bureau of Reclamation[6.94] made some thermal cycle tests on concrete at a constant